NASA TECHNICAL NOTE

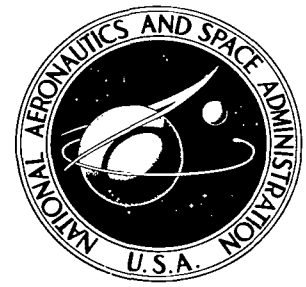

WIND-TUNNEL INVESTIGATION OF A LARGE 35° SWEPT-WING JET TRANSPORT MODEL WITH AN EXTERNAL-FLOW JET-AUGMENTED DOUBLE-SLOTTED FLAP

by Kiyoshi Aoyagi and Leo P. Hall

Ames Research Center
Moffett Field, Calif. 94035

NATIONAL AERONAUTICS AND SPACE ADMINISTRATION • WASHINGTON, D. C. • AUGUST 1971

1. Report No.	2. Government Accession No.	3. Recipient's Catalog No.
NASA TN D-6482		

4. Title and Subtitle	5. Report Date
WIND-TUNNEL INVESTIGATION OF A LARGE 35° SWEPT-WING JET TRANSPORT MODEL WITH AN EXTERNAL-FLOW JET-AUGMENTED DOUBLE-SLOTTED FLAP	August 1971
	6. Performing Organization Code

7. Author(s)	8. Performing Organization Report No.
Kiyoshi Aoyagi and Leo P. Hall	A-3523
	10. Work Unit No.
9. Performing Organization Name and Address	721-52-11-01-00-21
NASA Ames Research Center Moffett Field, California, 94035	11. Contract or Grant No.
	13. Type of Report and Period Covered
12. Sponsoring Agency Name and Address	Technical Note
National Aeronautics and Space Administration Washington, D.C. 20546	14. Sponsoring Agency Code

15. Supplementary Notes

16. Abstract

The model had a low-mounted wing of aspect ratio 7.82 and four pod-mounted jet engines under the wing. The lift of the flap system was augmented by impingement of the exhaust of the jet engines on the main flap and a small auxiliary flap. The auxiliary flap may be used for direct-lift control. Results were obtained for several main and auxiliary flap deflections at gross thrust coefficients of 0 to 2.0. Three-component longitudinal data are presented with the operation of four and two engines. Limited longitudinal and lateral data are presented for the operation of three engines.

17. Key Words (Suggested by Author(s))	18. Distribution Statement
External blowing jet-flap Direct lift control Wind tunnel model	Unclassified - Unlimited

19. Security Classif. (of this report)	20. Security Classif. (of this page)	21. No. of Pages	22. Price*
Unclassified	Unclassified	74	$3.00

SYMBOLS

a_n	vehicle incremental acceleration normal to flight path, $\frac{\Delta C_{L_{aux}}}{C_{L_{trim}}}$
b	wing span, m (ft)
c	wing chord measured parallel to the plane of symmetry, m (ft)
$\bar{c}$	mean aerodynamic chord of wing, $\frac{2}{S}\int_0^{b/2} c^2\, dy$, m (ft)
C_D	drag coefficient, $\frac{drag}{q_\infty S}$
C_L	lift coefficient, $\frac{lift}{q_\infty S}$
$C_{L_{\alpha=0}}$	lift coefficient at $\alpha = 0°$
$C_{L_{C_T=0}}$	lift coefficient without jet augmentation
C_{L_Γ}	jet-induced lift coefficient
$\Delta C_{L_{aux}}$	lift-coefficient increment due to auxiliary flap deflection
C_l	rolling-moment coefficient about stability axis, $\frac{rolling\ moment}{q_\infty Sb}$
C_{l_β}	rate of change of rolling-moment coefficient with sideslip
C_m	pitching-moment coefficient about $0.25\bar{c}$, $\frac{pitching\ moment}{q_\infty S\bar{c}}$
C_{m_0}	pitching-moment coefficient at zero lift
C_n	yawing-moment coefficient about stability axis, $\frac{yawing\ moment}{q_\infty Sb}$
C_{n_β}	rate of change of yawing-moment coefficient with sideslip
C_T	engine total gross thrust coefficient, $\frac{F_g}{q_\infty S}$
$C_{T_{net}}$	engine net thrust coefficient, $\frac{T}{q_\infty S}$
C_Y	side-force coefficient about stability axis, $\frac{side\ force}{q_\infty S}$
F_A	static incremental axial force, N (lb)

F_g	gross-thrust with flaps undeflected and $\delta_d = 0°$, N (lb) (obtained statically)
F_N	static incremental normal force due to flap deflection, N (lb)
F_R	resultant force, $\sqrt{F_A{}^2 + F_N{}^2}$, N (lb)
g	acceleration of gravity, 9.81 m/sec^2 (32.2 ft/sec^2)
i_t	horizontal-tail incidence, deg
q_∞	free-stream dynamic pressure, N/m^2 (lb/sq ft)
S	wing area, m^2 (sq ft)
T	gross thrust minus nacelle inlet ram drag
$\frac{T}{W}$	net thrust-to-weight ratio
V_S	1 g stall speed, m/sec (knots)
W	airplane gross weight, N (lb)
y	spanwise distance perpendicular to the plane of symmetry, m (ft)
α	angle of attack of fuselage, deg
β	angle of sideslip
γ	flight-path angle, deg
δ_d	jet exhaust deflector angle, deg (see fig. 2)
δ_e	horizontal-tail elevator deflection, deg
$\delta_{f_{aux}}$	trailing-edge auxiliary flap deflection relative to the main flap, measured normal to the hinge line, deg
δ_{f_m}	trailing-edge main flap deflection relative to the wing chord plane, measured normal to the hinge line, deg
δ_j	effective jet deflection angle obtained statically, $\tan^{-1} \frac{F_N}{F_A}$, deg
δ_s	slat deflection relative to the wing chord plane, measured perpendicular to the leading edge, deg

η wing semispan station, $\frac{y}{b/2}$

η_f flap-system static turning efficiency, $\frac{F_R}{F_g}$

Subscript

u uncorrected

WIND-TUNNEL INVESTIGATION OF A LARGE 35° SWEPT-WING JET TRANSPORT MODEL WITH AN EXTERNAL-FLOW JET-AUGMENTED DOUBLE-SLOTTED FLAP

Kiyoshi Aoyagi and Leo P. Hall

Ames Research Center

SUMMARY

An investigation has been conducted to determine the aerodynamic characteristics of a large-scale subsonic jet transport model with an externally jet-augmented flap system that would augment lift and provide direct-lift control. The model had a 35° swept wing of aspect ratio 7.82 and four pod-mounted engines under the wing. The lift of the flap system was augmented by impingement of the exhaust of the jet engines on the main flap and a small auxiliary flap. The auxiliary flap may be used for providing direct-lift control. Results were obtained for several main and auxiliary flap deflections at gross thrust coefficients of 0 to 2.0. Three-component longitudinal data are presented with the operation of four and two engines. Limited longitudinal and lateral data are presented with the operation of three engines.

Some performance computations were made using the data of the investigation. These calculations predict that the aircraft with one engine inoperative can have a rate of climb of 1.52 m/sec (300 ft/min) at a speed of 44.2 m/sec (86 knots) (1.2 V_S, 1 g flight) for takeoff and a rate of climb of 1.02 m/sec (200 ft/min) for a balked landing condition at an approach speed of 46.8 m/sec (91 knots, 1.3 V_S, 1 g flight) with a thrust-to-weight ratio of 0.375 and a wing loading of 4070 N/m^2 (85 psf). The calculations also predict that the flap system is capable of providing ±0.2 g incremental acceleration normal to the flight path at an approach speed of 41.1 m/sec (80 knots) (1 g flight, wing loading of 85 psf) with a thrust-to-weight ratio of 0.40.

INTRODUCTION

The principle of augmenting lift by directing jet engine exhaust toward the trailing-edge flap surface is currently being considered in some STOL turbofan transport designs. This principle was earlier reported in references 1 through 3. The feasibility of using a small auxiliary flap attached to a main flap for direct lift control has been demonstrated (refs. 4 and 5) with a swept-wing transport model with a flap system externally jet-augmented from two pod-mounted turbojet engines.

As part of continuing NASA STOL research, an investigation was undertaken in the Ames 40- by 80-Foot Wind Tunnel to determine the aerodynamic characteristics of a 35° swept-wing transport model with a flap system externally jet-augmented from four pod-mounted jet engines.

The model was equipped with a double-slotted flap that consisted of a main flap and a short chord auxiliary flap attached to the main flap. Results were obtained with several main and auxiliary flap deflections at gross thrust coefficients from 0 to 2.0. In addition, limited data were obtained with the operation of two and three engines. Some calculations also were made of the flight-path control capabilities of the flap system. The data were obtained at Reynolds numbers from 2.0×10^6 to 2.9×10^6, based on a mean aerodynamic chord of 1.59 m (5.22 ft) and at dynamic pressures of 215 to 479 N/m^2 (4.5 to 10.0 psf).

MODEL AND APPARATUS

Figure 1 is a photograph of the model in the 40- by 80-foot wind tunnel. Pertinent dimensions of the model are given in figure 2(a). The model was equipped with four T-58-6A engines modified to operate as conventional jet engines.

Wing

The basic wing had a quarter chord sweep of 35°, an aspect ratio of 7.82, a dihedral of 6°, and an incidence of 2°. The airfoil section had an NACA 65-012 thickness distribution at the root tapering linearly to an NACA 65-009 thickness distribution at the tip with a 230 mean line at these sections. The mean aerodynamic chord was 1.59 m (5.22 ft).

Leading-Edge Slats

The wing was equipped with full span 0.15c leading-edge slats except for breaks at each side of the nacelle pylons. The slats (fig. 2(b)) were deflected 35° with respect to the wing chord plane from η = 0.11 to 0.48 and 45° from η = 0.50 to 1.0 when the flaps were deflected. For flaps undeflected the slats were deflected 35°. The slats were in the extended position throughout the investigation.

Trailing-Edge Flap System

Flap details- The flap system was composed of a main flap and an auxiliary flap with fixed pivot points as shown in figure 2(c). Both flaps extended from 0.11 to 0.68 semispan with a break at 0.37 semispan and could be deflected 0° to 50° normal to their respective pivot lines. The total flap chord (main plus auxiliary flap chord) was 0.30 of the wing chord, and the auxiliary flap chord was 0.33 of the total flap chord.

Main and auxiliary flap arrangement- When the main flap was deflected, the flap left a 0.01 c gap below the shrouded wing trailing edge (located at 0.80 c), and the flap leading-edge location varied from 0.03 c forward of the 0.80 c line at a deflection of 20° to coincident with the 0.80 c line at a

deflection of 50° (see fig. 2(d)). The auxiliary flap was deflected from a fixed pivot point with a gap at the shrouded main flap trailing edge as shown in figure 2(d). Both flaps were deflected over the full spanwise extent (0.11 to 0.68 η) throughout the investigation.

Fuselage and Tail

The fuselage had a constant 1.22 m (4-ft) diameter except at the nose and tail. The nose section had elliptical outlines with circular cross sections; the tail section had transitions which tapered from a 1.22 m (4-ft) circular section to a small elliptical section at the rear.

The geometry of the horizontal and vertical tails is shown in figure 2(a). The rudder was fixed at 0°, and the horizontal tail incidence and elevator deflection were held at 0° throughout the investigation.

Engines

T-58-6A engines, modified to operate as conventional jet engines, were located at 0.28 and 0.49 of the wing semispan. The engine centerline was pitched 4.5° down to provide a better jet exhaust impingement on the flap surfaces. A 0.28 m (0.91 ft)-diameter ejector, 0.72 m (2.36 ft) long, and a faired leading-edge radius of 0.024 m (0.08 ft) (fig. 2(d)) was located behind the conventional tailpipe of each engine. Its purpose was to stimulate the jet exhaust wake of a turbofan jet engine. The combined ejector and jet exhaust flow provided external jet augmentation on the trailing-edge flap surface. A jet exhaust deflector was located behind the ejector, and was pivoted as shown in figure 2(d). The deflector had a constant chord of 0.36 m (1.17 ft) and a span equal to the ejector diameter. It was pivoted 15° from the engine centerline when the flaps were deflected, and 0° was used when the flaps were undeflected.

TESTING AND PROCEDURE

Tests were conducted at Reynolds numbers from 2.0×10^6 to 2.9×10^6, based on a mean aerodynamic chord of 1.59 m (5.22 ft) and dynamic pressures of 215 to 479 N/m^2 (4.5 and 10.0 psf), respectively. Force and moment measurements were made in most cases through the angle-of-attack range of -4° to 20°.

Tests With Constant C_T and Varying Angle of Attack

A constant C_T value was maintained as angle of attack was varied for each flap configuration tested. With the operation of each engine at equal thrust several nominal C_T values were investigated by varying thrust and/or dynamic pressure as shown below.

C_T (4 Engines)	q_u, N/m^2 (psf)
0	479 (10.0)
.25	479 (10.0)
.50	479 (10.0)
1.0	431 (9.0)
1.4	311 (6.5)
2.0	215 (4.5)

The C_T values were based on the calibration of the engine static thrust variation with engine rpm with both the flaps and jet exhaust deflector at 0°. Main flap deflections (δ_{f_m}) of 20°, 30°, 40°, and 50° were tested with auxiliary flap deflections ($\delta_{f_{aux}}$) of 0°, 20°, 40°, and 50° for each δ_{f_m} except the maximum $\delta_{f_{aux}}$ was 40° for δ_{f_m} = 30°. Tests were run with the plain wing (flaps up) at C_T values of 0, 0.50, and 1.0.

The data obtained with the operation of two inboard engines with symmetrical thrust were limited to main and auxiliary flap deflection of 40° at C_T = 0.26, 0.51, and 1.05.

The data obtained with the operation of three engines at approximately equal thrust (left hand outboard engine inoperative) were limited to main flap deflections of 20° and 40° for auxiliary flap deflection of 20° at C_T = 0.19, 0.39, 0.76, 1.0, and 1.6. These values were approximately 75 percent of those used with four engines. In addition, one asymmetrical auxiliary flap condition (40° (left hand side) and 0° (right hand side)) with main flap deflected 40° was tested at these same thrust coefficient values.

Tests With Constant C_T and Varying Angle of Sideslip

A constant C_T value was maintained at an angle of attack of 4° and 8° as sideslip was varied from 4° to -16°. The C_T values examined were 0, 1.0, and 1.4 (four engines operating) and 0.76 and 1.08 with three engines (outboard left engine inoperative). All tests were run with each engine set at equal thrust. These tests were limited to main flap deflection of 40° and an auxiliary flap deflection of 20°.

CORRECTIONS

The data were corrected for strut tares and wind-tunnel wall effects. The tunnel-wall corrections were as follows:

$$\alpha = \alpha_u + 0.375C_L$$

$$C_D = C_{D_u} + 0.0065C_L{}^2$$

$$C_m = C_{m_u} + 0.0122C_L$$

RESULTS AND DISCUSSION

The basic force data obtained from this investigation are presented in figures 3 through 21. An index to these basic data is given in table 1. Gross thrust coefficient was used as a parameter since the total exit momentum of the jet affects the augmentation of the flap lift. The relationship between gross thrust and net thrust coefficients is shown in figure 3. Parts of the basic data were used to estimate flight-path control characteristics during takeoff and descent with auxiliary flap. These results are presented in figures 22 through 33.

Longitudinal Characteristics of the Model With Plain Wing

The longitudinal characteristics of the model with and without power is shown in figure 4. The effect of four engines with $C_T = 1.0$ was to increase lift-curve slope 31 percent and $C_{L_{max}}$ by 27 percent. Approximately half of this increase was thrust and the remainder was jet-induced effect. Lift coefficient values for angles of attack below 5° were less with power on than with power off, indicating that a negative pressure field is induced on the underside of the wing by the adjacent jet flow with 4.5° engine tilt. The static margin obtained with power on was essentially the same as that obtained with power off. However, a positive C_{m_o} shift occurred with increasing power.

Longitudinal Characteristics of the Model With Flap Deflection and Four Engines Operating

Effect of variable angle of attack- The longitudinal characteristics of the model with main flap deflection of 20°, 30°, 40°, and 50° at several auxiliary flap deflections are shown in figures 5, 6, 7, and 8, respectively. These figures show that jet augmentation (C_T values) and auxiliary flap deflection increased the lift coefficient but did not significantly affect the slope of the linear portion of the lift curve. In addition the upper limit of the region of constant lift-curve slope was extended from an angle of attack of 4° to 10° when C_T value increased from 0.25 to 1.0. Figure 9 shows the variation of trimmed $C_{L_{max}}$ with auxiliary flap deflection at several main flap deflections. This figure shows that maximum trimmed lift coefficient increased with jet augmentation and with auxiliary flap deflection up to 40° for all main flap deflections investigated. A maximum trimmed C_L of 5.25 was obtained at $\delta_{f_m} = 50°$ and $\delta_{f_{aux}} = 40°$ with a C_T value of 2.0. Note that for a constant auxiliary flap deflection the angle of attack at maximum lift did not significantly increase with jet augmentation.

Neither jet augmentation nor auxiliary flap deflection affected the longitudinal stability of the model below the stall angle but both did produce large nose-down pitching moments (see figs. 5 through 8). Static margin was reduced with jet augmentation compared to that without jet augmentation. For example, at $\delta_{f_m} = 40°$ and $\delta_{f_{aux}} = 20°$ there was approximately a 45 percent reduction between $C_T = 0$ and 2.0.

Analysis of lift with jet augmentation at 0° angle of attack- The total lift for a given flap chord and deflection is the sum of the lift without jet augmentation, effective jet reaction $[\sin(\delta_j + \alpha)\eta_f C_T]$, and jet induced lift. The lift component due to jet augmentation is therefore dependent on the effectiveness of the flap system in turning the jet. Figure 10 shows the variation of static jet turning angle and turning efficiency with auxiliary flap deflection, $\delta_{f_{aux}}$. With $\delta_{f_{aux}} = 0°$ the effective jet turning angle was always less than the geometric main flap deflection δ_{f_m}, ranging from 73 percent of $\delta_{f_m} = 20°$ to 82 percent of $\delta_{f_m} = 50°$. With $\delta_{f_{aux}} = 50°$ the effective jet turning angle δ_j increased an additional 30° for $\delta_{f_m} = 20°$, 30°, and 40° and 26° for $\delta_{f_m} = 50°$. The static resultant force due to the jet decreased with increasing main and auxiliary flap deflections because of the turning losses (shown in fig. 10(b)). Static jet turning efficiency ranged from 79 percent to 70 percent at $\delta_{f_{aux}} = 0°$ and from 62 percent to 46 percent at $\delta_{f_{aux}} = 50°$ for $\delta_{f_m} = 20°$ and 50°, respectively.

The lift components at $\delta_{f_m} = 20°$ and 50° for $\alpha = 0°$ and several auxiliary flap deflections are shown in figure 11. The jet-induced lift is based on the effective jet turning angle and turning efficiency shown in figure 10. Figures 11(a) and (b) show that the jet-induced lift (C_{L_T}) becomes larger as C_T increases. For example, at $C_T = 2.0$ and $\delta_{f_{aux}} = 40°$ this lift component accounted for as much as 54 percent of the total lift ($\delta_{f_m} = 50°$).

Longitudinal Characteristics of the Model With Flap Deflection and Two Engines Operating

Figure 12 shows the longitudinal characteristics of the model with the main and auxiliary flaps deflected 40° and only the inboard engines operating at equal thrust. Figure 13 compares two inboard engines with four engines for trimmed lift, drag, and pitching-moment coefficients. Note that trimmed lift and drag coefficients were essentially the same for both configurations (see also refs. 1 and 6) while nose-down pitching-moment coefficient values with only the inboard engines operating were approximately 50 percent of the values for four engines. This result suggests that a four-engine jet transport with two side-by-side engines located close to the fuselage may reduce longitudinal trim requirements as well as improve lateral and directional control with asymmetric thrust.

Longitudinal and Lateral Characteristics of the Model With Asymmetric Thrust

The longitudinal and lateral characteristics of the model with left outboard engine out are limited to an auxiliary flap deflection of 20° and main flap deflections of 20° and 40° (figs. 14 and 15, respectively). Longitudinal characteristics are not significantly affected by the loss of one engine. Figure 16 shows a comparison of data for three and four engines. These data show that lift and drag coefficients were essentially unchanged for the same total C_T. Pitching-moment coefficients were approximately 20 to 25 percent less negative at $C_T = 1.6$ than those obtained with four engines.

Rolling- and yawing-moment coefficient increased negatively with C_T.

The variation of rolling- and yawing-moment coefficient with sideslip is shown in figure 17 with the operation of three and four engines at $\delta_{f_m} = 40°$ and $\delta_{f_{aux}} = 20°$. In each case the dihedral effect is larger with jet augmentation ($C_T > 0$), but rolling-moment coefficients were more negative with one engine out because of the lift loss on the left side. The model was directionally stable for the sideslip range (4° to -16°) investigated, and C_{n_β} remained the same with or without jet augmentation. The variation of the ratio C_{l_β}/C_{n_β}, an important handling quality parameter, with jet augmentation was greater with three engines than with four engines as shown in figure 18. At $C_T = 1.0$, the value of C_{l_β}/C_{n_β} was 1.4 times greater than that with four engines and two times greater than that with $C_T = 0$.

Effect of asymmetric auxiliary flap deflection- Figure 19 shows the longitudinal and lateral characteristics of the model with asymmetric auxiliary flap deflection and with one engine out. Figure 20 shows the effectiveness of differential auxiliary flap deflection for roll control under these conditions. Nearly trimmed roll was attained over the range of C_T values investigated. The use of differential flap deflection, however, increased yawing-moment coefficient approximately 60 percent.

Comparison of Flap Lift Increment With Theory

Theoretical jet-flap-induced lift increments were calculated assuming that the jet efflux spreads over the entire span of the flap. The measured effective jet angle and resulting force were used with the method of reference 7 to calculate the theoretical curves shown in figure 21. At $\delta_{f_m} = 20°$, good agreement was obtained between measured and theoretical values with $\delta_{f_{aux}} = 0°$ and 20°, but poor agreement was obtained with $\delta_{f_{aux}} = 40°$. At $\delta_{f_m} = 50°$, poor agreement was obtained with $\delta_{f_{aux}} = 0°$, 20°, and 40°. The values measured at $C_T = 0$ were always less than the theoretical values. This suggests that some jet exhaust flow is required to attach the local airflow over the flap.

Estimated Flight-Path Control Characteristics Using Auxiliary Flap During Takeoff and Descent

Figures 22 through 25 show the longitudinal characteristics of the model at T/W = 0.40 and 0.50 (four engines operating) and 0.30 and 0.375 (representing three engines operating). These curves were obtained by interpolation of the data in figures 5 through 8 with four engines operating. The data with three engines operating were obtained from these figures since the effect of one engine out on the longitudinal characteristics was small for the same thrust as shown in figure 16. In the following analysis it is assumed that the aircraft can be trimmed with one engine out and the three remaining engines at full power.

Takeoff- Figure 26 shows the variation of the steady-state flight path angle[1] with auxiliary flap deflection at 1.2 V_S (1 g flight) for main flap deflections of 20° and 30°. At either main flap deflection, variable auxiliary flap deflection provides a wide range of flight path climb angles with an outboard engine inoperative (T/W = 0.3 and 0.375). However, at T/W = 0.30 and δ_{f_m} = 30° the auxiliary flap did not provide a wide range of positive climb angles. Maximum climb angles of 3.7° and 6.1° are attainable at T/W = 0.30 and 0.375, respectively, with δ_{f_m} = 20°. As expected, four engines provided a greater climb angle range than did three engines for both main-flap deflections (maximum γ attained is 12°, T/W = 0.50, δ_{f_m} = 20°, $\delta_{f_{aux}}$ = 0°). The variation of forward speed with auxiliary flap deflection is presented in figure 27 for the flight path angles in figure 26. The forward speeds (1.2 V_S) needed to maintain either a rate of climb of 1.52 m/sec (300 ft/min) or a steady gradient of 3 percent[2] (1.7°) are given in figure 27 for W/S = 3352, 4070, and 4788 N/m^2 (70, 85, and 100 psf). Results that meet the climbout requirement are presented below. The table shows that the requirement is met with either main-flap

δ_{f_m}, deg	T/W	W/S = 3352 N/m^2 (70 psf)		W/S = 4070 N/m^2 (85 psf)		W/S = 4788 N/m^2 (100 psf)	
		γ, deg	1.2 V_S, m/sec (knots)	γ, deg	1.2 V_S, m/sec (knots)	γ, deg	1.2 V_S, m/sec (knots)
20	0.30	2.0	44.5 (86.5)	1.85	48.8 (94.9)	1.7	52.9 (102.9)
	.375	2.25	40.3 (78.4)	2.00	44.0 (85.7)	1.8	47.7 (92.8)
30	.30	---	---	1.7	51.0 (99.2)	1.7	55.4 (107.7)
	.375	2.1	41.0 (79.8)	1.95	45.1 (87.7)	1.8	48.8 (95.0)

[1]Flight-path angle was computed as follows (see figs. 22-25):

$$\sin \gamma = T/W - D/W + [(dv/dt)/g]$$

Assume steady 1 g flight (dv/dt = 0)

$$\sin \gamma = C_D/C_L \qquad C_L q_\infty S = W \qquad C_D q_\infty S = T - D$$

[2]This climbout requirement is based on the tentative Federal Air Regulations of reference 8 for climb with landing gear retracted and one critical engine inoperative.

deflection except at T/W = 0.30, W/S = 3352 N/m^2 (70 psf), and δ_{f_m} = 30°. A main-flap deflection of 20° is the better take-off flap setting because the requirement is met at lower speed.

Landing- Figure 28 shows the variation of the flight path angle with auxiliary flap deflection at 1.3 V_S (steady 1 g flight) for main flap deflections of 30°, 40°, and 50°. Positive climb angle using auxiliary flap deflection with one outboard engine inoperative is available only at δ_{f_m} = 30° (T/W = 0.30 and 0.375) and δ_{f_m} = 40° (T/W = 0.375). With T/W = 0.375 maximum climb angles of 6.8° and 2.2° are attained at δ_{f_m} = 30° and 40°, respectively. With all engines operative, positive climb angles are attained at any of the three main-flap deflections. The variation of approach speed with auxiliary flap deflection is presented in figure 29 at the flight path angles shown in figure 28. The forward speeds needed for 1 g flight to maintain a rate of climb of 1.02 m/sec (200 ft/min) with one engine inoperative during a balked landing approach are indicated by tick marks in the figure and are tabulated below. This landing requirement is again based on the tentative

δ_{f_m}, deg	T/W	W/S = 2633 N/m^2 (55 psf)		W/S = 3352 N/m^2 (70 psf)		W/S = 4070 N/m^2 (85 psf)	
		γ, deg	1.3 V_S, m/sec (knots)	γ, deg	1.3 V_S, m/sec (knots)	γ, deg	1.3 V_S, m/sec (knots)
30	0.30	1.35	43.5 (84.7)	1.2	48.9 (95.1)	1.1	53.6 (104.4)
30	.375	1.55	38.3 (74.5)	1.35	43.1 (83.8)	1.25	47.5 (92.4)
40	.375	1.55	37.7 (73.4)	1.4	42.6 (82.9)	1.3	46.6 (90.6)

regulations of reference 8. At T/W = 0.30, the requirement is met only for a main flap deflection of 30°. Although main-flap deflections of both 30° and 40° meet the requirement at T/W = 0.375, a flap deflection of 40° is a better landing flap setting because of the lower approach speed and greater descent angle range available during descent (fig. 28).

Figure 30 show the variation of flight path angle with auxiliary flap deflection at 1.2 V_S for main flap deflections of 30° and 40°. A substantial positive climb angle range (fig. 30) with an engine inoperative is available using a main flap deflection of 30° at T/W = 0.30 and 0.375. The forward speeds needed to satisfy the climbout requirement are shown in figure 31.

The investigation of reference 9 shows that the use of a rapidly responding auxiliary flap can provide not only flight path angle change but can also provide a more rapid build-up in normal acceleration than elevator control. The maximum pull-up incremental accelerations for the model investigated are presented in figure 32 at forward speeds of 1.2 V_S and 1.3 V_S. This figure shows that 0.3 g is available for the 1.3 V_S approach and 0.2 g for the 1.2 V_S approach. Figure 33 shows the calculated incremental normal acceleration available based on trimmed level flight at 20° auxiliary flap deflection, the midpoint of the useful $\delta_{f_{aux}}$ range as shown in figures 23, 24, and 25.

The angle of attack and $C_{L_{trim}}$ values for trimmed flight ($a_n = 0$) are tabulated below for the approach speed 1.3 V_S. Flight studies (refs. 10 and 11)

T/W = 0.30					T/W = 0.40			
δ_{f_m}, deg	α, deg	$C_{L_{trim}}$	W/S = 4070 N/m^2 (85 psf) approach speed 1.3 V_S, m/sec (knots)	γ, deg	α, deg	$C_{L_{trim}}$	W/S = 4070 N/m^2 (85 psf) approach speed 1.3 V_S, m/sec (knots)	γ, deg
30	7.5	2.53	51.2 (99.6)	-1.7	5.5	2.53	51.2 (99.6)	3.2
40	6.8	2.96	47.3 (92.0)	-1.9	4.0	2.96	47.3 (92.0)	1.0
50	4.5	3.11	46.2 (89.8)	-6.1	1.4	3.11	46.2 (89.8)	-3.9

have indicated that 0.2 g is a reasonable margin for maneuvering during the landing approach. This criterion is met when the main flap is deflected 30° or 40° at T/W = 0.40. With the main flap deflected 50°, a_n values ranged from -0.22 to 0.12 g at T/W = 0.30 and -0.27 to 0.13 g at T/W = 0.40.

SUMMARY OF RESULTS

An investigation of a large scale externally jet-augmented double-slotted flap transport model has been conducted to determine the aerodynamic characteristics of the model. Significant results of the investigation are summarized below.

Jet exhaust impingement on the trailing-edge flap surfaces with $C_T = 2.0$ increased maximum lift by as much as 3.5 times the maximum lift at $C_T = 0$. An auxiliary flap provided a method of direct-lift control and had a useful range of 40°.

For a given C_T the operation of two inboard engines with symmetrical thrust resulted in essentially the same lift and drag coefficient values as those obtained with four engines, but 50 percent reduction of pitching-moment coefficient values also resulted.

Good agreement was obtained between measured lift with flap deflection and jet flap theory (ref. 7) at the low flap deflection $\delta_{f_m} = 20°$ but not at the higher flap deflection $\delta_{f_m} = 50°$.

Performance computations indicate that an aircraft based on the test configuration could meet tentative Federal Air Regulations for climb during takeoff or balked landing with one engine inoperative and landing gear retracted. For the take-off condition a main-flap deflection of 20° with auxiliary flap deflected can provide a rate of climb of 1.52 m/sec (300 ft/min) at approximately 44.2 m/sec (86 knots) with one outboard engine inoperative. For a balked landing condition a main-flap deflection of 40° with auxiliary

flap deflected can provide a rate of climb of 1.02 m/sec (200 ft/min) at approximately 46.8 m/sec (91 knots). The auxiliary flap could also provide a normal acceleration response of ±0.2 g at an approach speed of 47.3 m/sec (92.0 knots) with $\delta_{f_m} = 40°$.

Ames Research Center
National Aeronautics and Space Administration
Moffett Field, Calif., 94035, April 16, 1971

REFERENCES

1. Campbell, John P.; and Johnson, Joseph L., Jr.: Wind-Tunnel Investigation of an External-Flow Jet-Augmented Slotted Flap Suitable for Application to Airplanes With Pod-Mounted Jet Engines. NACA TN 3898, 1956.

2. Lowry, John G.; Riebe, John M.; and Campbell, John P.: The Jet-Augmented Flap. Preprint 715, Inst. Aeron. Sci., Jan. 1957.

3. Johnson, Joseph L., Jr.: Wind-Tunnel Investigation of the Static Longitudinal Stability and Trim Characteristics of a Sweptback-Wing Jet-Transport Model Equipped With an External-Flow Jet-Augmented Flap. NACA TN 4177, 1958.

4. Kirk, Jerry V.; Hickey, David H.; and Aoyagi, Kiyoshi: Large-Scale Wind Tunnel Investigation of a Model With an External Jet-Augmented Flap. NASA TN D-4278, 1967.

5. Aoyagi, Kiyoshi, Dickinson, Stanley O.; and Soderman, Paul T.: Investigation of a 0.3-Scale Jet-Transport Model Having a Jet-Augmented Boundary-Layer-Control Flap With Direct-Lift Control Capability. NASA TN D-5129, 1969.

6. Parlett, Lysle P.; Fink, Marvin P.; and Freeman, Delma C., Jr.: Wind-Tunnel Investigation of a Large Jet Transport Model Equipped With an External-Flow Jet Flap. NASA TN D-4928, 1968.

7. Williams, J.; Butler, S. F. J.; and Wood, M. N.: The Aerodynamics of Jet Flaps. Rep. no. Aero. 2646, British RAE, 1961.

8. Anon.: Tentative Airworthiness Standards for Verticraft/Powered Lift Transport Category Aircraft. Dept. of Transportation, Federal Aviation Administration, Flight Standards Service, July 1968.

9. Rolls, Stewart L.; Cook, Anthony M.; and Innis, Robert C.: Flight-Determined Aerodynamic Properties of a Jet-Augmented, Auxiliary-Flap, Direct-Lift Control System Including Correlation With Wind-Tunnel Results. NASA TN D-5128, 1969.

10. Drinkwater, Fred J., III: Operational Technique for Transition of Several Types of V/STOL Aircraft. NASA TN D-774, 1961.

11. Staff of the Langley Research Center: Determination of Flight Characteristics of Supersonic Transport During the Landing Approach With a Large Jet Transport in-Flight Simulator. NASA TN D-3971, 1967.

TABLE 1.- LIST OF BASIC DATA FIGURES

Figure	δ_{f_m}, deg	$\delta_{f_{aux}}$, deg	C_T	Number of engines	α_u, deg	δ_d, deg	β, deg	Remarks
4	0	0	0 .53 1.00	4	-4 to 24	0	0	Longitudinal characteristics of model with plain wing
5(a)	20	0	0 .25 .52 1.01 1.40 2.00		-4 to 26 -4 to 26 -4 to 24 -4 to 24 -4 to 22 -4 to 24	15		Longitudinal characteristics of model with auxiliary flap deflection
5(b)		20	0 .26 .51 1.01 1.38 1.95		-4 to 18 -4 to 20 -4 to 20 -4 to 18			
5(c)		40	0 .25 .50 1.01 1.38 2.08					
5(d)		50	.52 1.02 1.38 2.06		-4 to 16 -4 to 22 -4 to 20 -4 to 20			
6(a)	30	0	0 .25 .52 1.01 1.40 2.10		0 to 24 -4 to 22 -4 to 24 -4 to 24			
6(b)		20	0 .25 .50 1.03 1.41 2.01		-4 to 18 -4 to 20			
6(c)		40	0 .25 .50 .99 1.37 2.01		-4 to 18 -4 to 20 -4 to 20			
7(a)	40	0	0 .28 .59 1.06 1.51 2.17		-4 to 18 -4 to 20			
7(b)		20	0 .27 .52 1.01 1.42 1.98		-4 to 18			
7(c)		30	.27 .54 1.02 1.45					
7(d)		40	0 .26 .52 1.01 1.44 2.09		0 to 20 -4 to 16 -4 to 18 -4 to 18 -4 to 16 -4 to 16			
7(e)		50	0 .27 .51 1.03 1.47 2.06		0 to 16 -4 to 18			
8(a)	50	0	0 .27 .52 1.00 1.42 2.04		-4 to 18 -4 to 16 -4 to 18			
8(b)		20	0 .26 .51 1.00 1.41 2.01		0 to 16 -4 to 16 -4 to 18 -4 to 16			
8(c)		40	0 .30 .57 1.04 1.41 2.04		-4 to 18 -4 to 18 -4 to 16			
8(d)		50	0 .26 .53 1.03 1.42 2.12		-4 to 20 -4 to 16			Longitudinal characteristics of model with flap deflections

TABLE 1.- LIST OF BASIC DATA FIGURES - Concluded.

Figure	δ_{f_m}, deg	$\delta_{f_{aux}}$, deg	C_T	Number of engines	α_u, deg	δ_d, deg	β, deg	Remarks
9	20 30 40 50	0 to 50	0, 1.0, 2.0	4	- - -	15	0	Trimmed $C_{L_{max}}$ variation with auxiliary flap deflection
10	20 30 40 50	0, 20, 50 20, 40 0, 30, 40 0, 20, 40, 50	- - -		0			Static jet deflection and turning efficiency with auxiliary flap deflection
11	20, 50	0, 20, 40, 50	0 to 2.0					Lift components due to direct jet reaction, induced effect of jet, and no jet augmentation
12	40	40	0.26 .51 1.05	2	-4 to 14 -4 to 18 -4 to 16			Longitudinal characteristics of model with two inboard engines operating
13			0 to 1.05	4 & 2	0			Comparison of C_L, C_D, and C_m between operation of two inboard engines and four engines
14(a)	20	20	0.19 .39 .76 1.05 1.57	3 (left hand outboard engine off)	-4 to 22			Asymmetric thrust effect on longitudinal characteristics of model
14(b)			.19 .39 .76 1.05 1.57					Asymmetric thrust effect on lateral characteristics of model
15(a)	40		.19 .39 .77 1.05 1.60		-4 to 20 -4 to 20 -4 to 18 -4 to 20			Asymmetric thrust effect on longitudinal characteristics of model
15(b)			.19 .39 .77 1.05 1.60		-4 to 18 -4 to 20 -4 to 20			Asymmetric thrust effect on lateral characteristics of model
16(a)	20	20	0 to 2.0	3 & 4	0			Comparison of longitudinal characteristics of the model between operation of three and four engines
16(b)	40							
17(a)			1.10, 1.00, 0	4	4 & 8		-16 to 4	Effect of sideslip
17(b)			1.08, 0.76	3				
18			0 to 1.5	3 & 4				Variation of C_{y_β}/C_{n_β} with three and four engines operating
19(a)		40 (left) 0 (right)	0.19 .37 .75 1.05 1.50	3 (left hand outboard engine (off)	-4 to 20 -4 to 20 -4 to 18 -4 to 20		0	Asymmetric auxiliary flap deflection effect on longitudinal characteristics of model
19(b)	40	40 (left) 0 (right)	.19 .37 .75 1.05 1.50		-4 to 18 -4 to 20 -4 to 20			Asymmetric auxiliary flap deflection effect on lateral characteristics of model
20		20 (left and right hand side)	0 to 1.60		0			Comparison of rolling and yawing moment coefficients between symmetric and asymmetric auxiliary flap deflection
		40 (left) and 0 (right)	0 to 1.18					

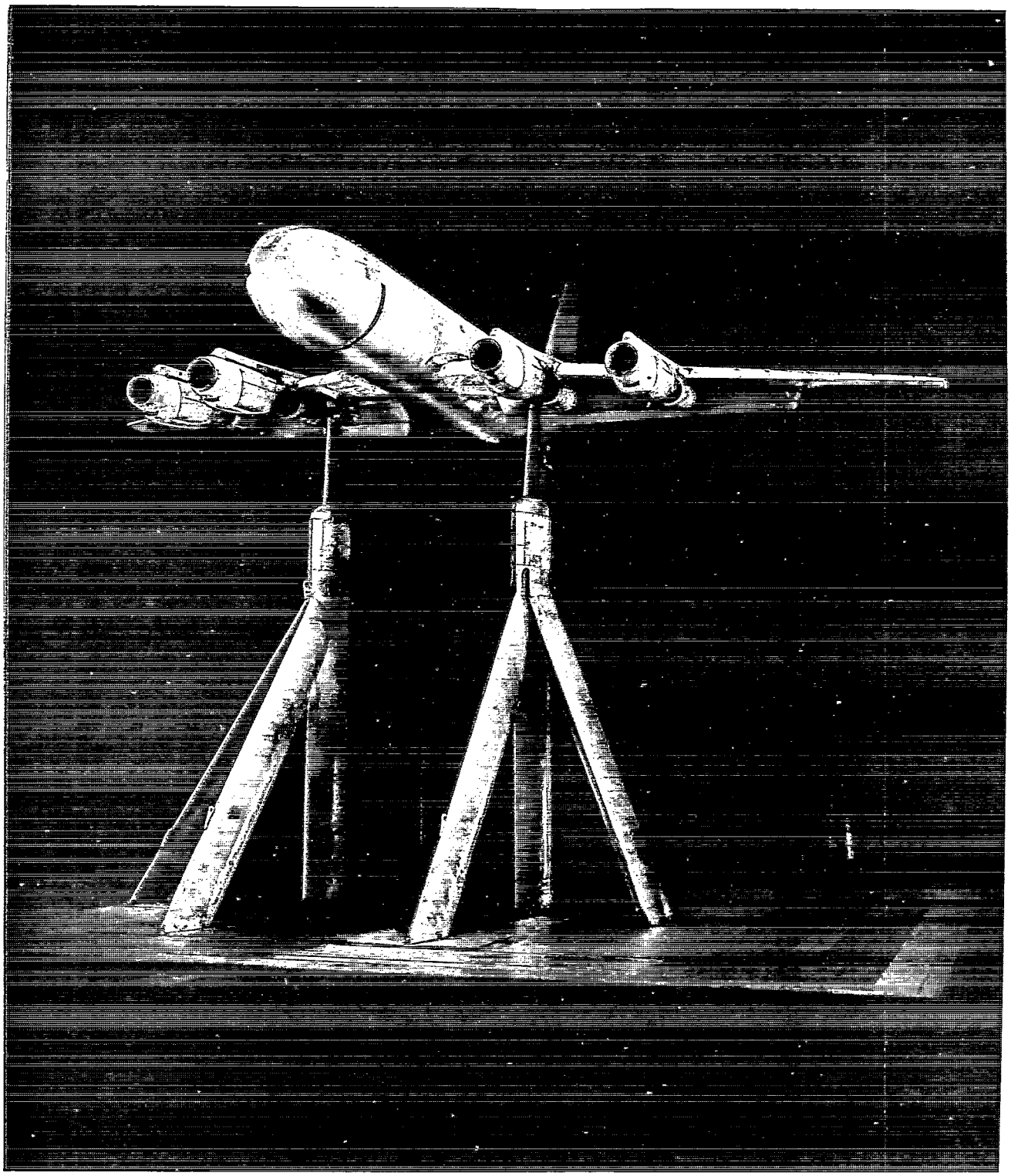

Figure 1.- Photograph of the model as mounted in the Ames 40- by 80-Foot Wind Tunnel.

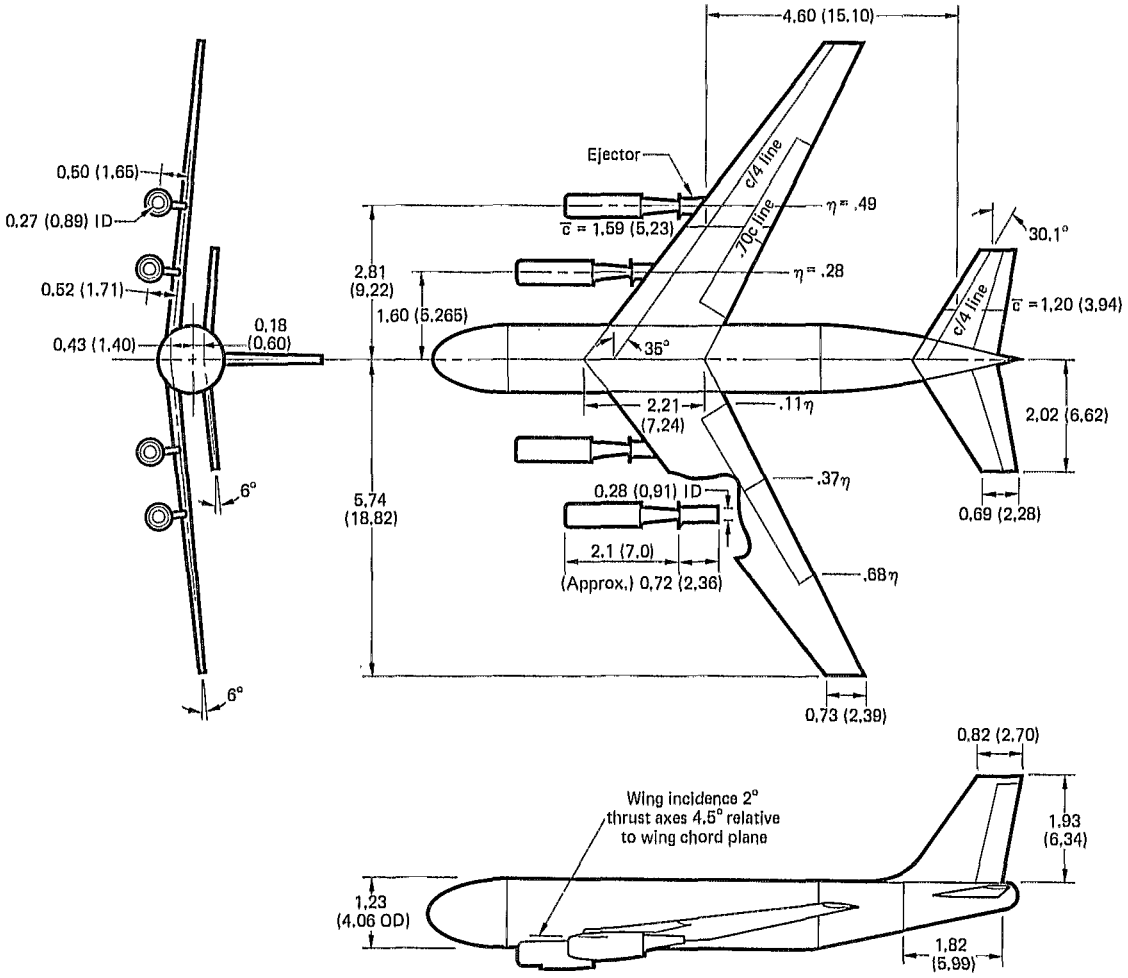

	Wing	Horizontal Tail	Vertical Tail
Aspect ratio	7.82	3.56	1.46
Tip chord/root chord	0.33	0.44	0.45
Area m^2 (ft^2)	16.85 (181.24)	4.64 (50.0)	2.55 (27.5)
Airfoil section	See note 2	66-010	0009

Note:

1. All dimensions in meters (feet) except as noted.
2. Basic wing t/c = 0.12 (root) & 0.09 (tip), 65 airfoil thickness distribution with 230 mean line.

(a) General arrangement of the model.

Figure 2.- Geometric details of the model.

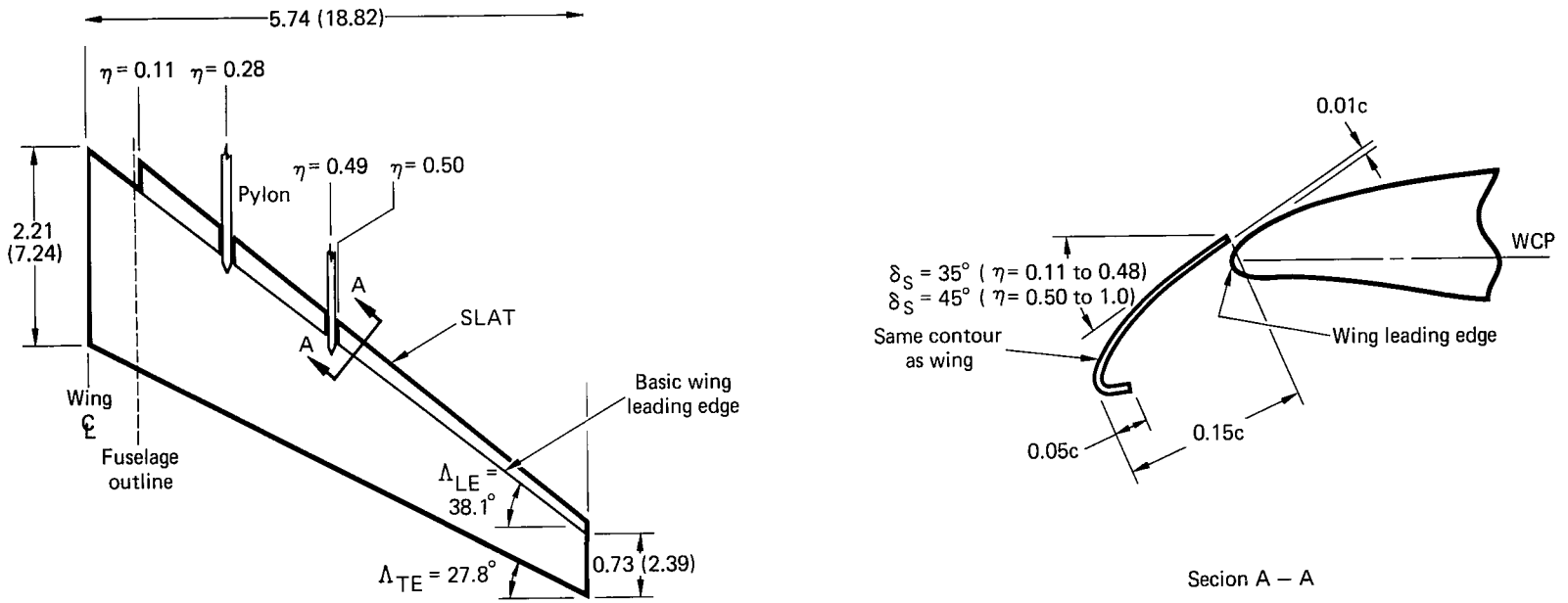

Note: All dimensions in meters (feet) unless otherwise noted.

(b) Leading-edge slat.

Figure 2.- Continued.

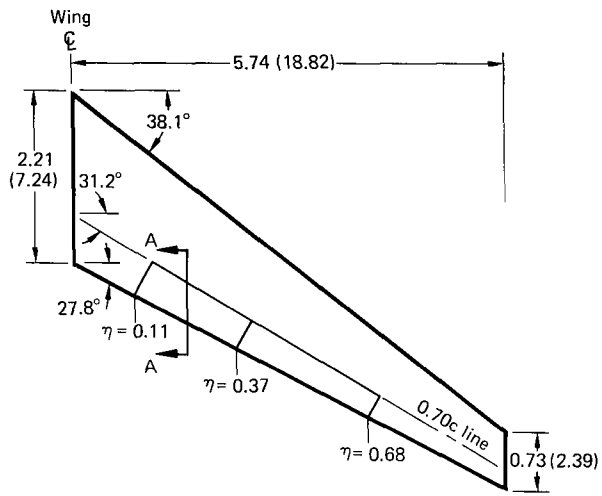

STREAMWISE DIRECTION					
MAIN FLAP ORDINATES			AUXILIARY FLAP ORDINATES		
x, %c	y_U, %c	y_L, %c	x, %c	y'_U, %c	y'_L, %c
0	-1.274	-1.274	20.000	-0.348	-0.348
0.448	-0.314	-2.018	20.274	0.049	-0.679
0.814	0.041	-2.166	20.502	0.251	-0.743
1.543	0.603	-2.420	20.731	0.396	-0.792
2.269	1.023	-2.550	21.416	0.686	-0.823
3.003	1.377	-2.548	21.872	0.799	-0.807
4.448	1.902	—	22.328	0.871	—
5.888	2.252	-2.342	22.783	0.903	—
7.333	2.519	-2.207	23.238	0.902	-0.700
8.755	2.564	—	23.692	0.853	—
10.181	2.511	—	26.308	0.500	-0.410
11.612	2.392	-1.764	30.000	0.058	-0.062
16.902	—	-1.250			
17.547	1.685	—			
17.823	—	-0.997			
18.743	—	-0.502			
19.660	—	0.073			
19.962	1.375	—			
20.585	—	0.501			
21.498	—	0.856			
22.410	1.097	0.968			

Note: All dimensions in meters (feet) except as noted.

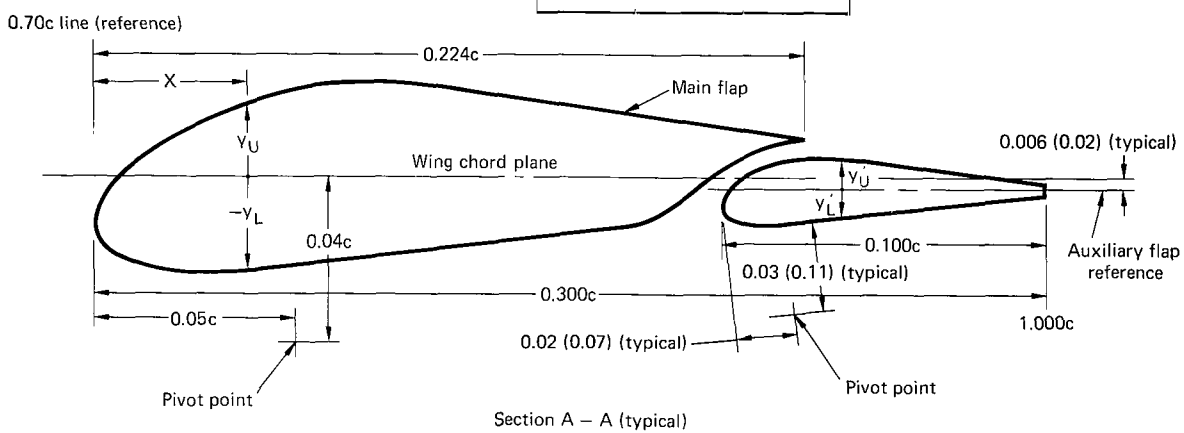

(c) Trailing-edge flap detail.

Figure 2.- Continued.

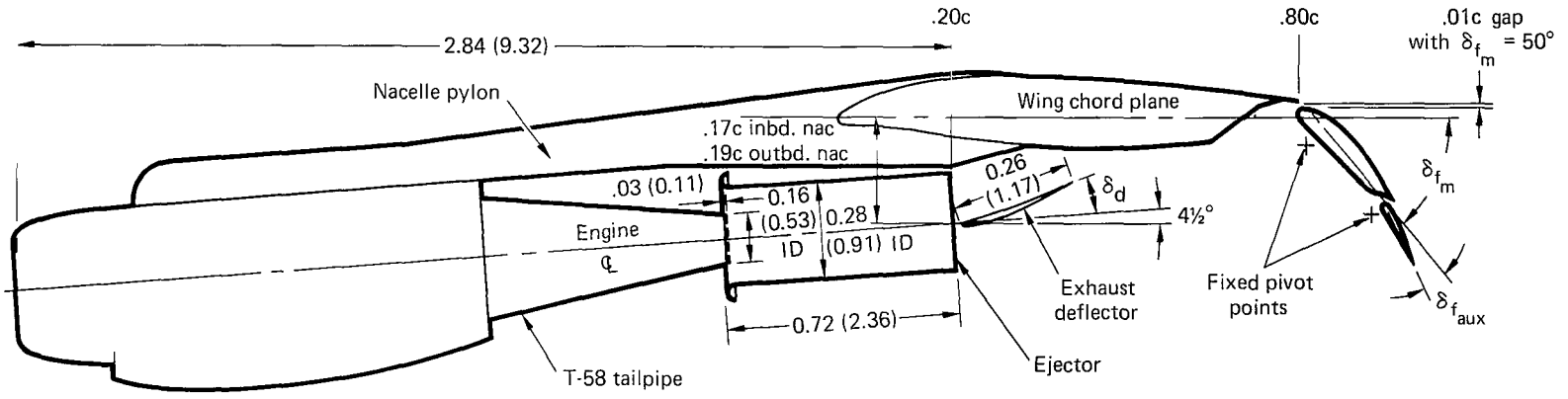

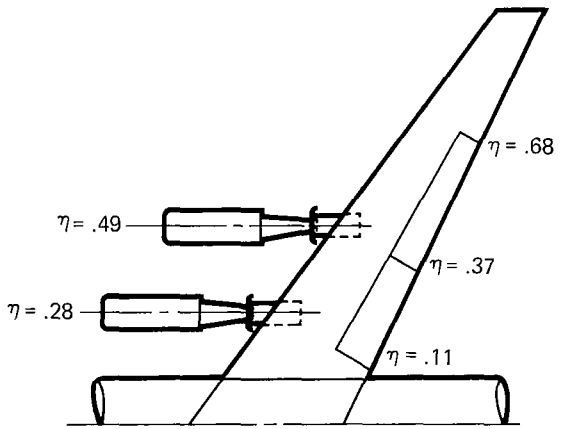

Notes:
1. All dimensions in meters (feet) except as noted
2. "c" - local wing chord

(d) Jet-augmented flap arrangement.

Figure 2.- Concluded.

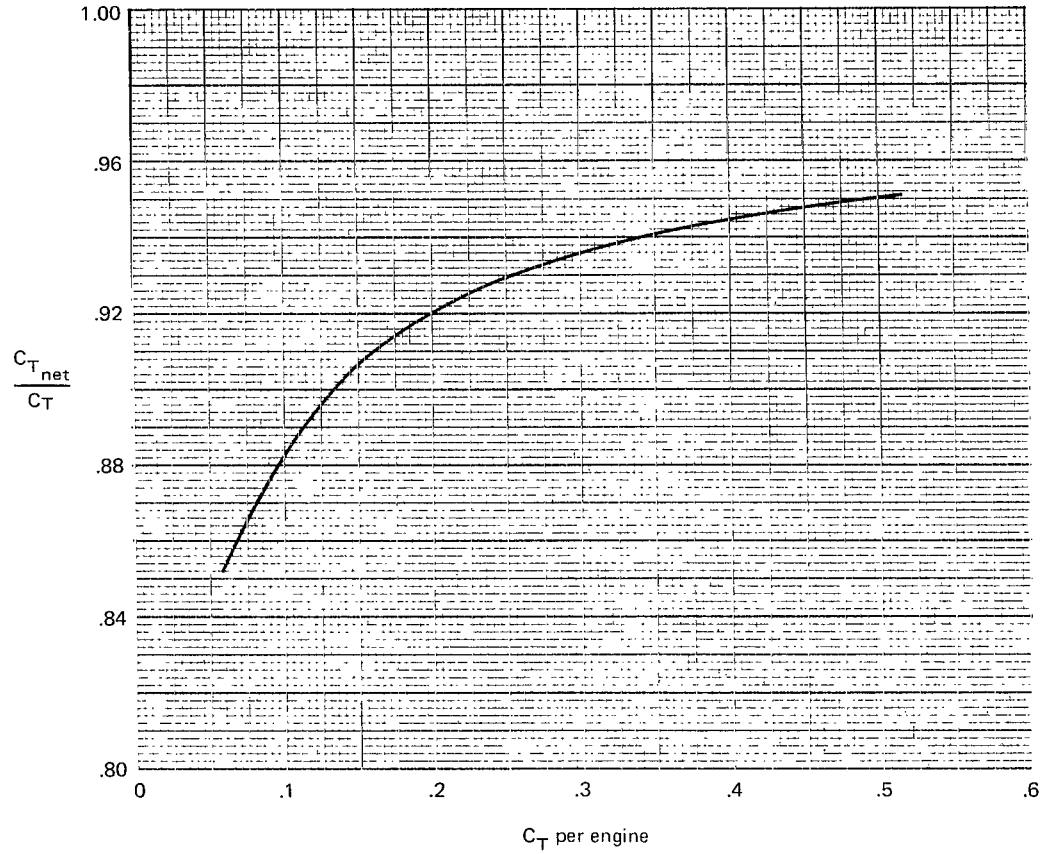

Figure 3.- Relationships between C_T and $C_{T_{net}}$ for engines of present investigation.

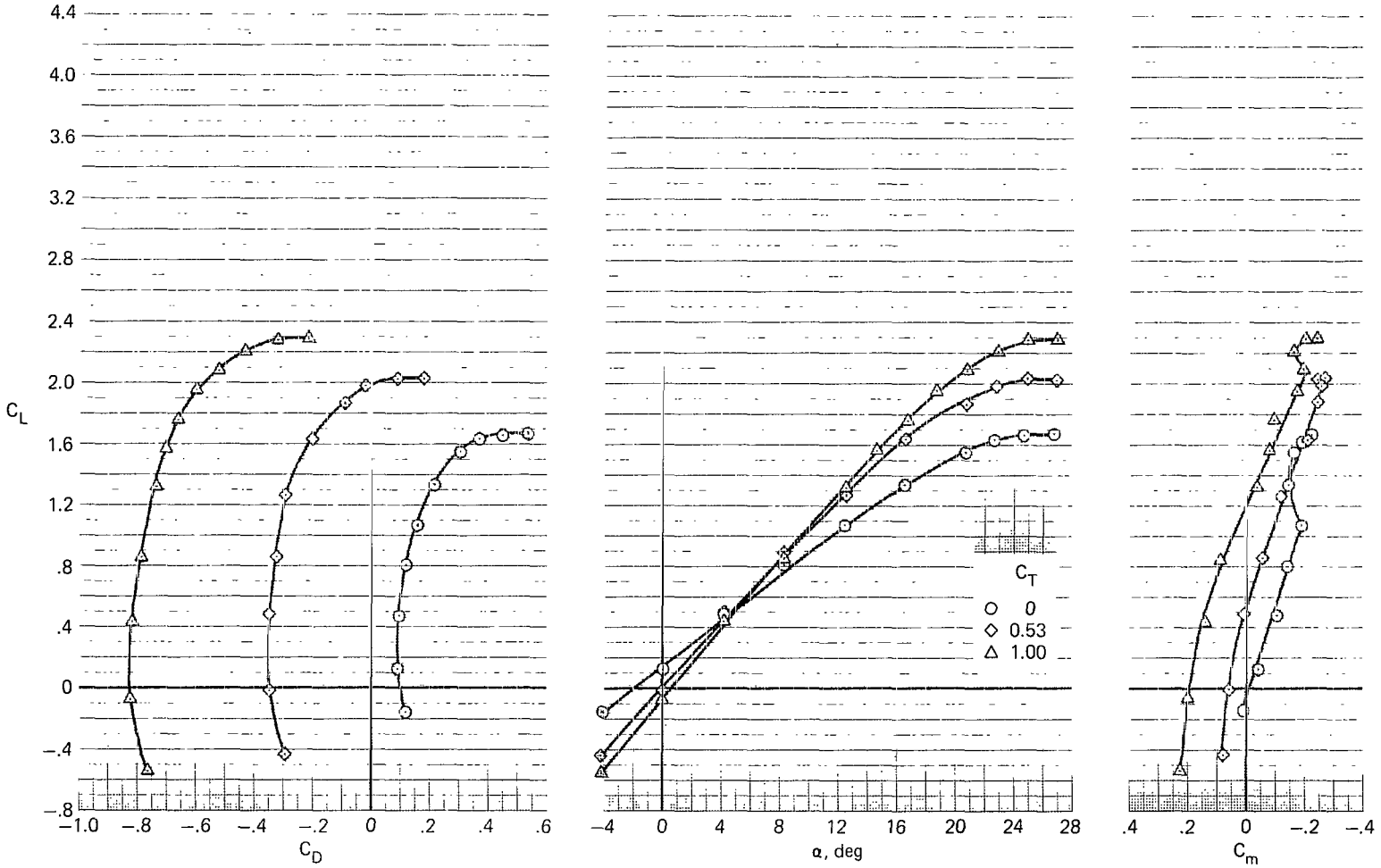

Figure 4.- Longitudinal characteristics of the model with plain wing.

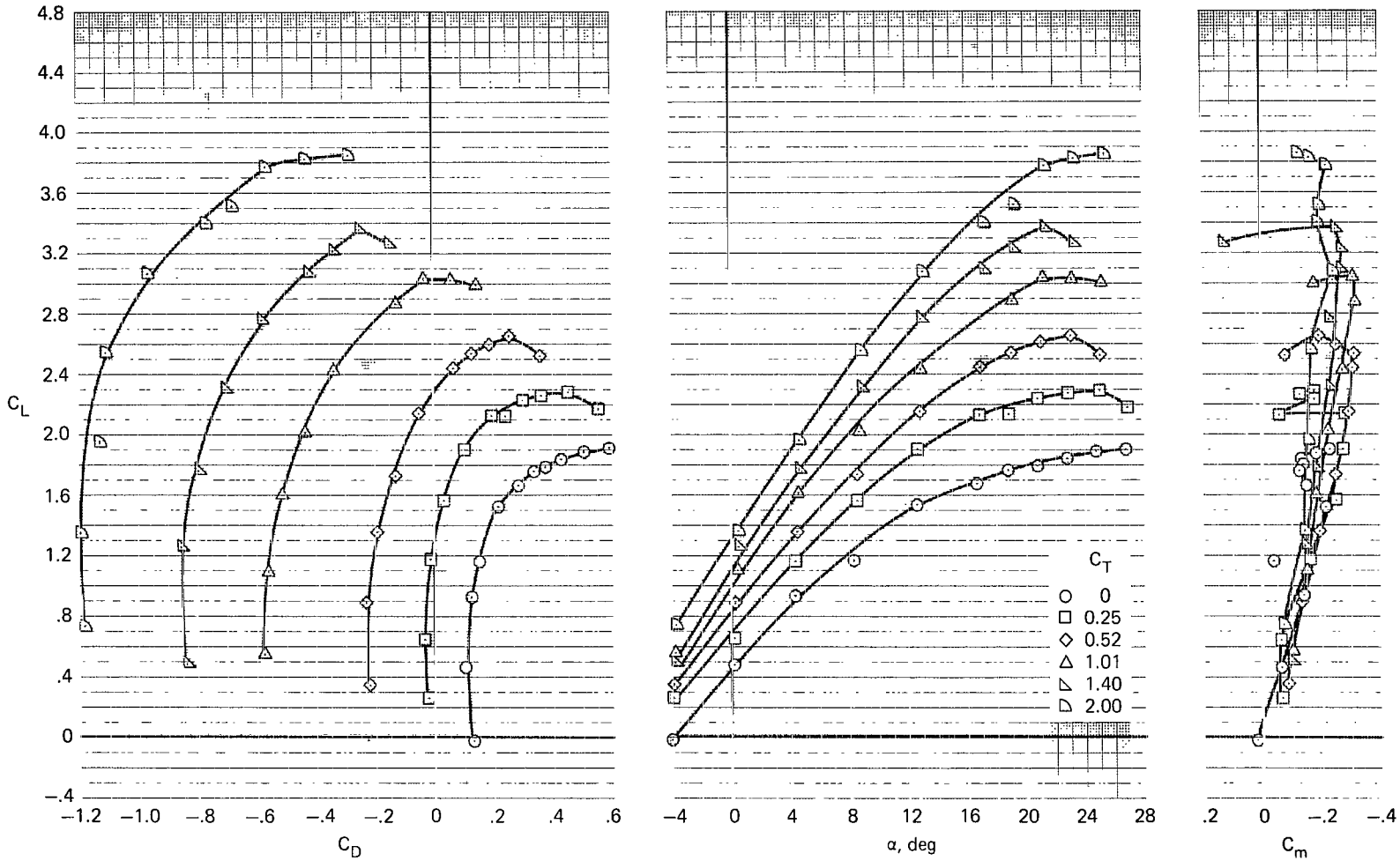

(a) $\delta_{f_{aux}} = 0°$

Figure 5.- Longitudinal characteristics of the model with main flap deflected 20°.

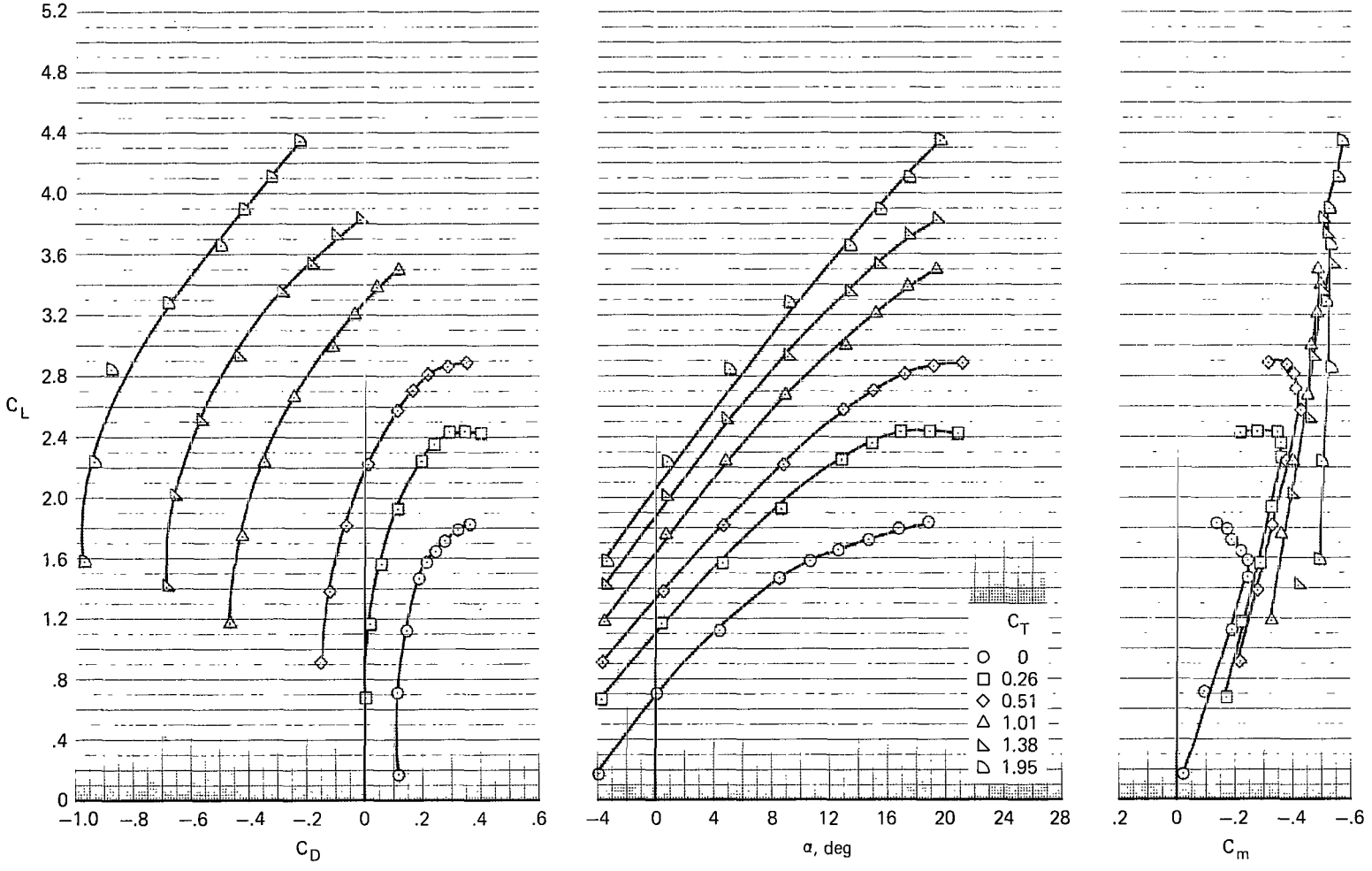

(b) $\delta_{f_{aux}} = 20°$

Figure 5.- Continued.

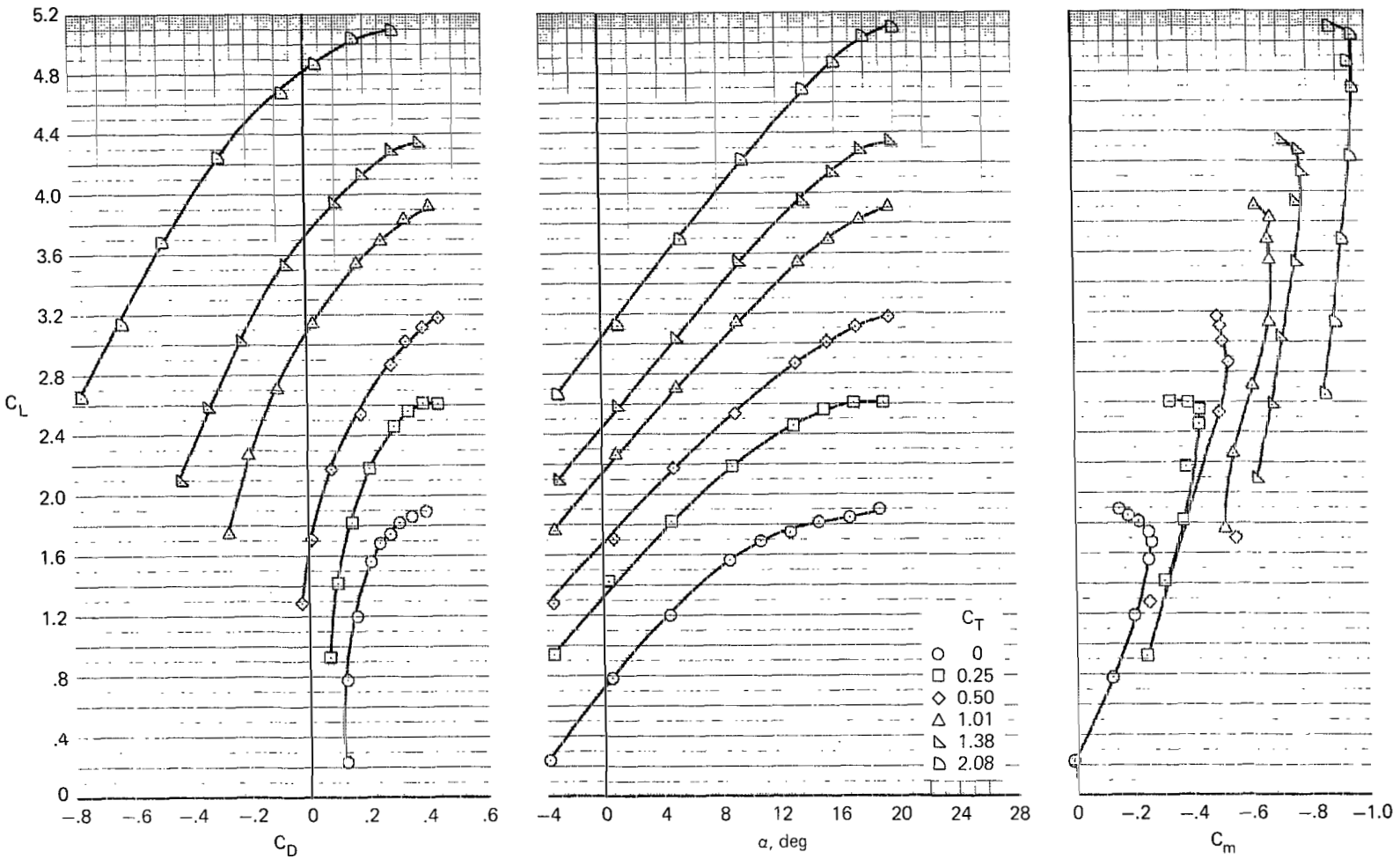

(c) $\delta_{f_{aux}} = 40°$

Figure 5.- Continued.

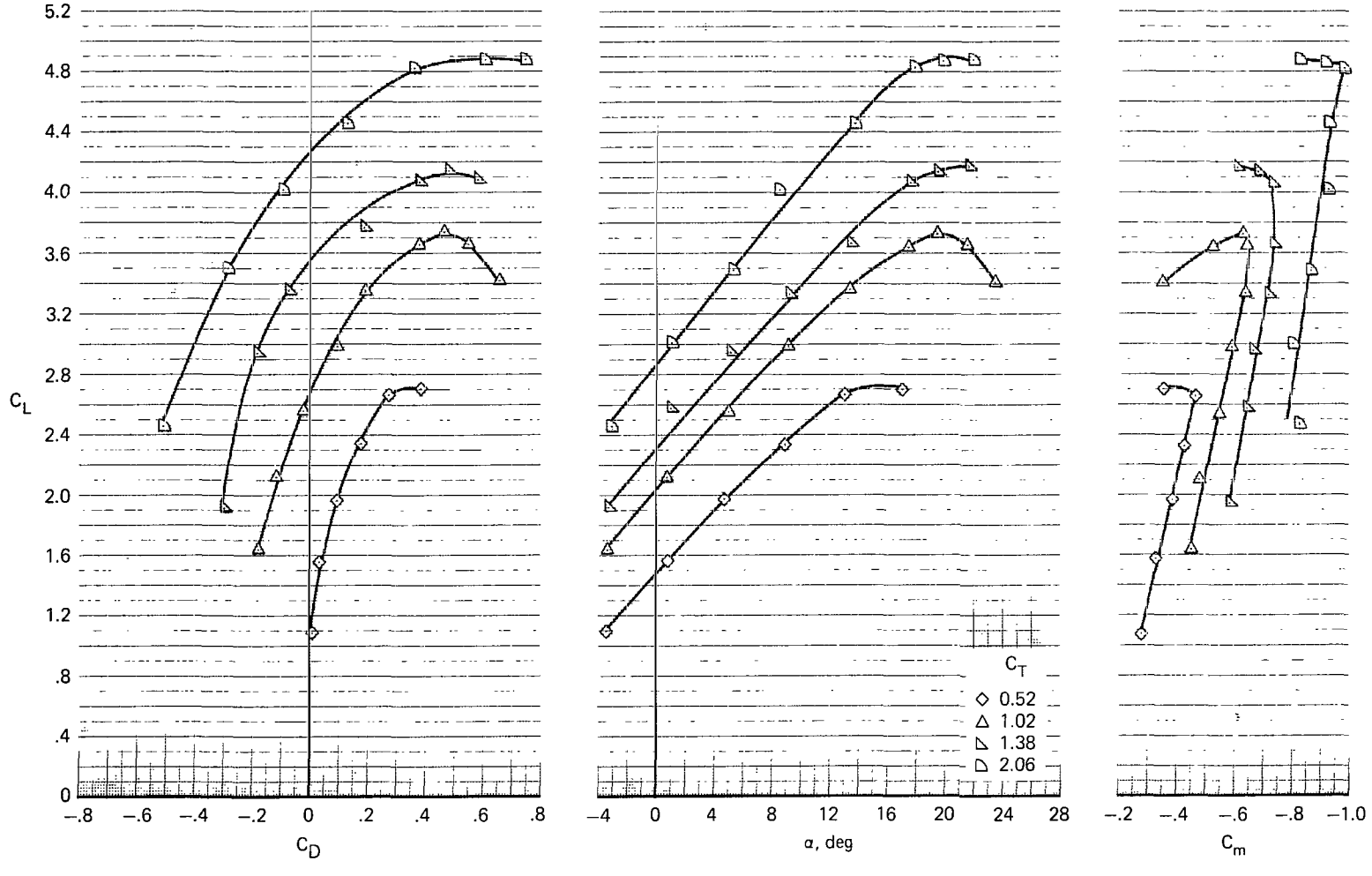

(d) $\delta_{f_{aux}} = 50°$

Figure 5.- Concluded.

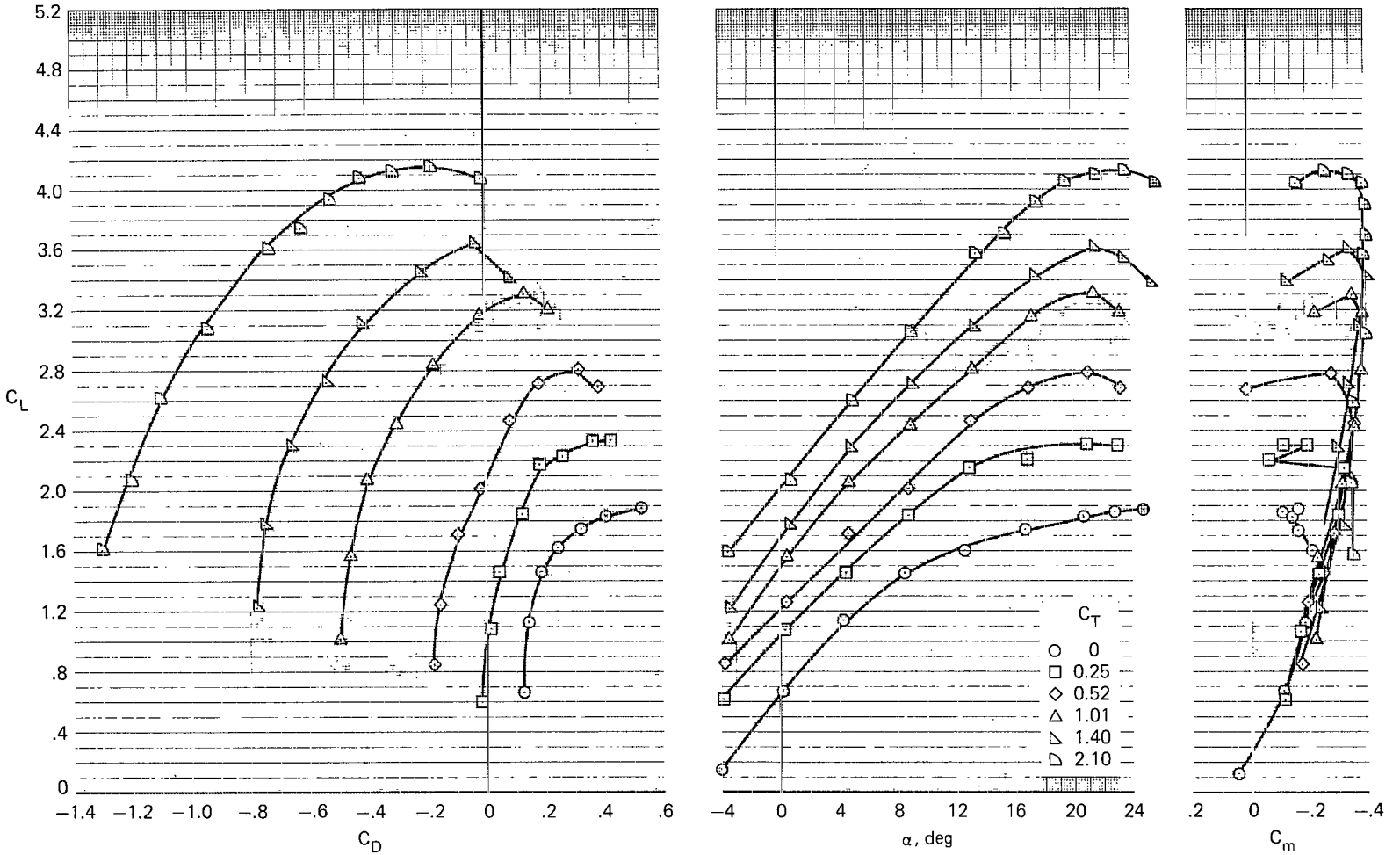

(a) $\delta_{f_{aux}} = 0°$

Figure 6.- Longitudinal characteristics of the model with main flap deflected 30°.

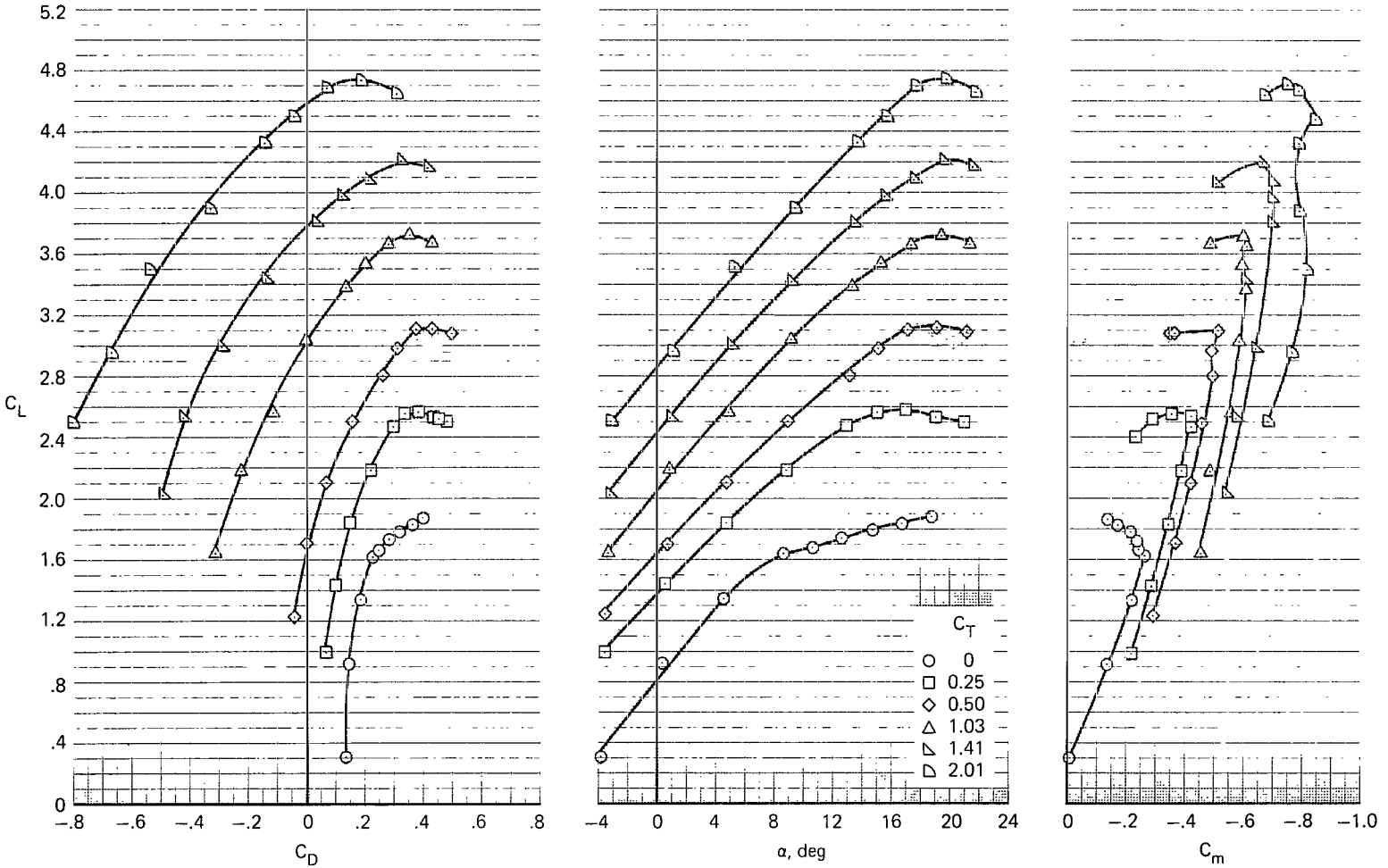

(b) $\delta f_{aux} = 20°$

Figure 6.- Continued.

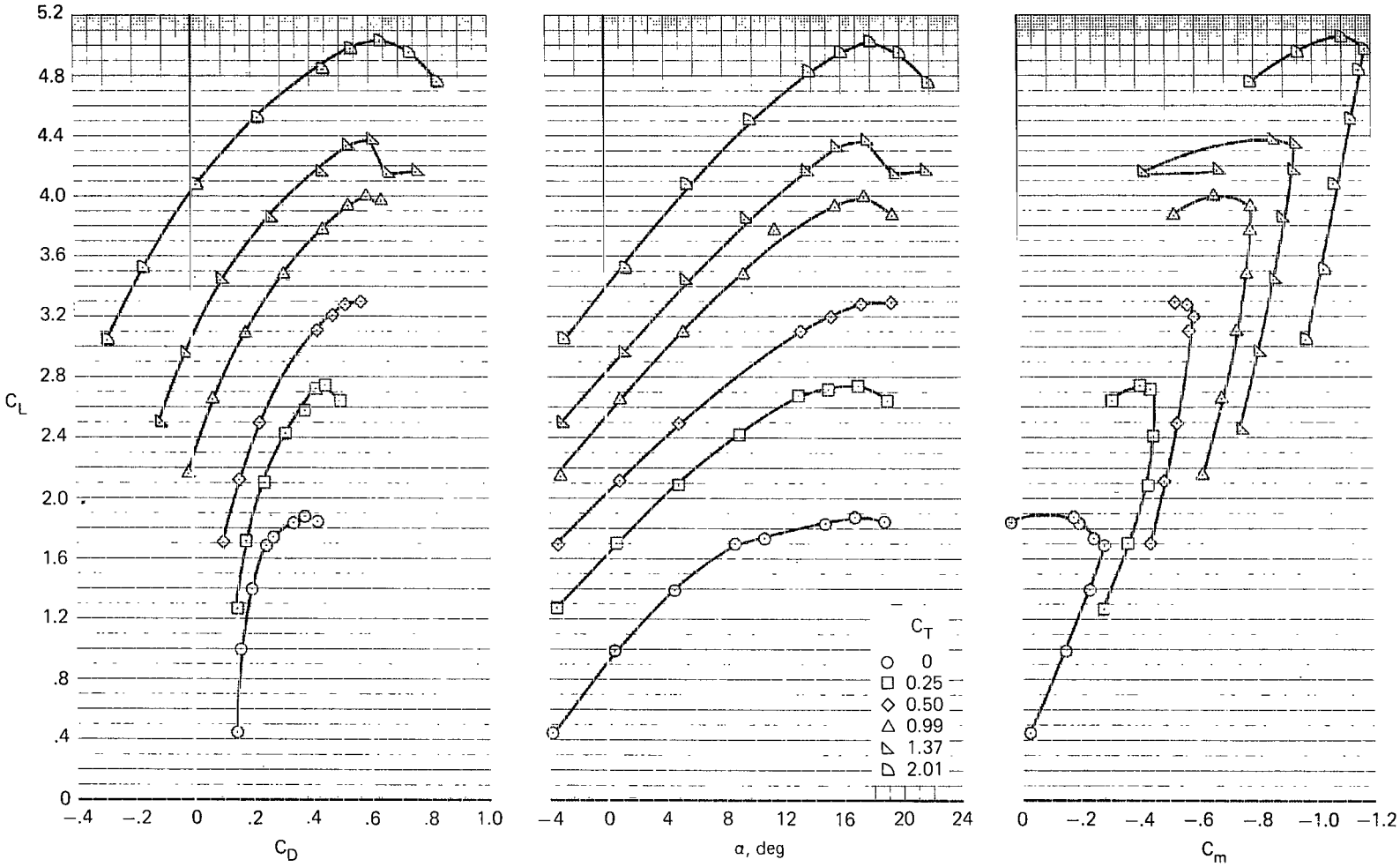

(c) $\delta_{f_{aux}} = 40°$

Figure 6.- Concluded.

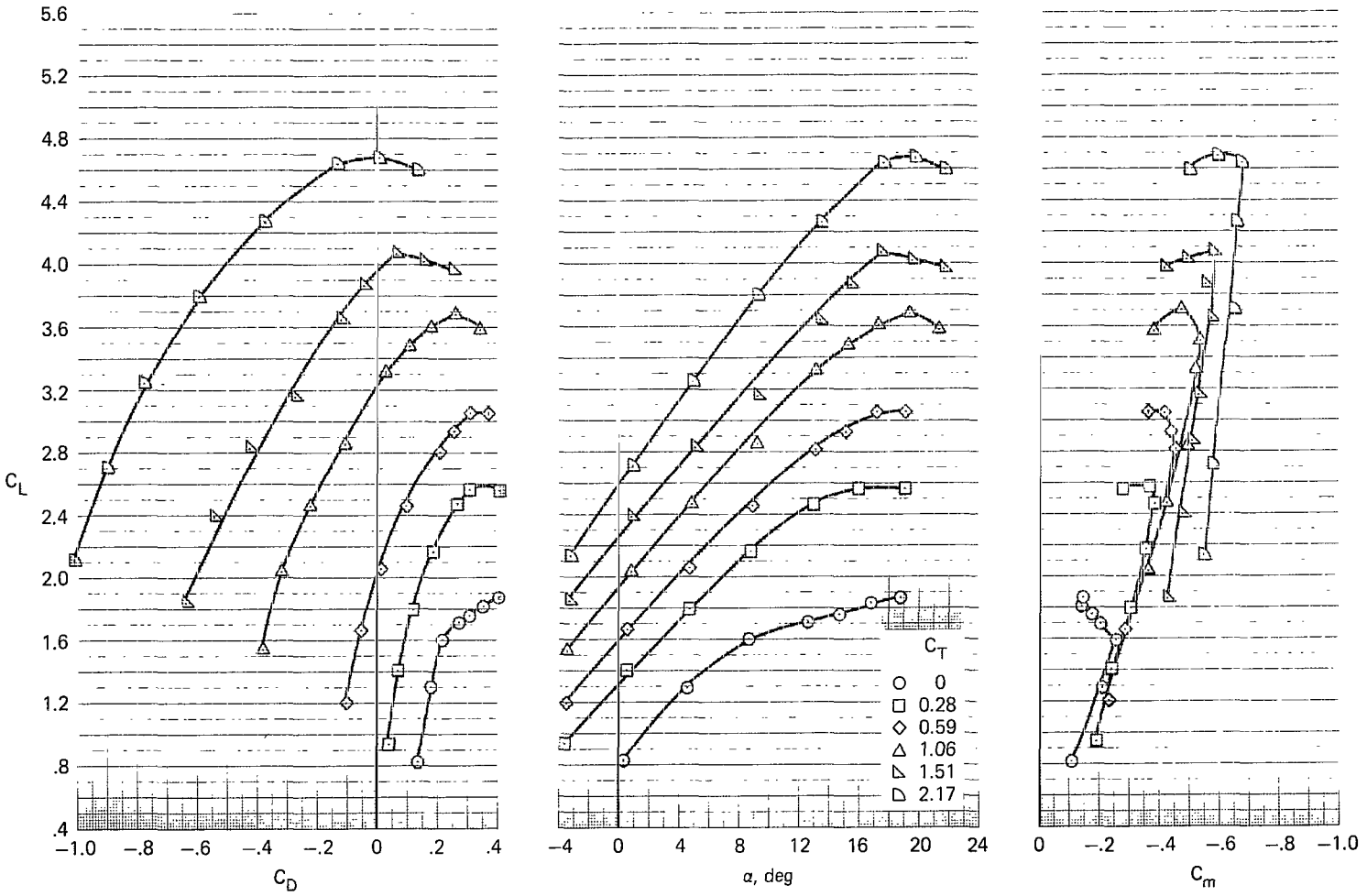

(a) $\delta_{f_{aux}} = 0°$

Figure 7.- Longitudinal characteristics of the model with the main flap deflected 40°.

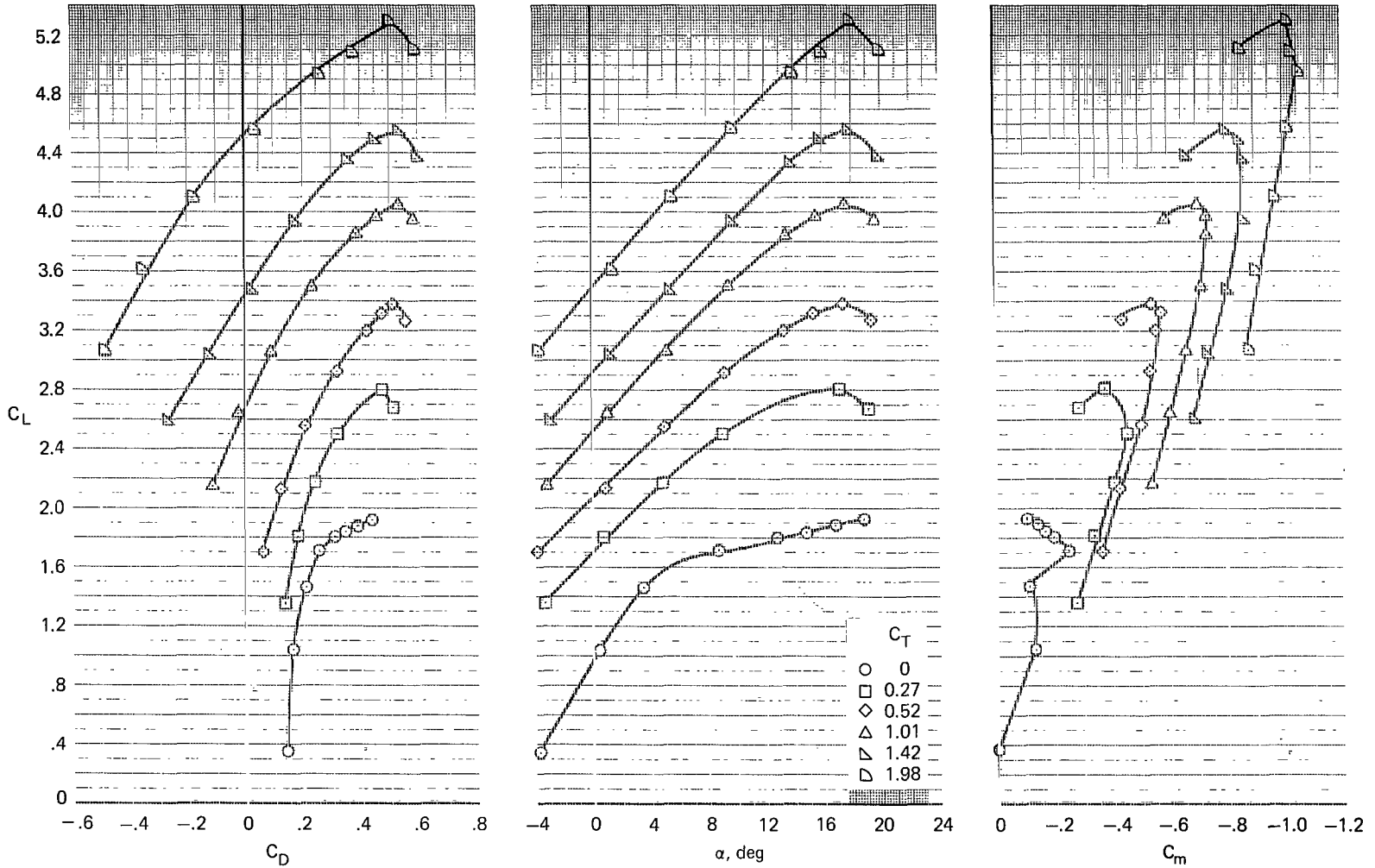

(b) $\delta_{f_{aux}} = 20°$

Figure 7.- Continued.

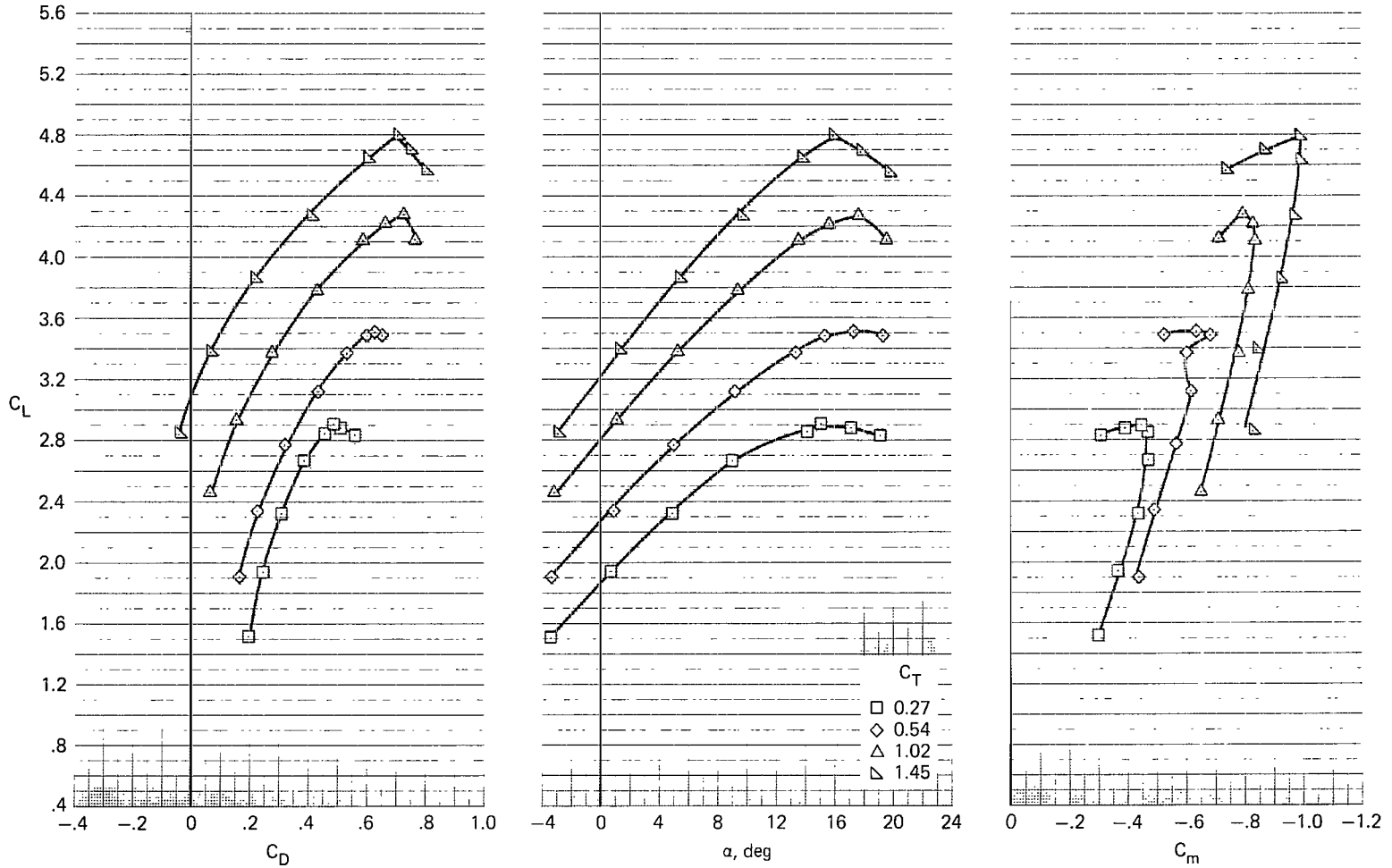

(c) $\delta_{f_{aux}} = 30°$

Figure 7.- Continued.

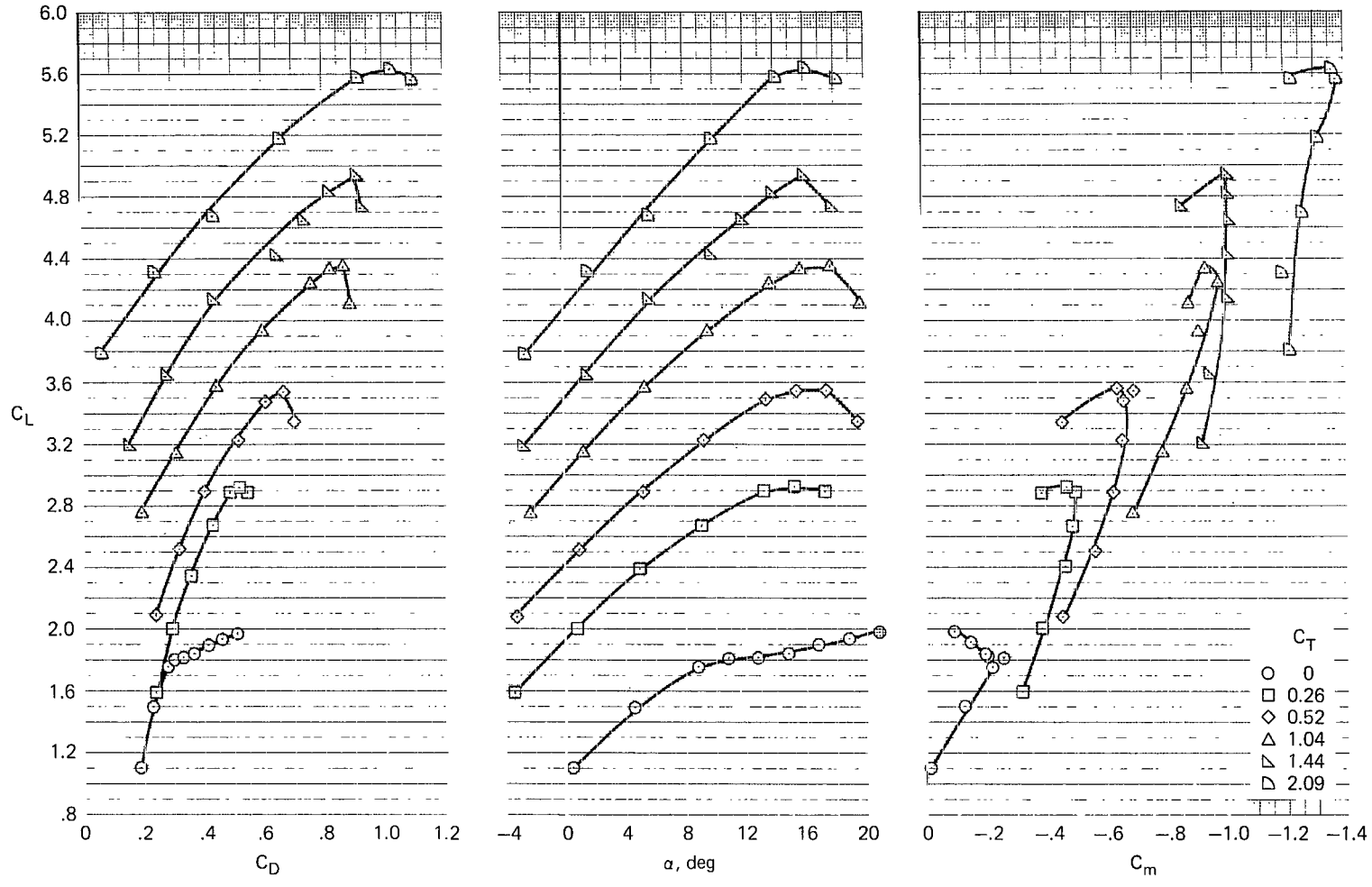

(d) $\delta_{f_{aux}} = 40°$

Figure 7.- Continued.

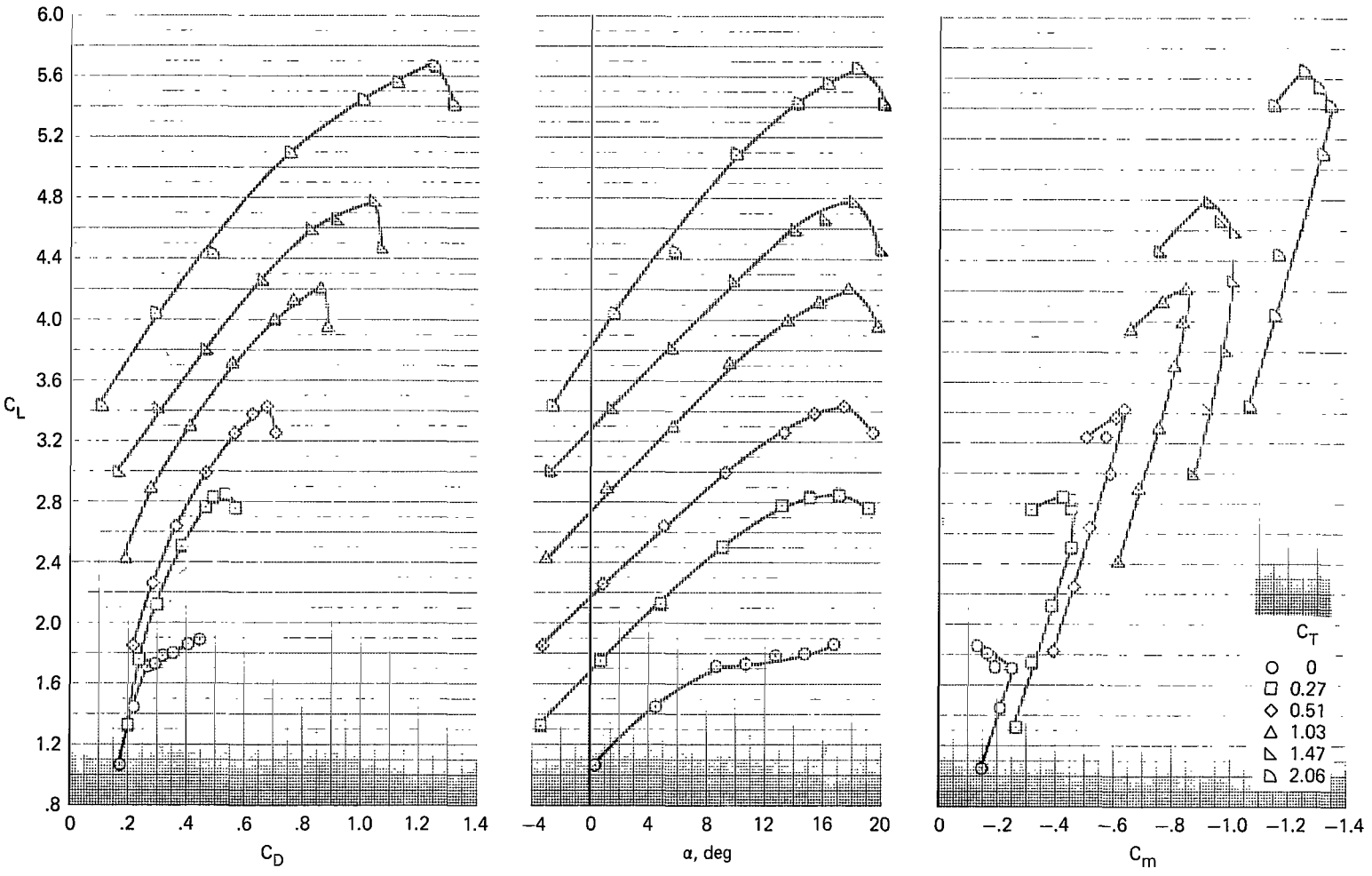

(e) $\delta_{f_{aux}} = 50°$

Figure 7.- Concluded.

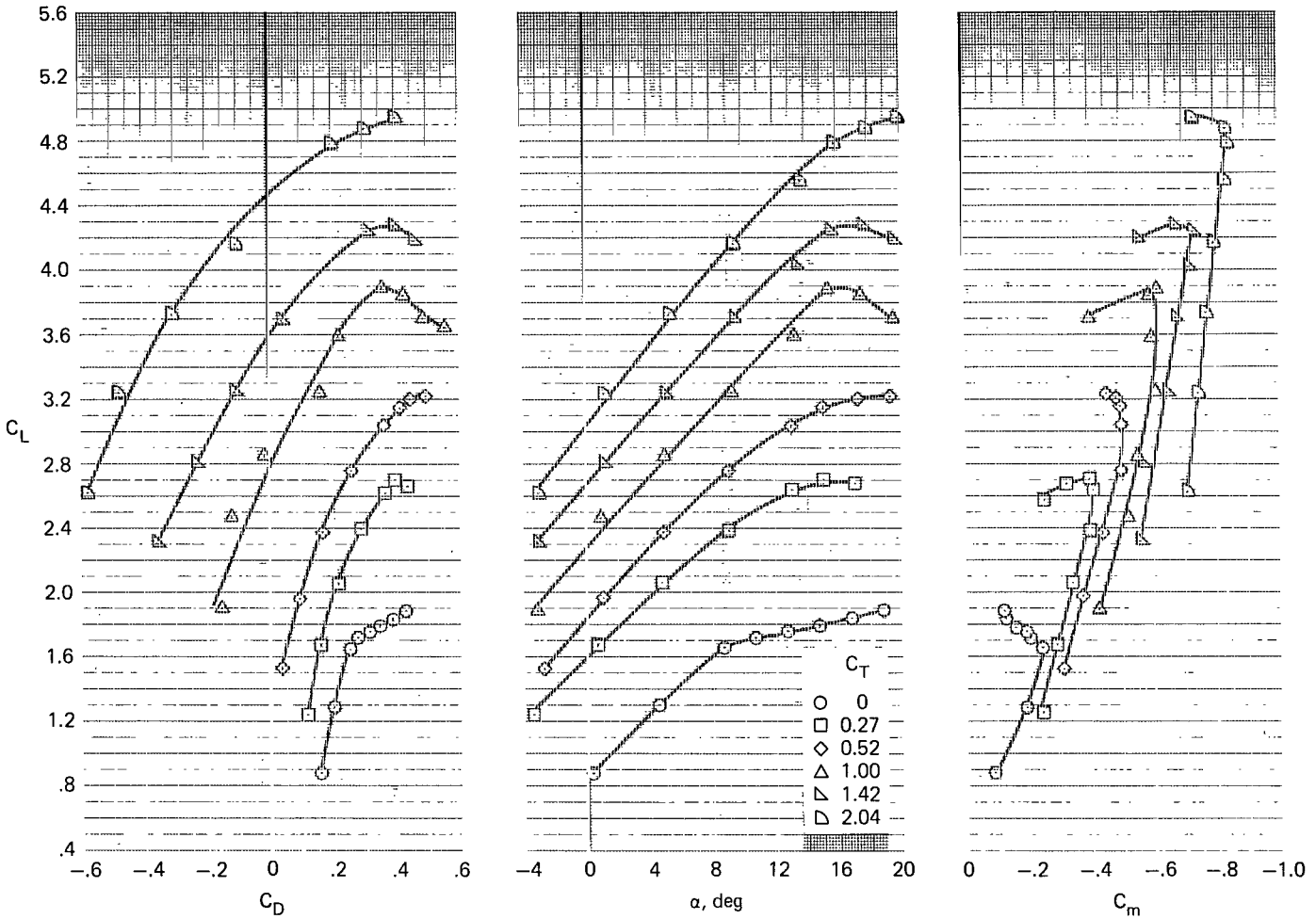

(a) $\delta_{f_{aux}} = 0°$

Figure 8.- Longitudinal characteristics of the model with main flap deflected 50°.

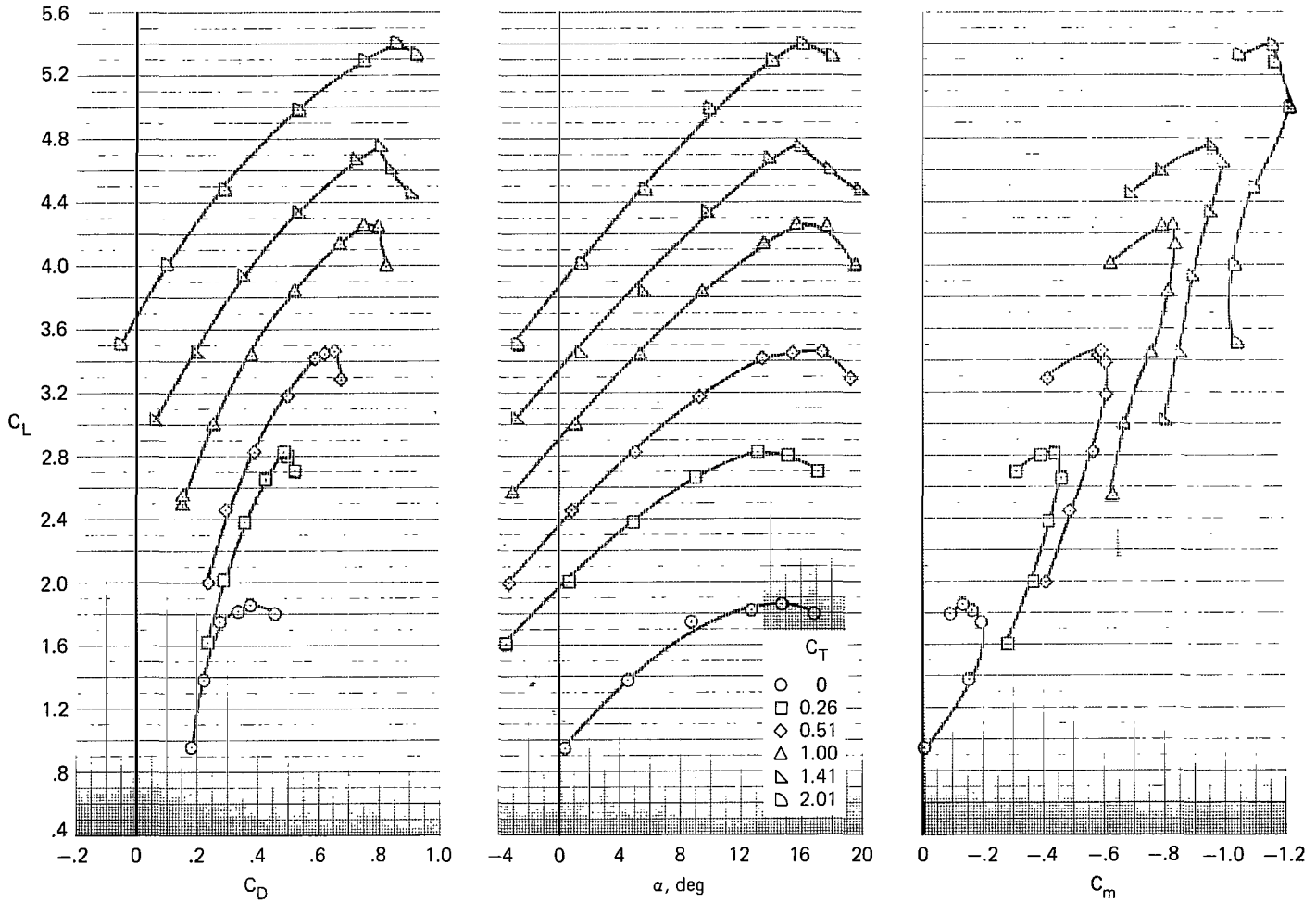

(b) $\delta_{f_{aux}} = 20°$

Figure 8.- Continued.

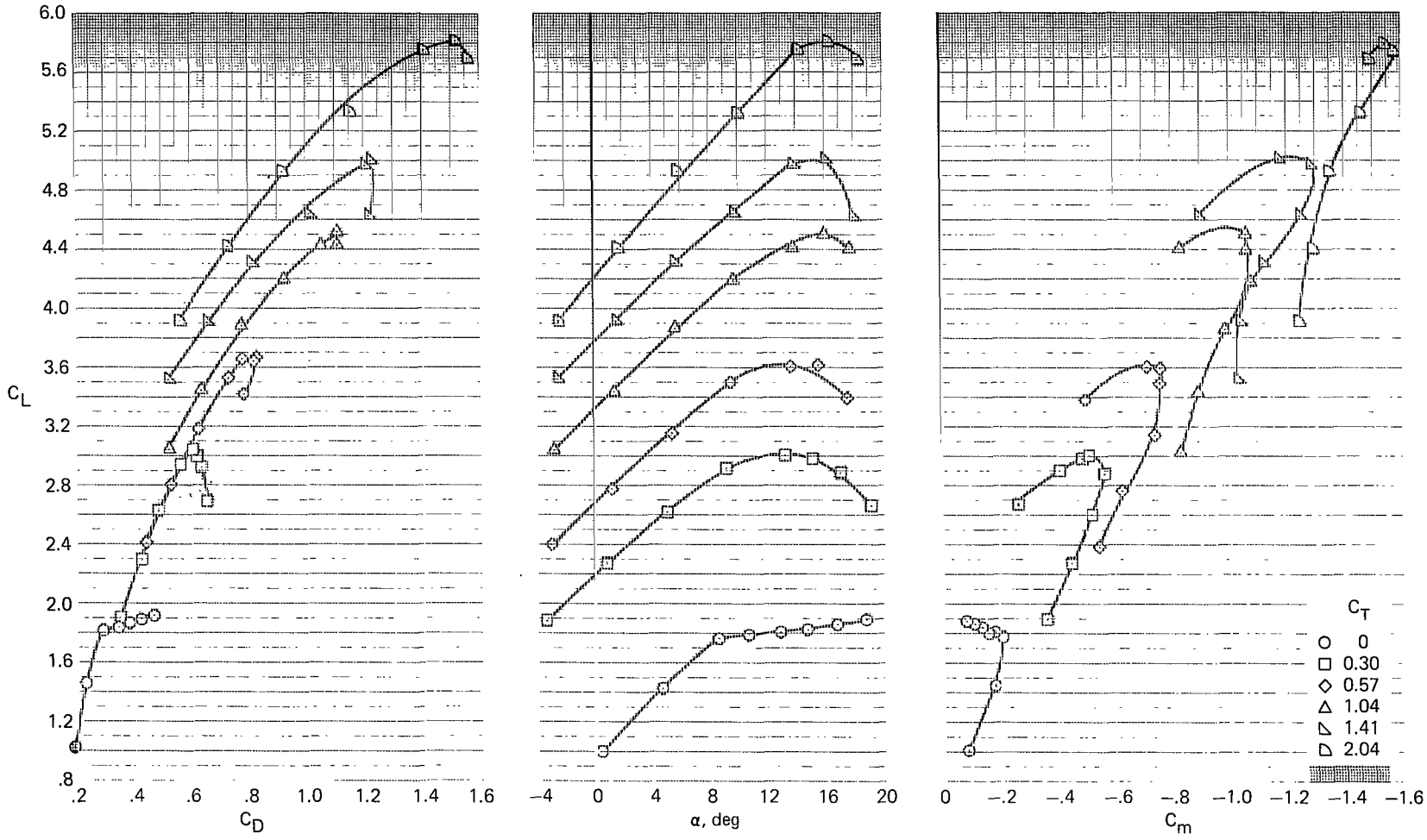

(c) $\delta_{f_{aux}} = 40°$

Figure 8.- Continued.

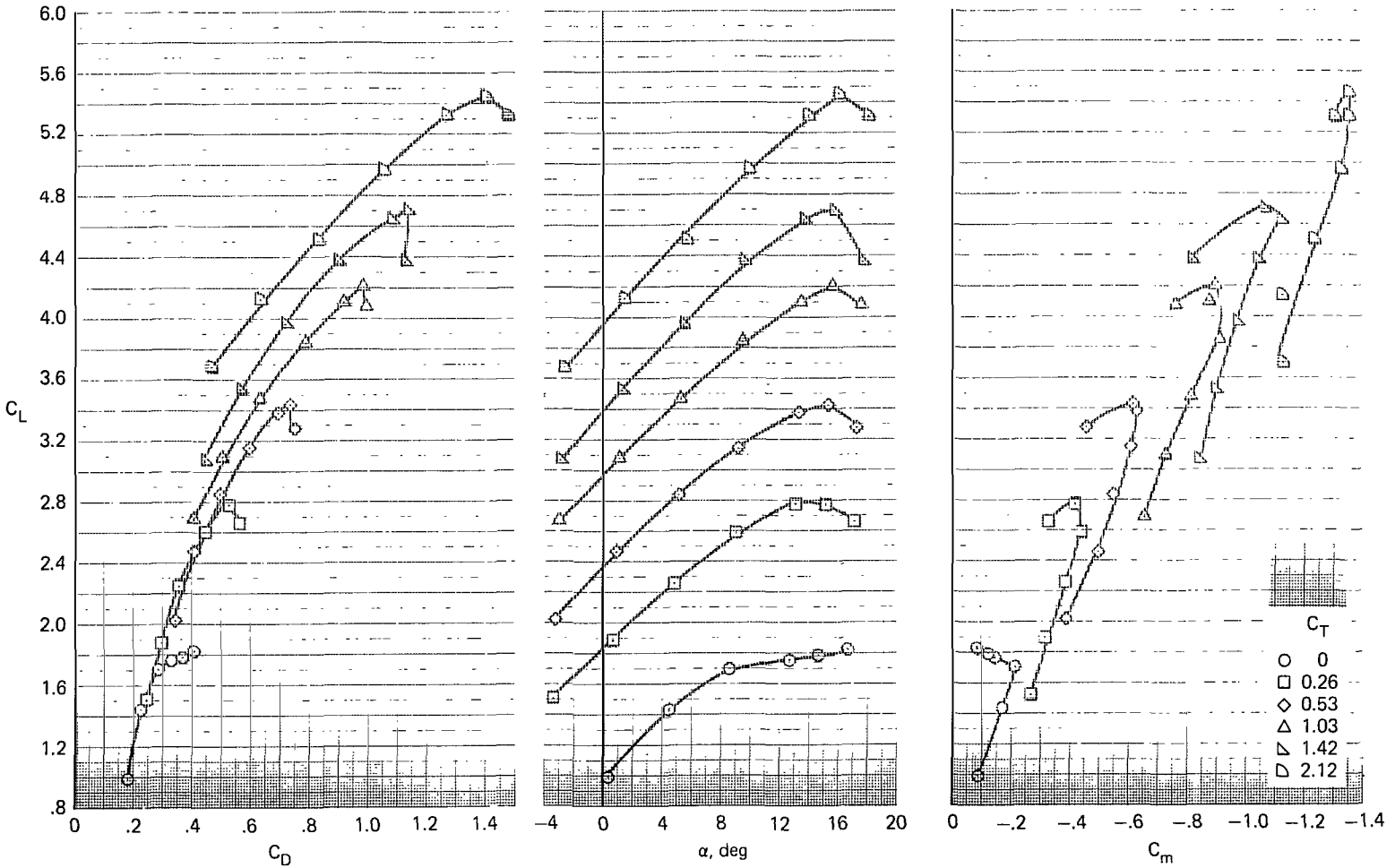

(d) $\delta_{f_{aux}} = 50°$

Figure 8.- Concluded.

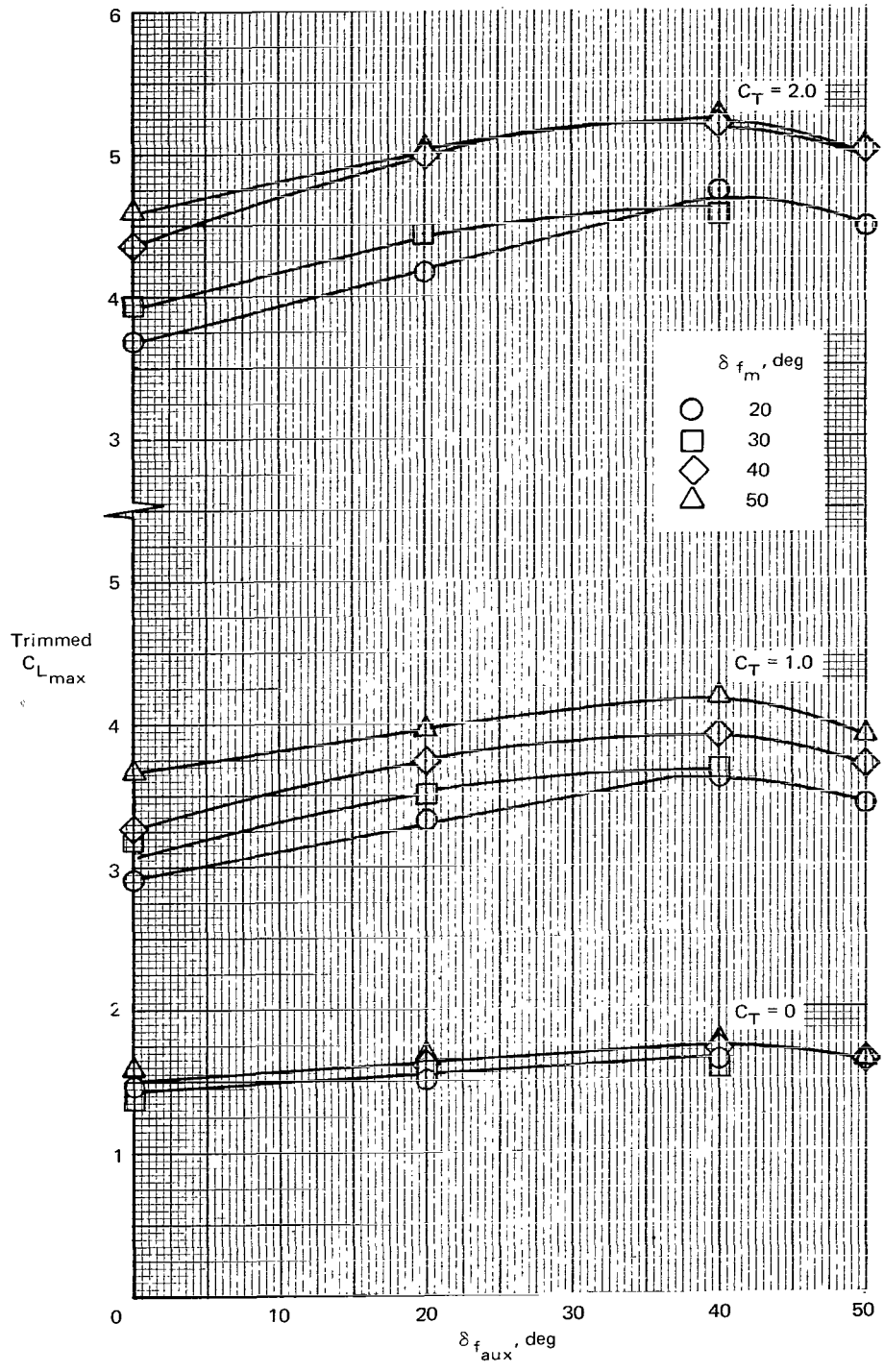

Figure 9.- Variation of trimmed $C_{L_{max}}$ with auxiliary flap deflection.

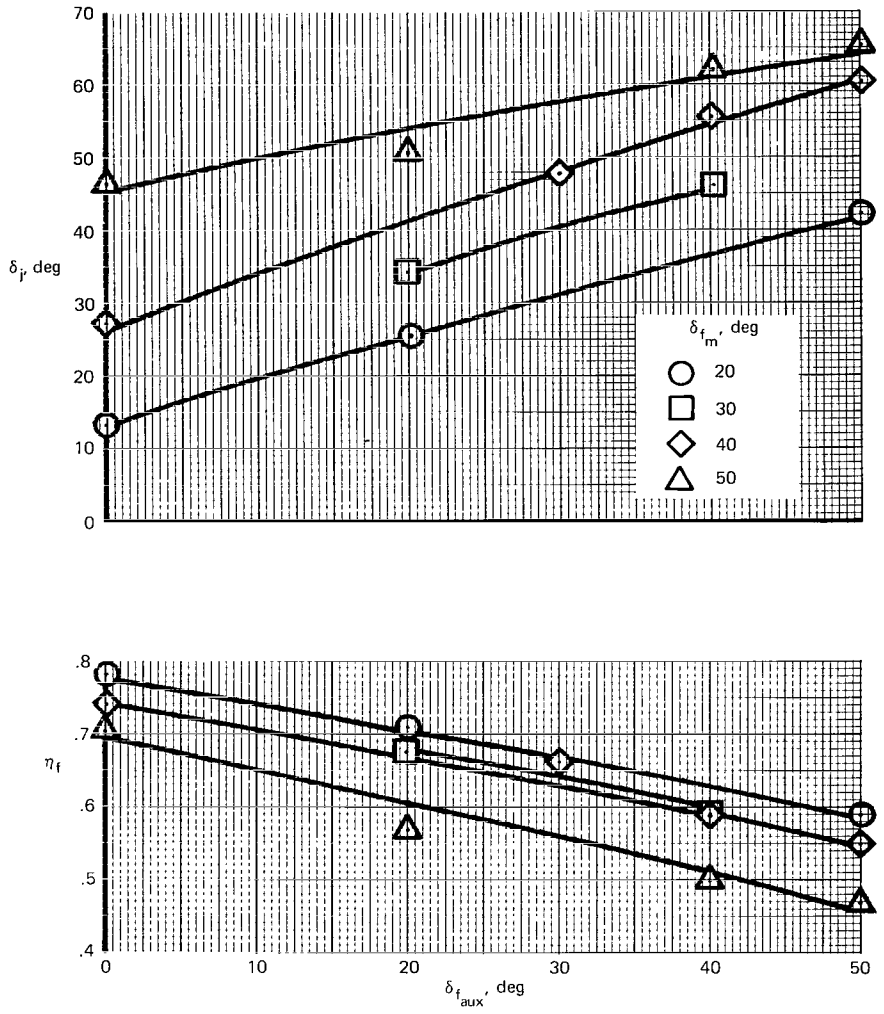

Figure 10.- Variations of resultant static jet deflection angle and turning efficiency with auxiliary flap deflection, $\alpha = 0°$, $\delta_d = 15°$.

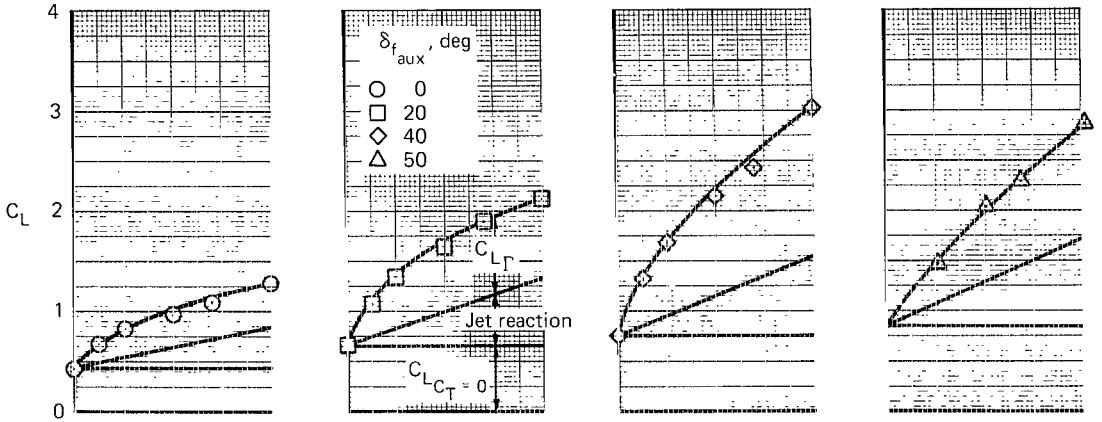

(a) $\delta_{f_m} = 20°$

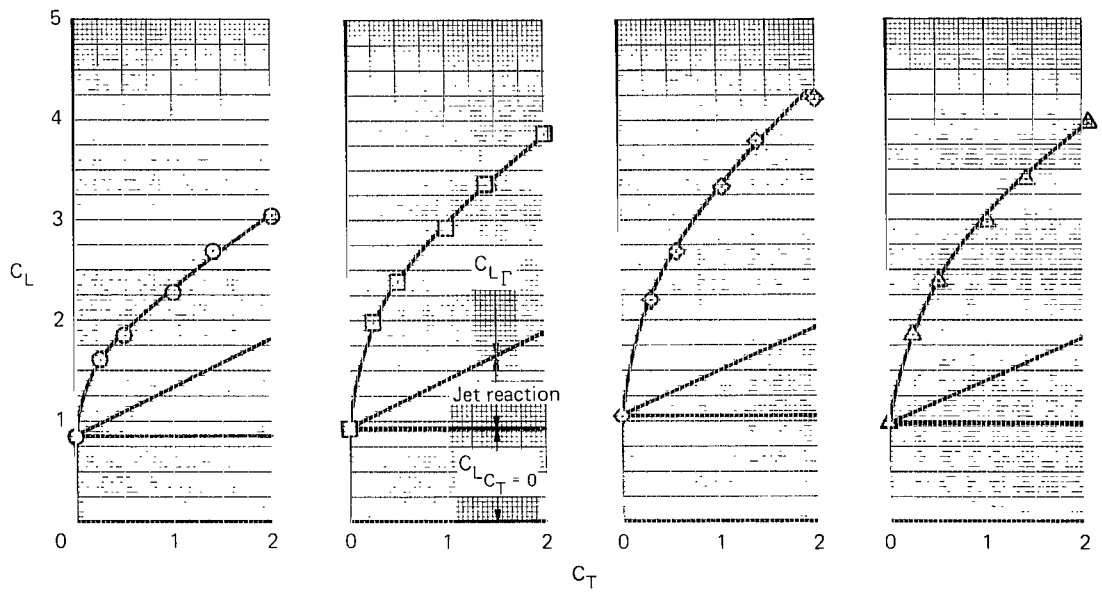

(b) $\delta_{f_m} = 50°$

Figure 11.- Variation of lift coefficient with gross thrust coefficient; $\alpha = 0°$.

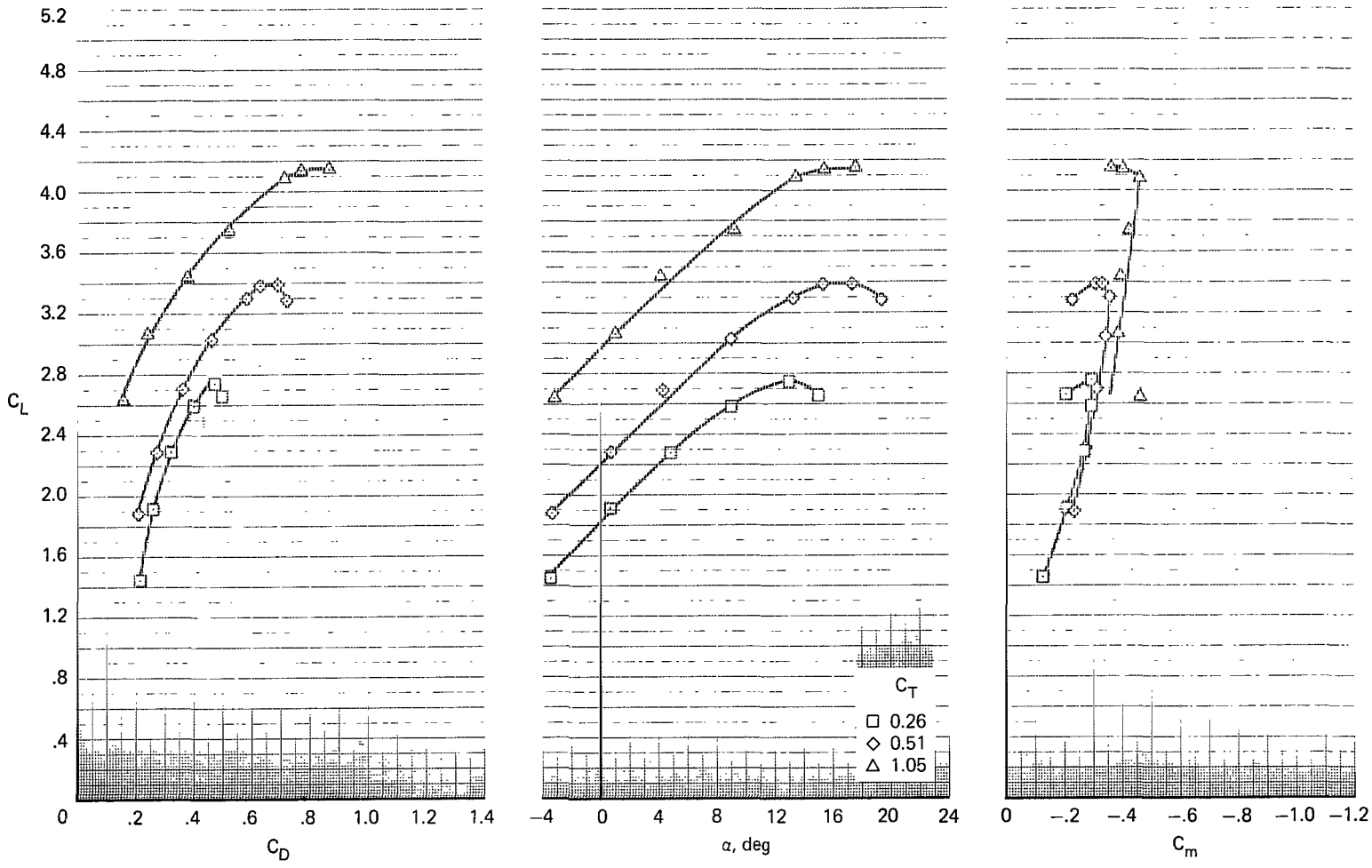

Figure 12.- Longitudinal characteristics of the model with the operation of two inboard engines; $\delta_{f_m} = 40°$, $\delta_{f_{aux}} = 40°$.

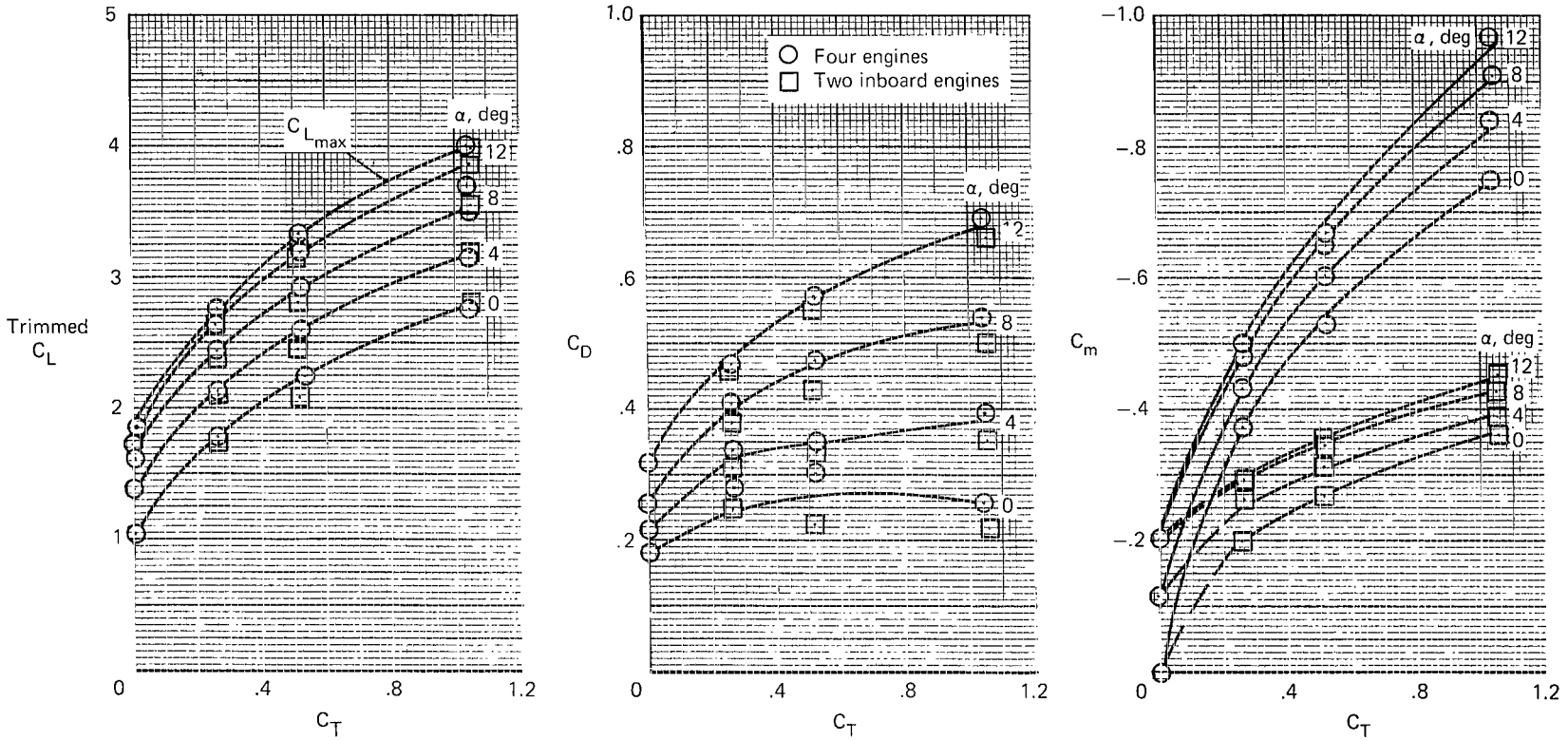

Figure 13.- Comparison of lift, drag, pitching-moment coefficients for operation of two inboard engines and four engines; $\delta_{f_m} = 40°$, $\delta_{f_{aux}} = 40°$.

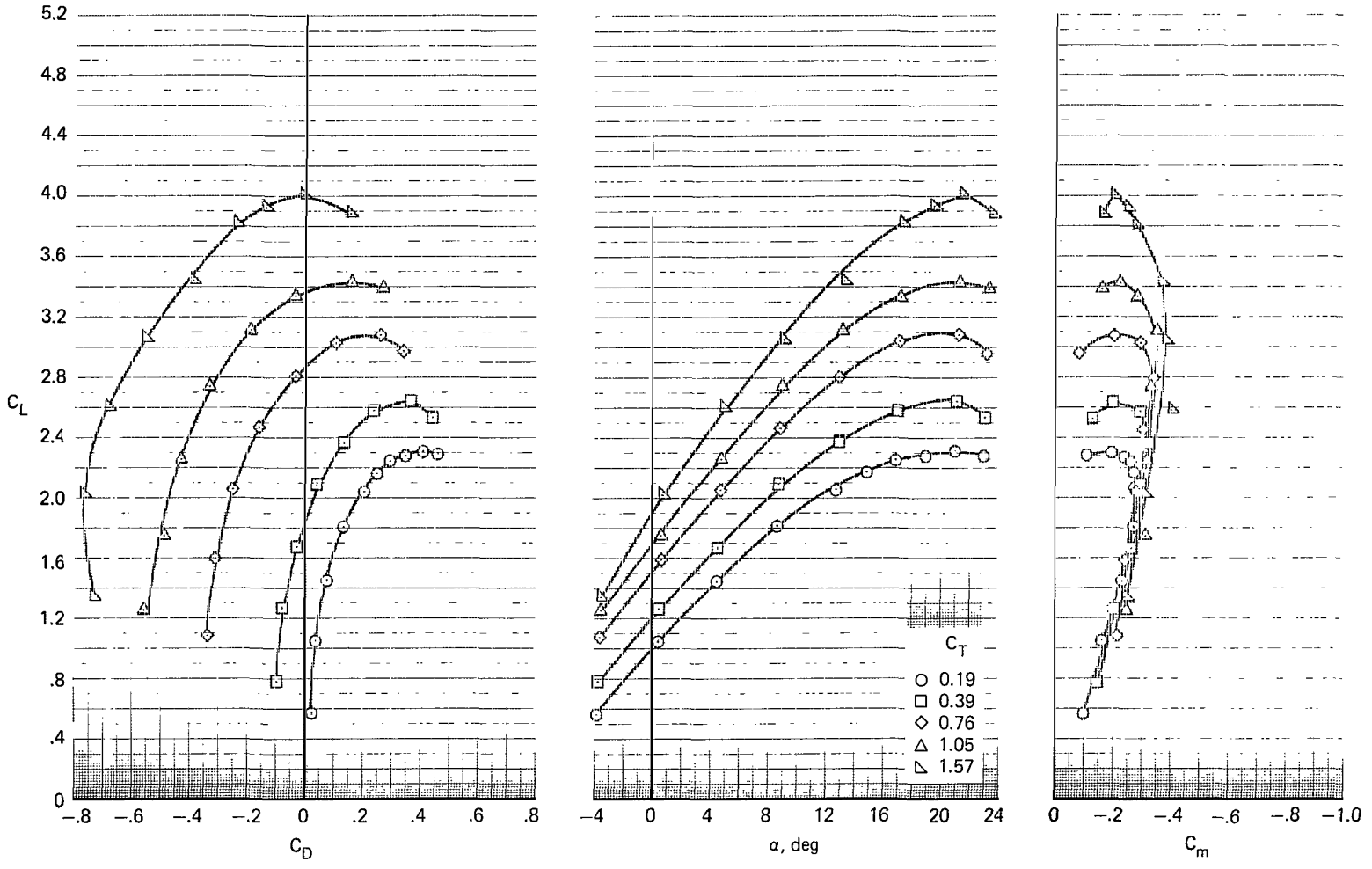

(a) Longitudinal characteristics.

Figure 14.- Aerodynamic characteristics of the model with left hand outboard engine out; $\delta_{f_m} = 20°$, $\delta_{f_{aux}} = 20°$.

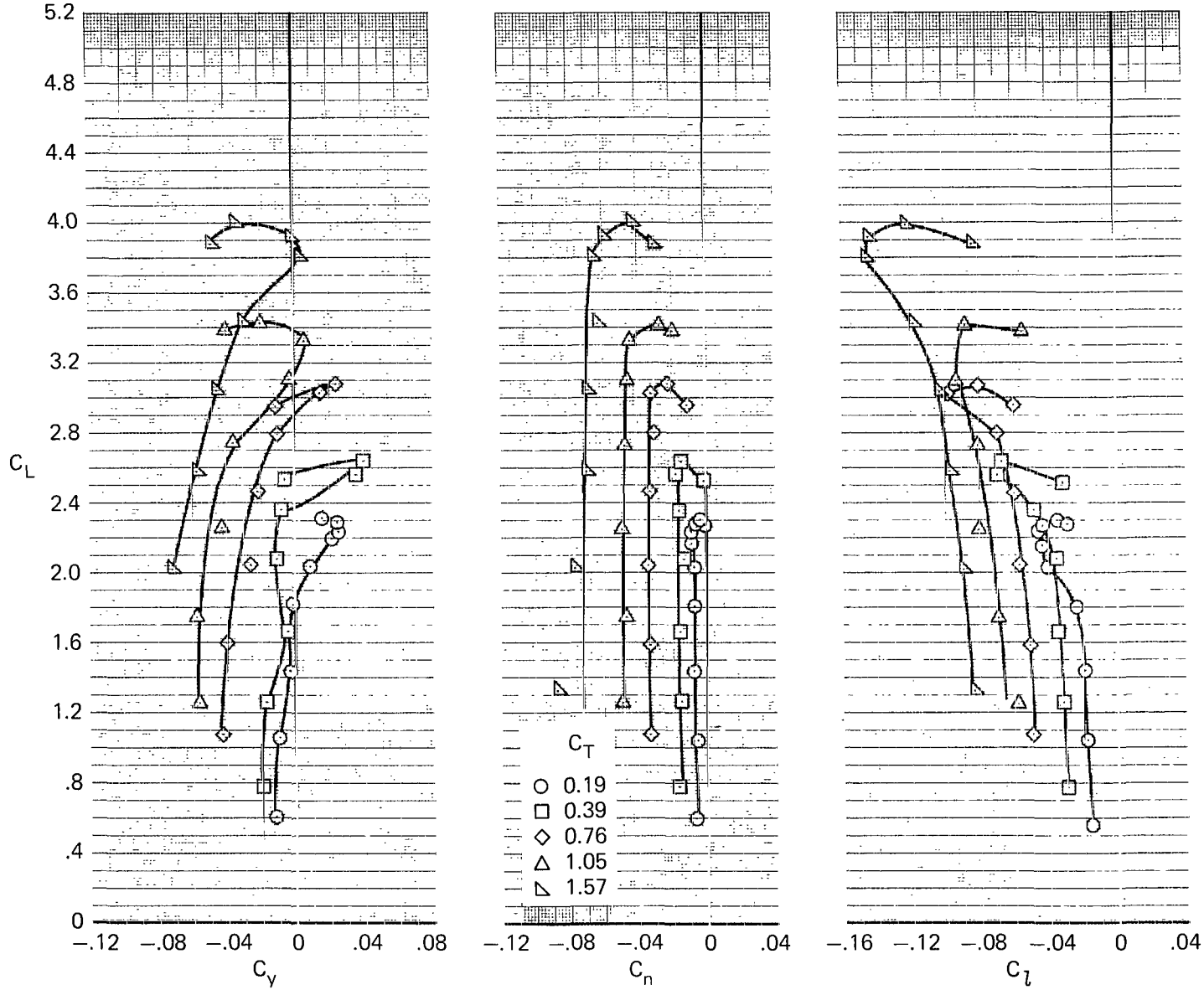

(b) Lateral characteristics.

Figure 14.- Concluded.

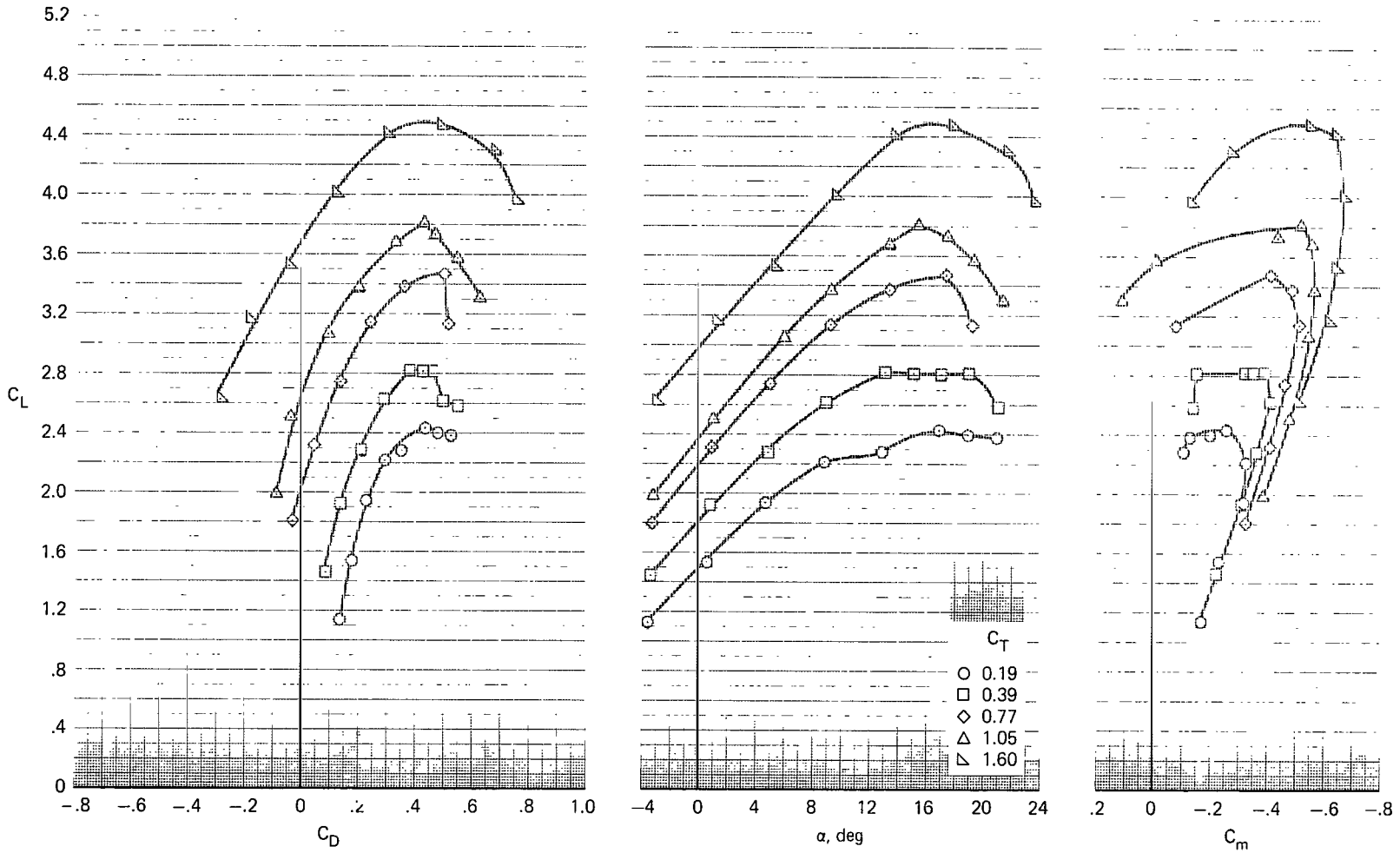

(a) Longitudinal characteristics.

Figure 15.- Aerodynamic characteristics of the model with left hand outboard engine out; $\delta_{f_m} = 40°$, $\delta_{f_{aux}} = 20°$.

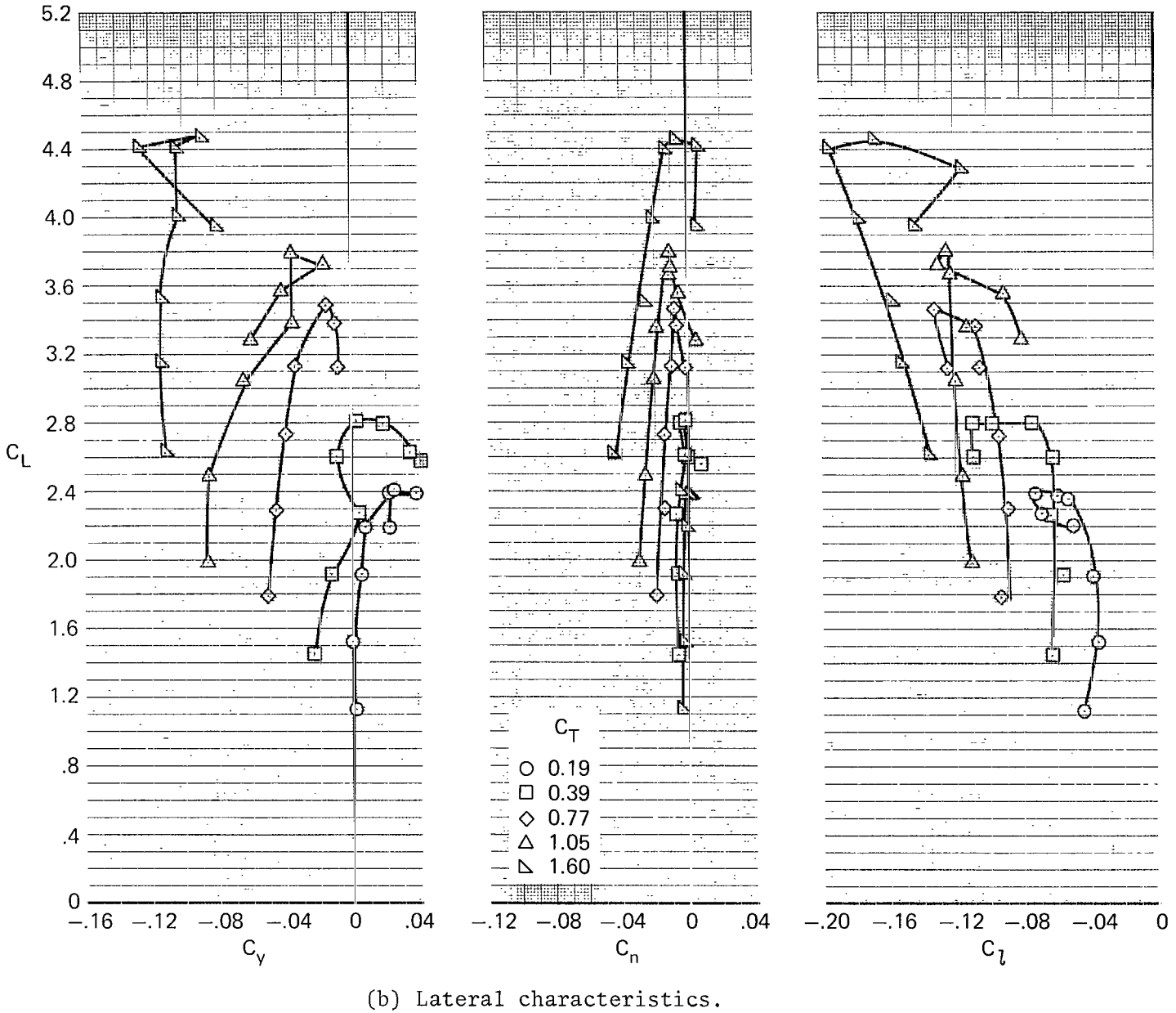

(b) Lateral characteristics.

Figure 15.- Concluded.

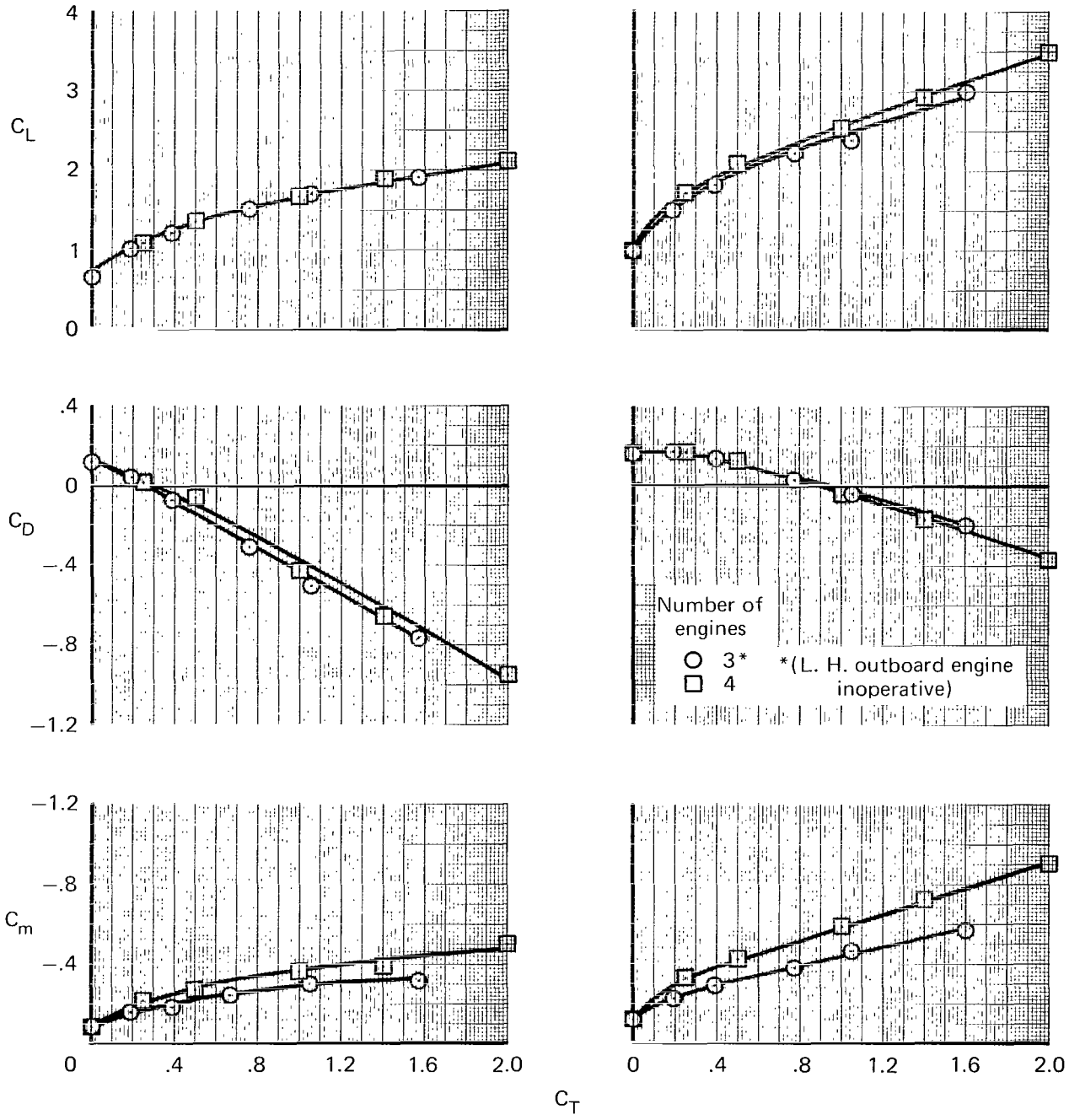

(a) $\delta_{f_m} = 20°$ (b) $\delta_{f_m} = 40°$

Figure 16.- Effect of operating three engines on the longitudinal characteristics of the model; $\alpha = 0°$, $\delta_{f_{aux}} = 20°$.

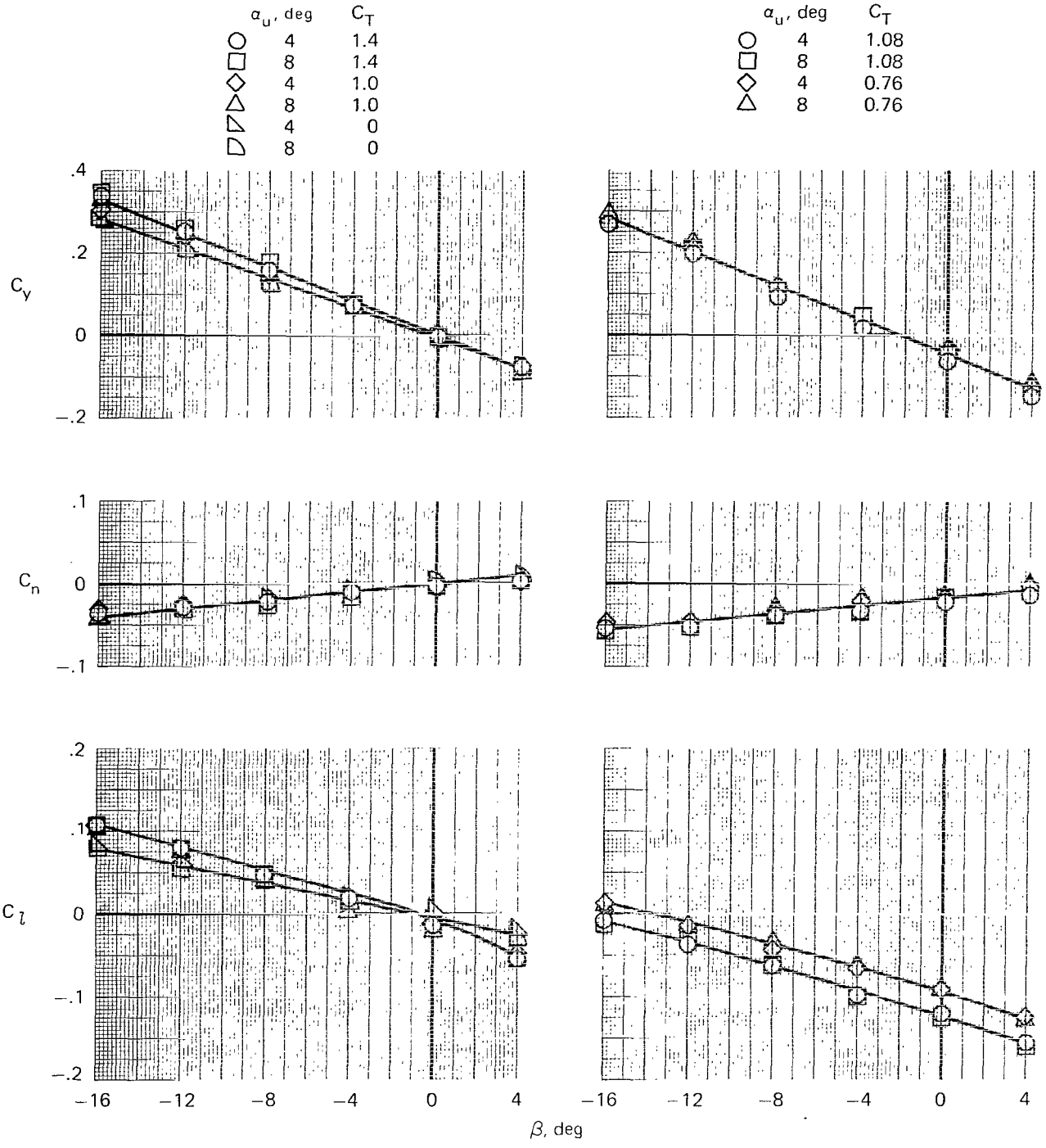

(a) Four engines.

(b) Three engines.

Figure 17.- Variation of side force, yawing, and rolling-moment coefficients with sideslip; $\delta_{f_m} = 40°$, $\delta_{f_{aux}} = 20°$, $\delta_r = 0°$.

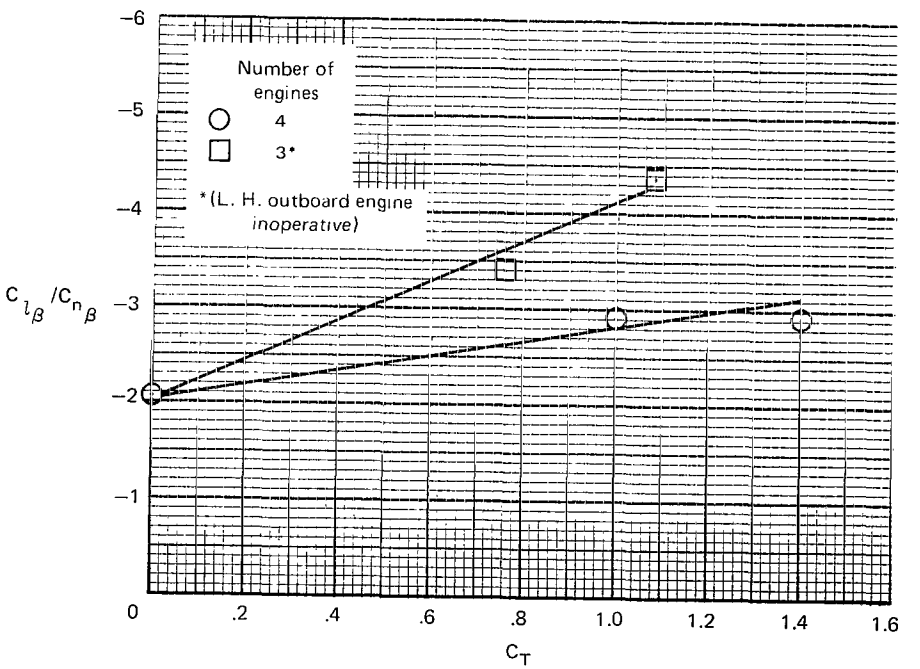

Figure 18.- Variations of C_{l_β}/C_{n_β} with gross thrust coefficient; $\delta_{f_m} = 40°$, $\delta_{f_{aux}} = 20°$.

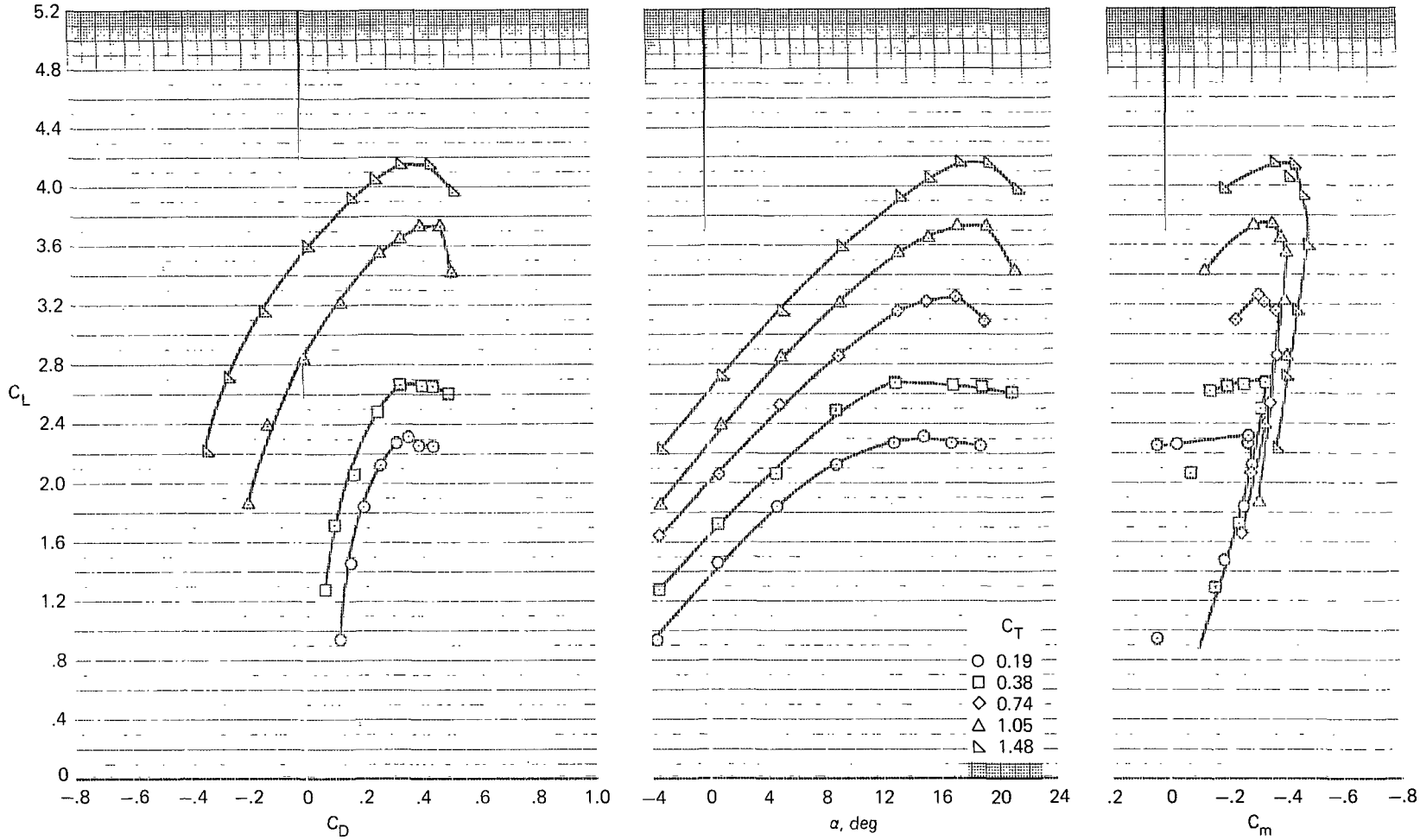

(a) Longitudinal characteristics.

Figure 19.- Aerodynamic characteristics of the model with asymmetric auxiliary flap deflection and left hand outboard engine out; $\delta_{f_m} = 40°$, $\delta_{f_{aux}} = 40°$ (left side), $\delta_{f_{aux}} = 0°$ (right side), $\beta = 0°$.

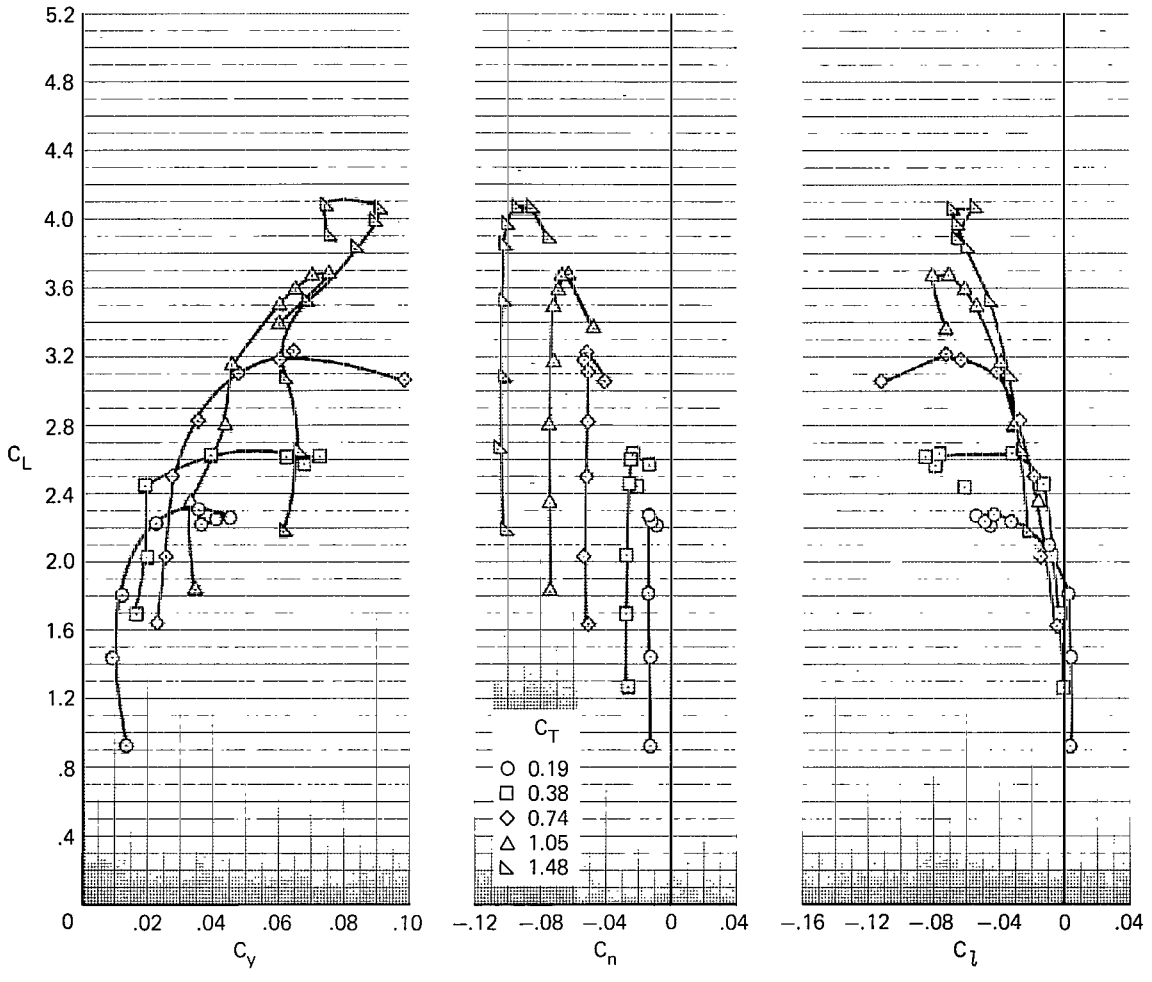

(b) Lateral characteristics.

Figure 19.- Concluded.

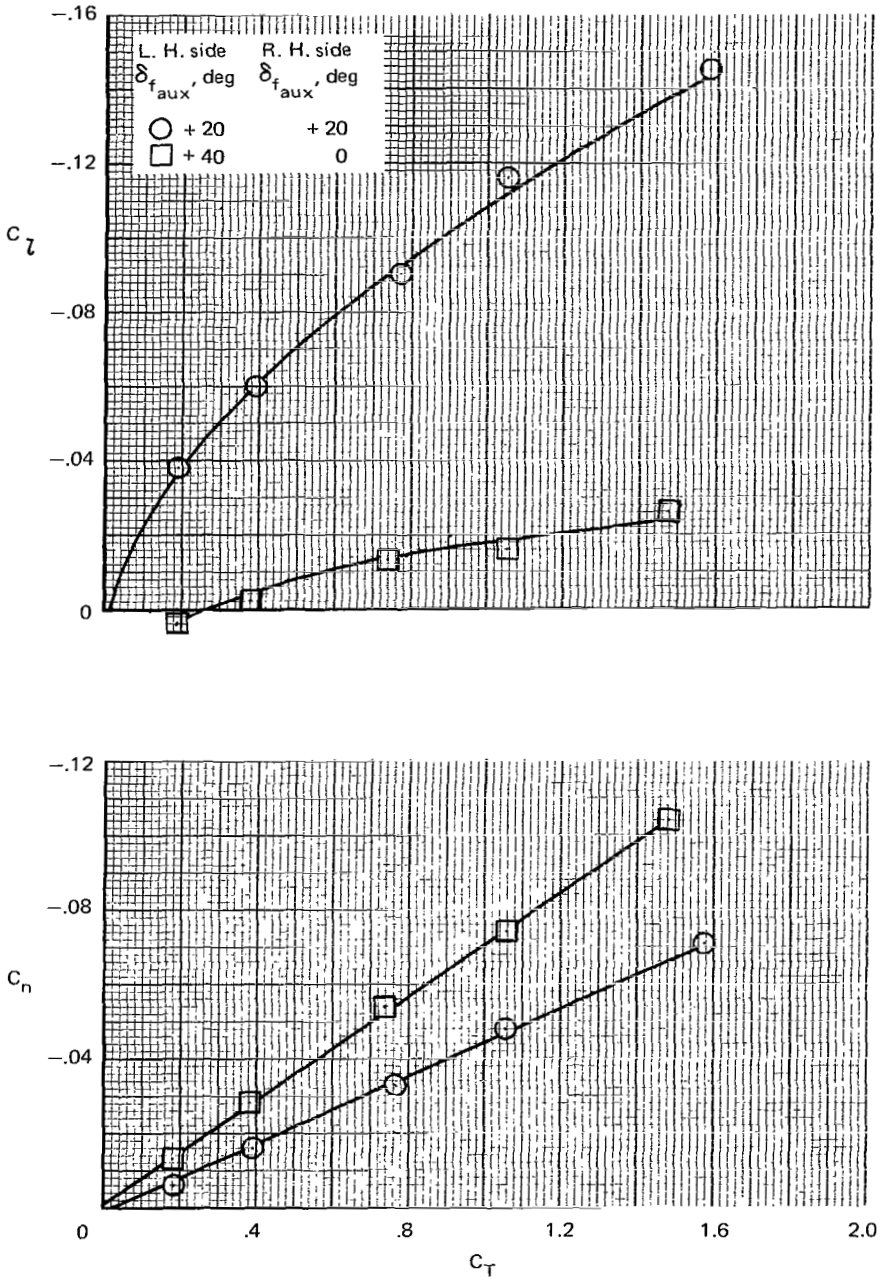

Figure 20.- Effect of asymmetric auxiliary flap deflection with three engines operating (left hand outboard engine off) on the variation of rolling and yawing moment coefficients with gross thrust coefficient; $\delta_{f_m} = 40°$, $\alpha = 0°$, $\beta = 0°$.

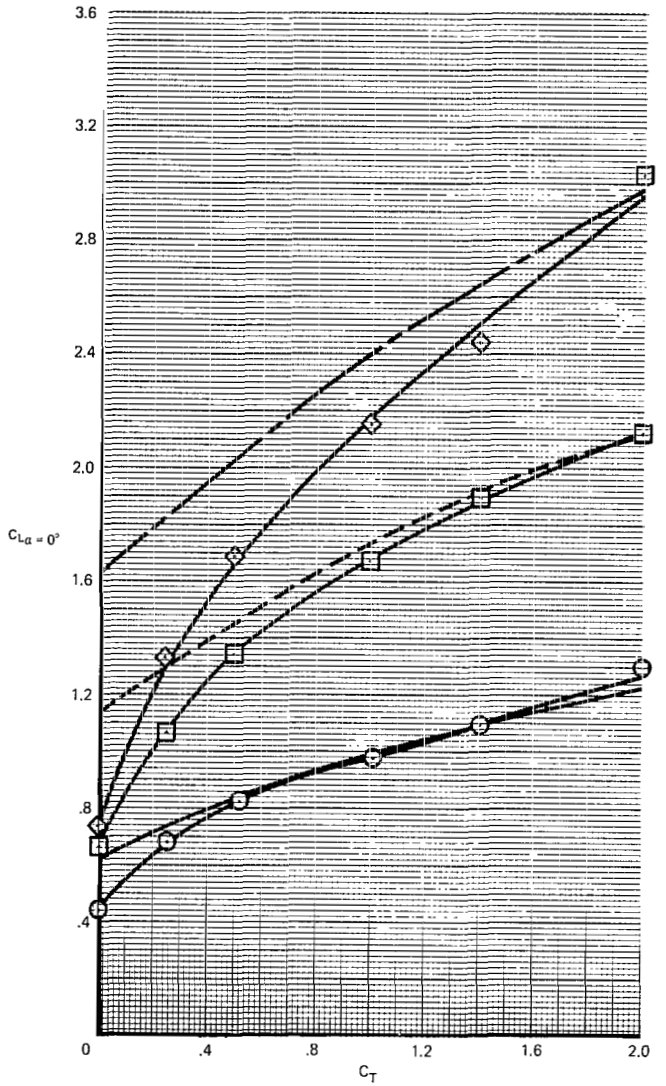

(a) $\delta_{f_m} = 20^\circ$

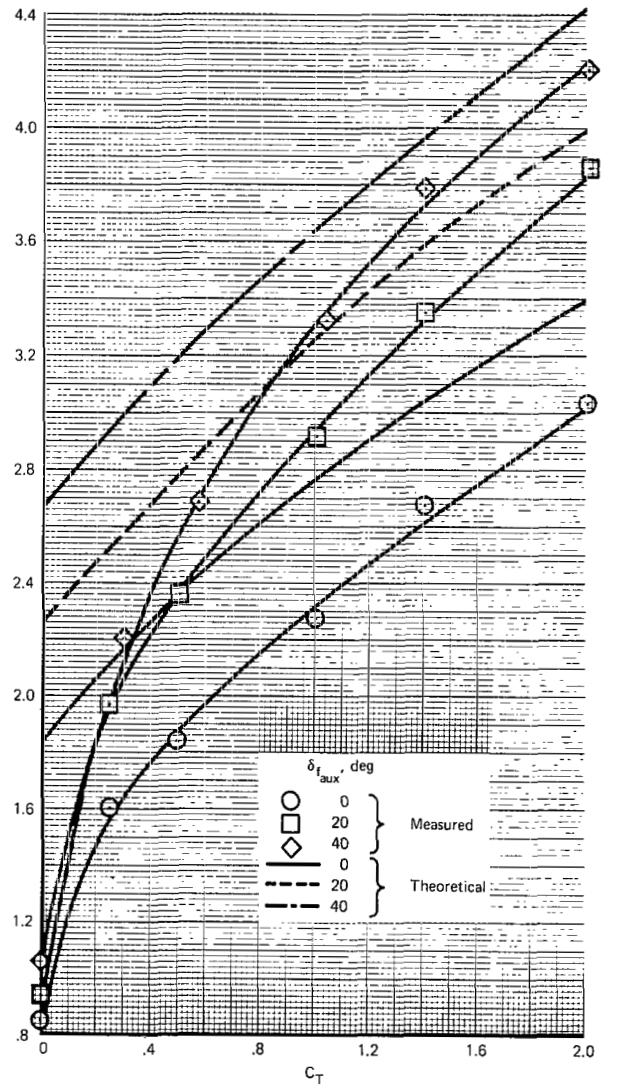

(b) $\delta_{f_m} = 50^\circ$

Figure 21.- Comparison of lift coefficients for measured and theoretical lift coefficient; $\alpha = 0^\circ$.

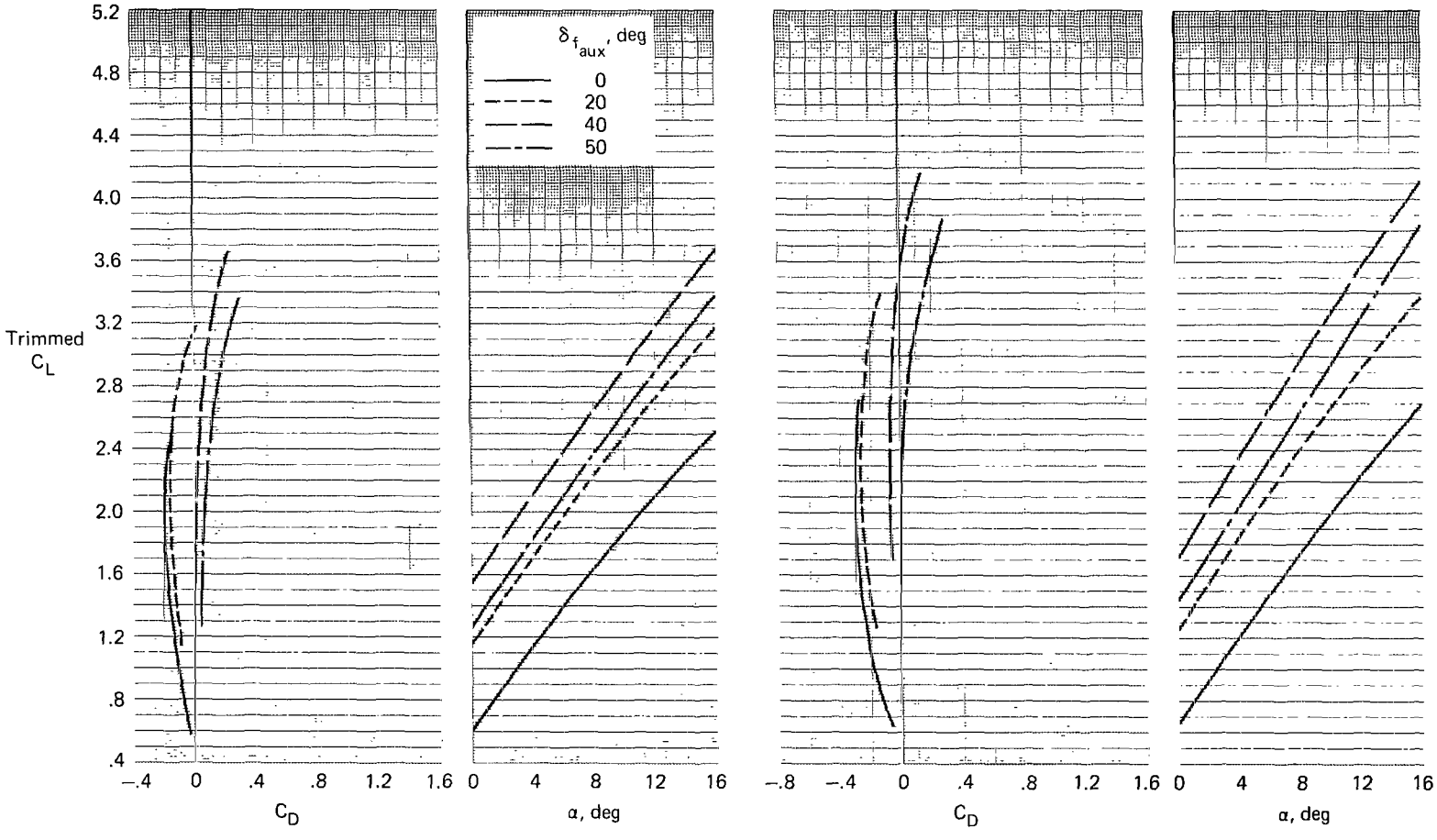

(a) T/W = 0.300 (3 engines)

(b) T/W = 0.375 (3 engines)

Figure 22.- Longitudinal characteristics of the model used in performance computations; $\delta_{f_m} = 20°$.

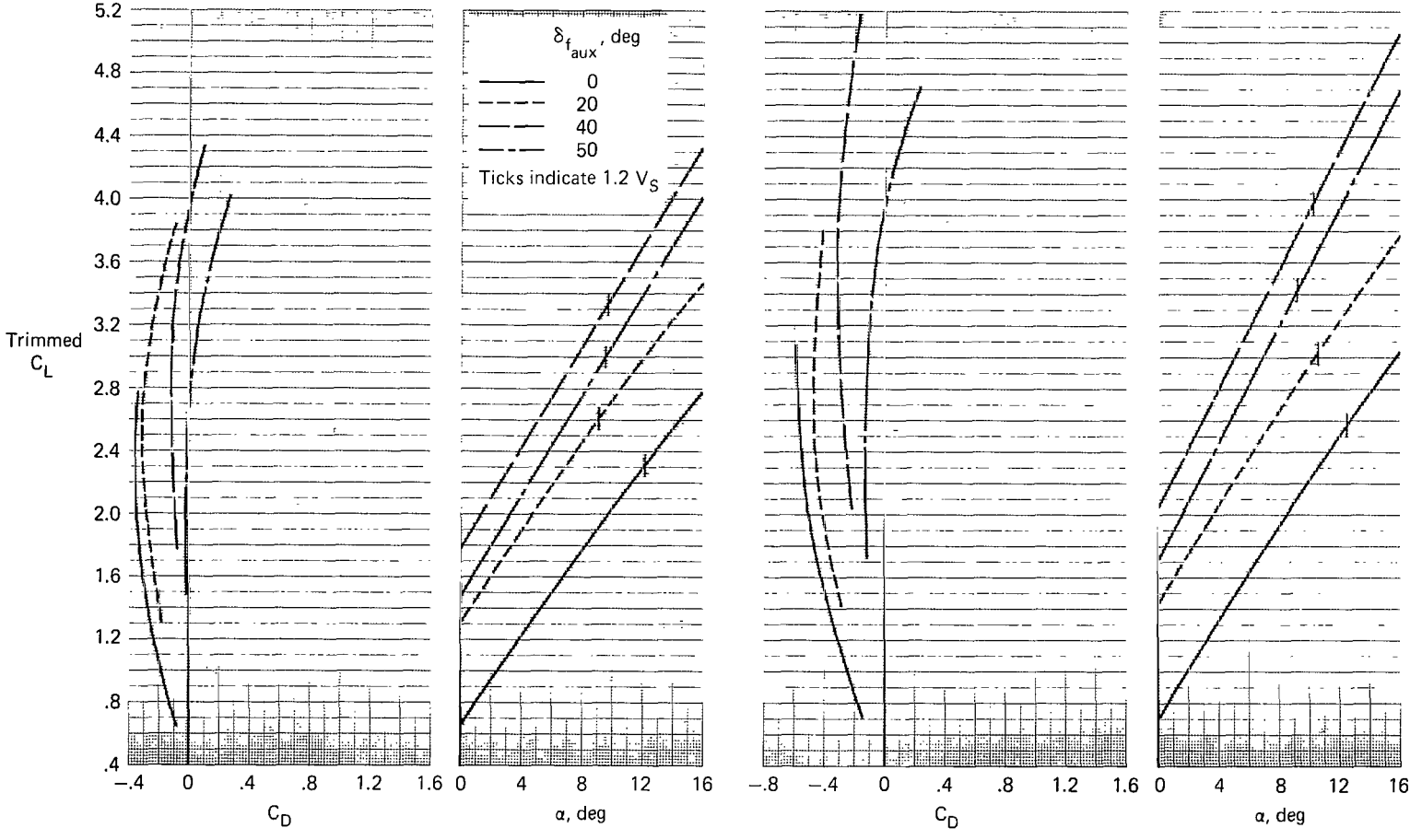

(c) T/W = 0.40 (4 engines)

(d) T/W = 0.50 (4 engines)

Figure 22.- Concluded.

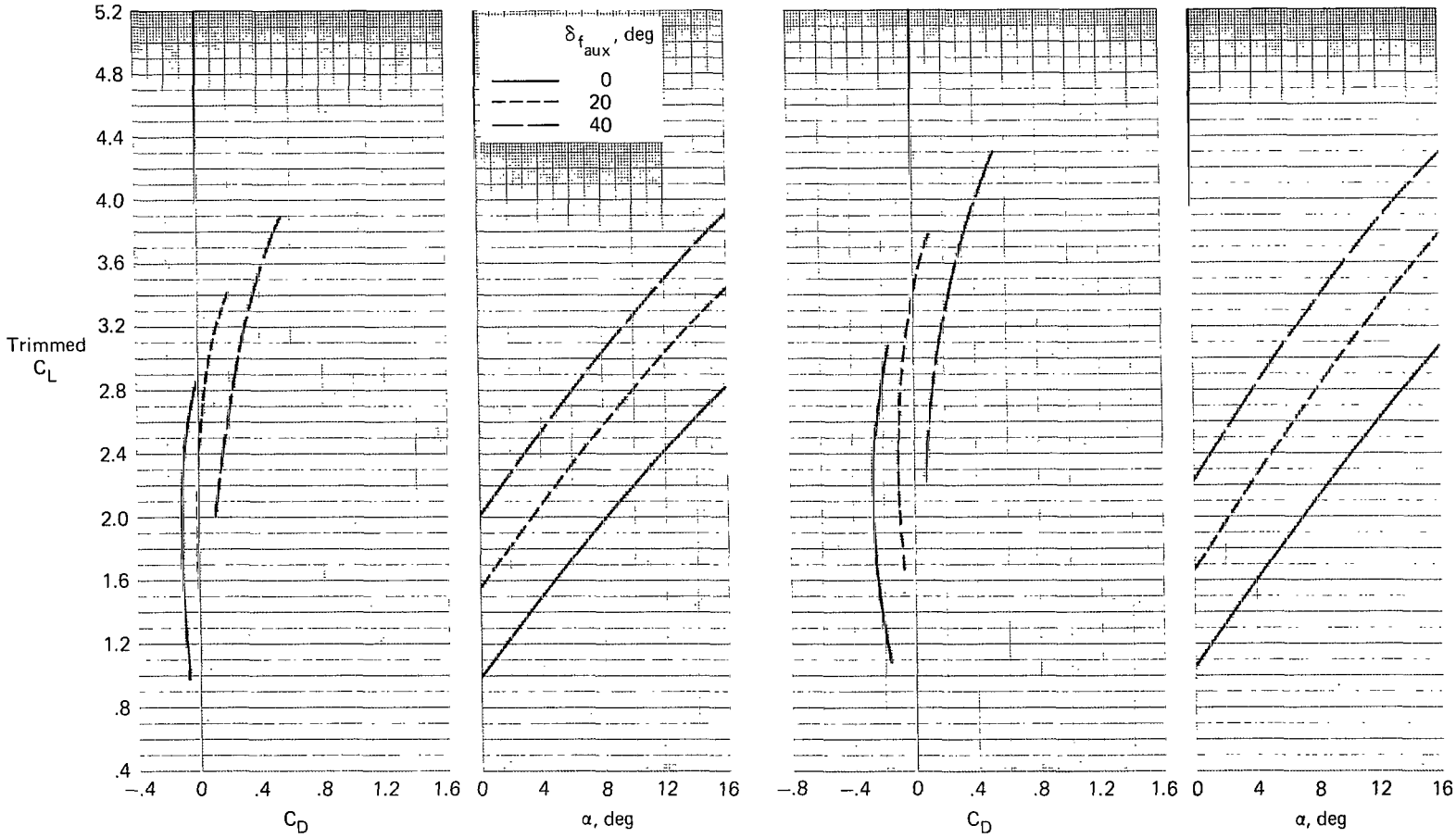

(a) T/W = 0.300 (3 engines)

(b) T/W = 0.375 (3 engines)

Figure 23.- Longitudinal characteristics of the model used for performance computations; $\delta_{f_m} = 30°$.

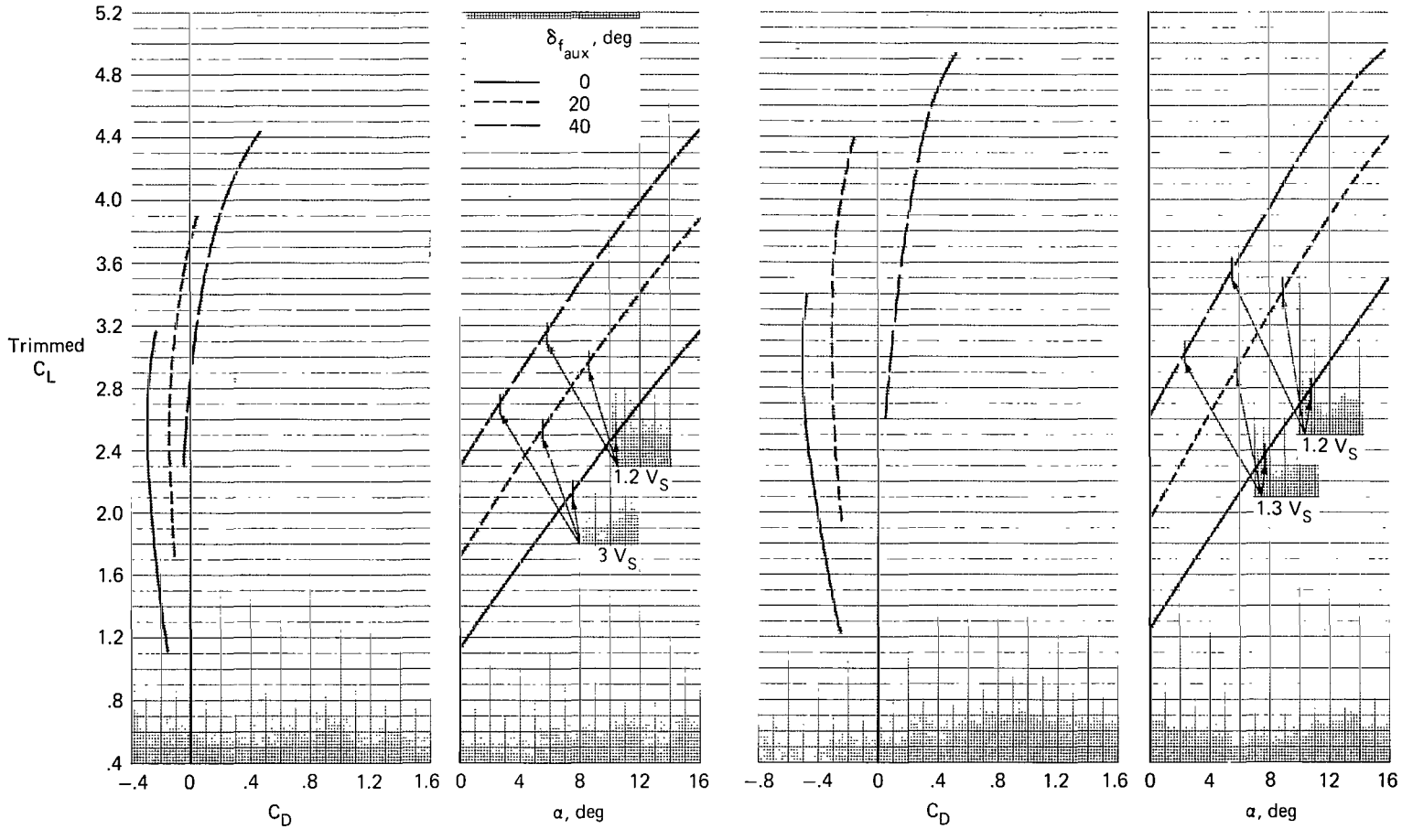

(c) T/W = 0.40 (4 engines)

T/W = 0.50 (4 engines)

Figure 23.- Concluded.

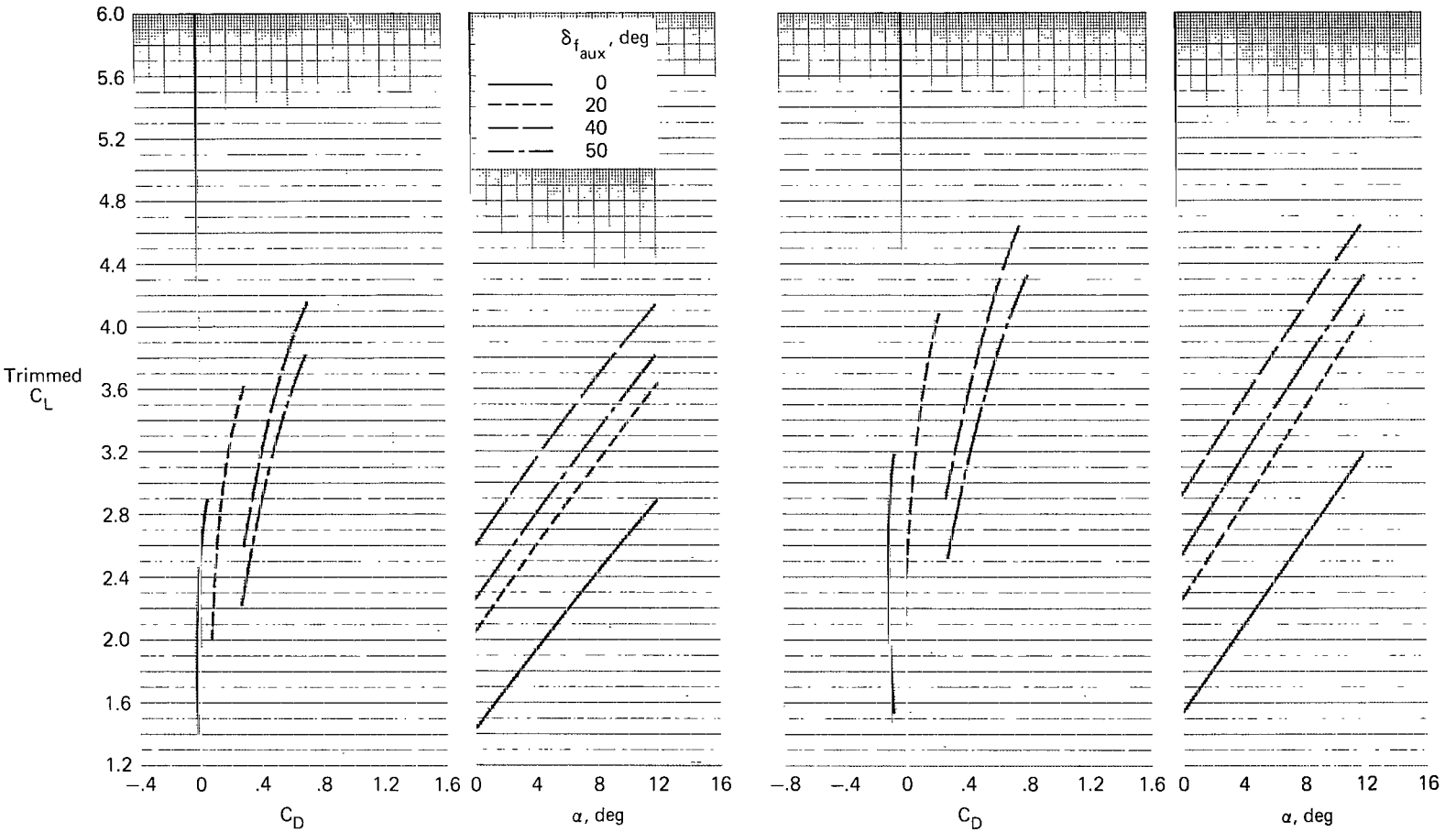

(a) T/W = 0.300 (3 engines)

(b) T/W = 0.375 (3 engines)

Figure 24.- Longitudinal characteristics of the model used for performance computation; $\delta_{f_m} = 40°$.

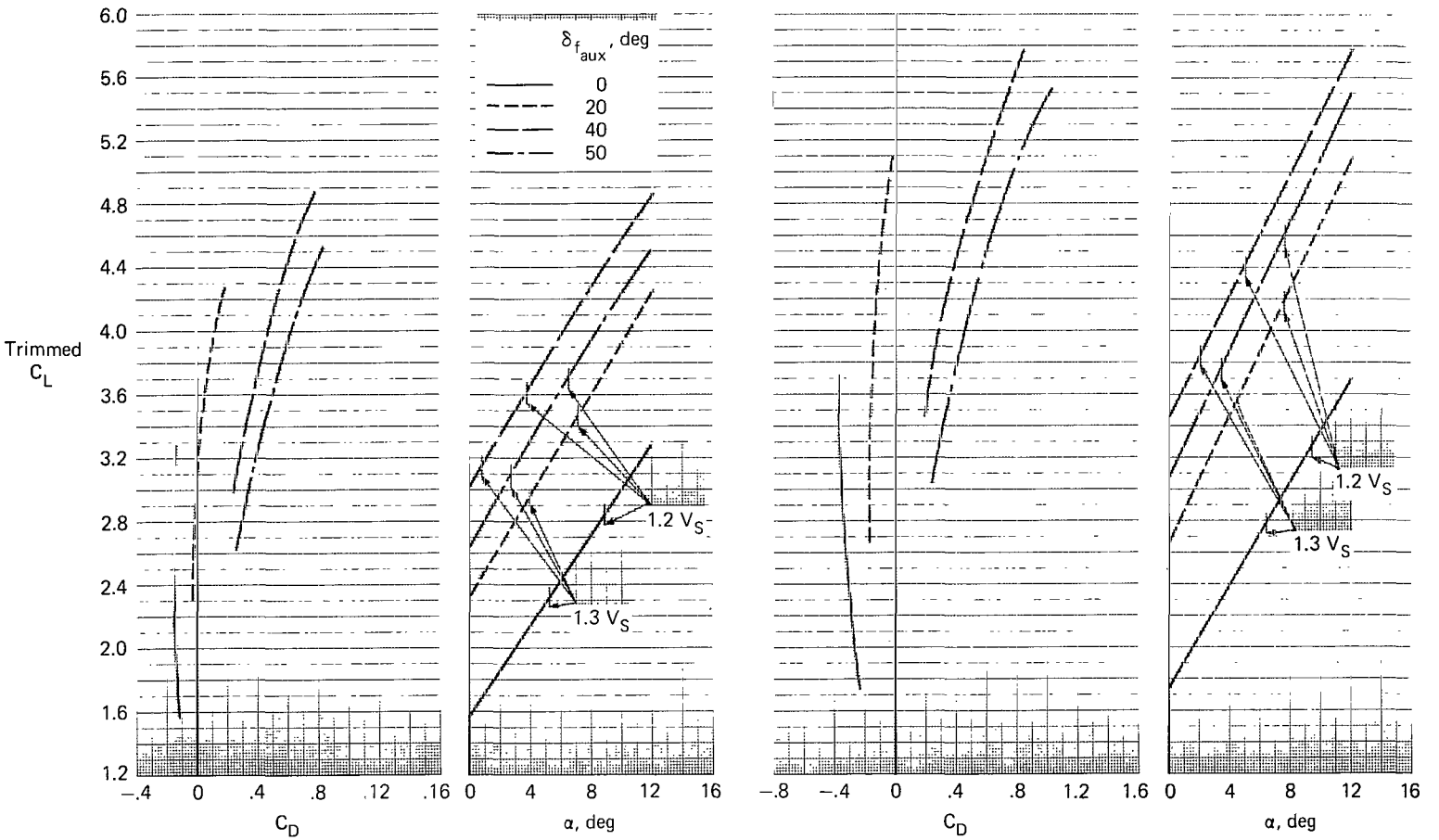

(c) T/W = 0.40 (4 engines)

(d) T/W = 0.50 (4 engines)

Figure 24.- Concluded.

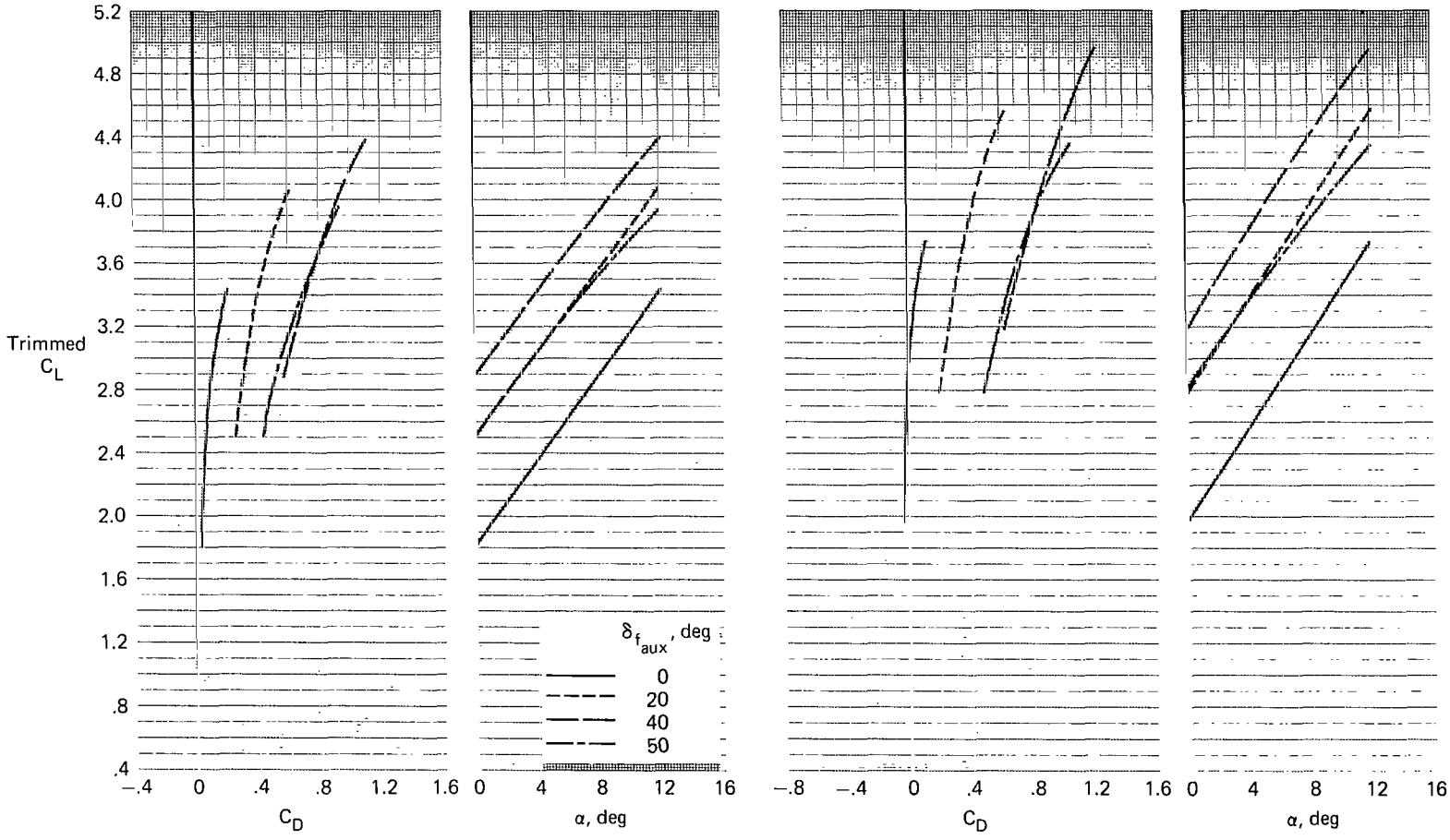

(a) T/W = 0.300 (3 engines)

(b) T/W = 0.375 (3 engines)

Figure 25.- Longitudinal characteristics of the model used in performance computation; $\delta_{f_m} = 50°$.

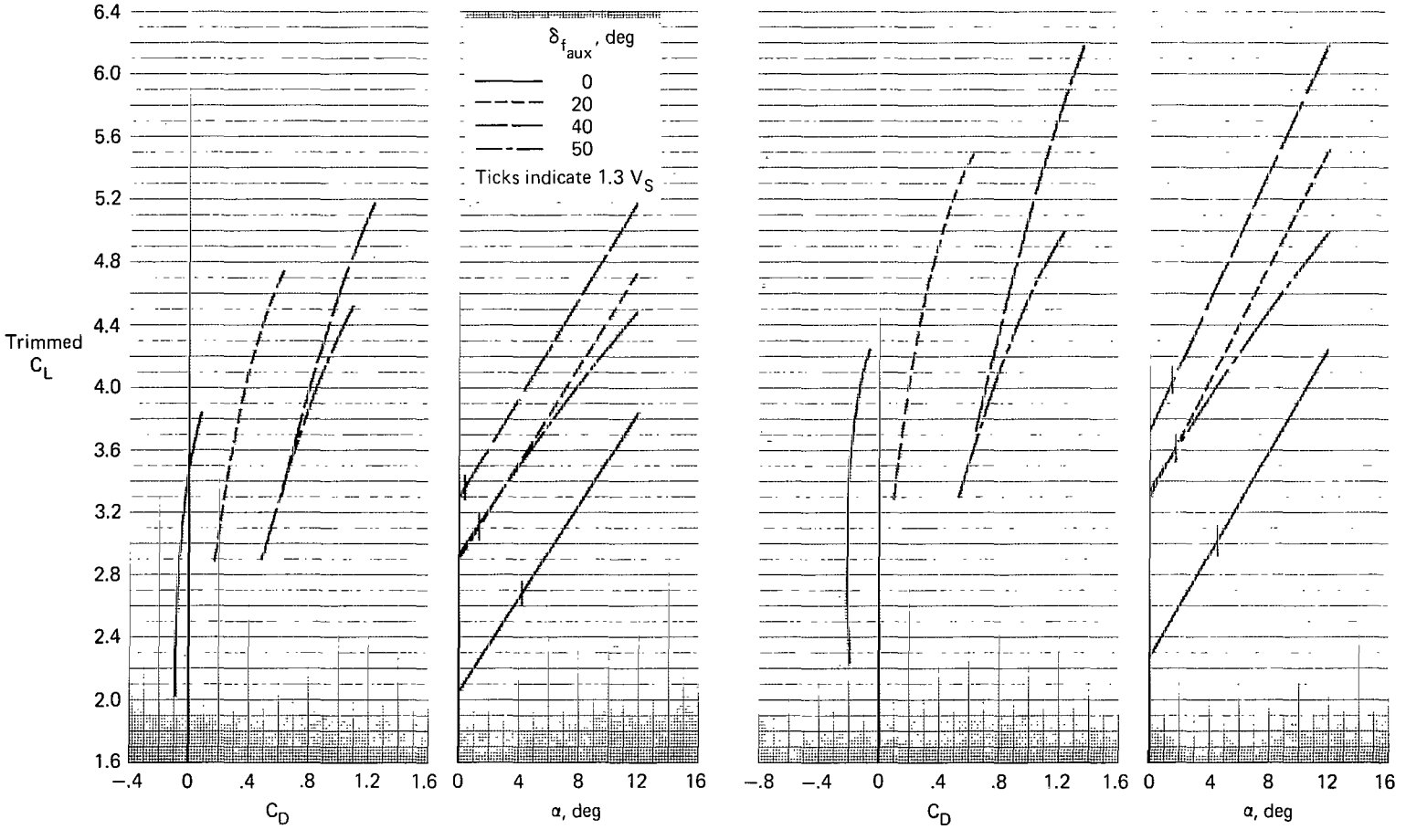

(c) T/W = 0.40 (4 engines)

(d) T/W = 0.50 (4 engines)

Figure 25.- Concluded.

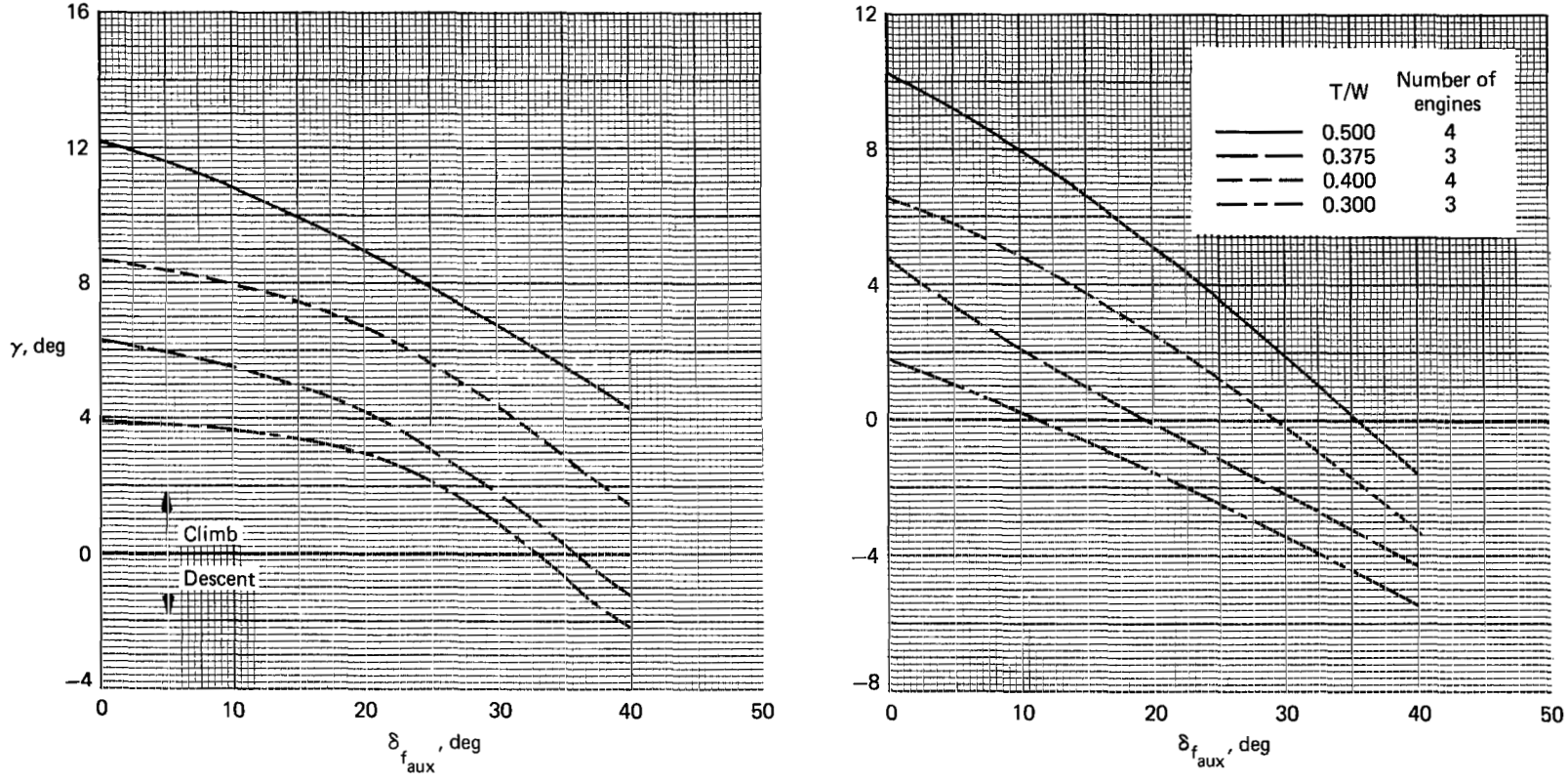

(a) $\delta_{f_m} = 20°$

(b) $\delta_{f_m} = 30°$

Figure 26.- Variation of flight path angle with auxiliary flap deflection at 1.2 V_S (1 g flight).

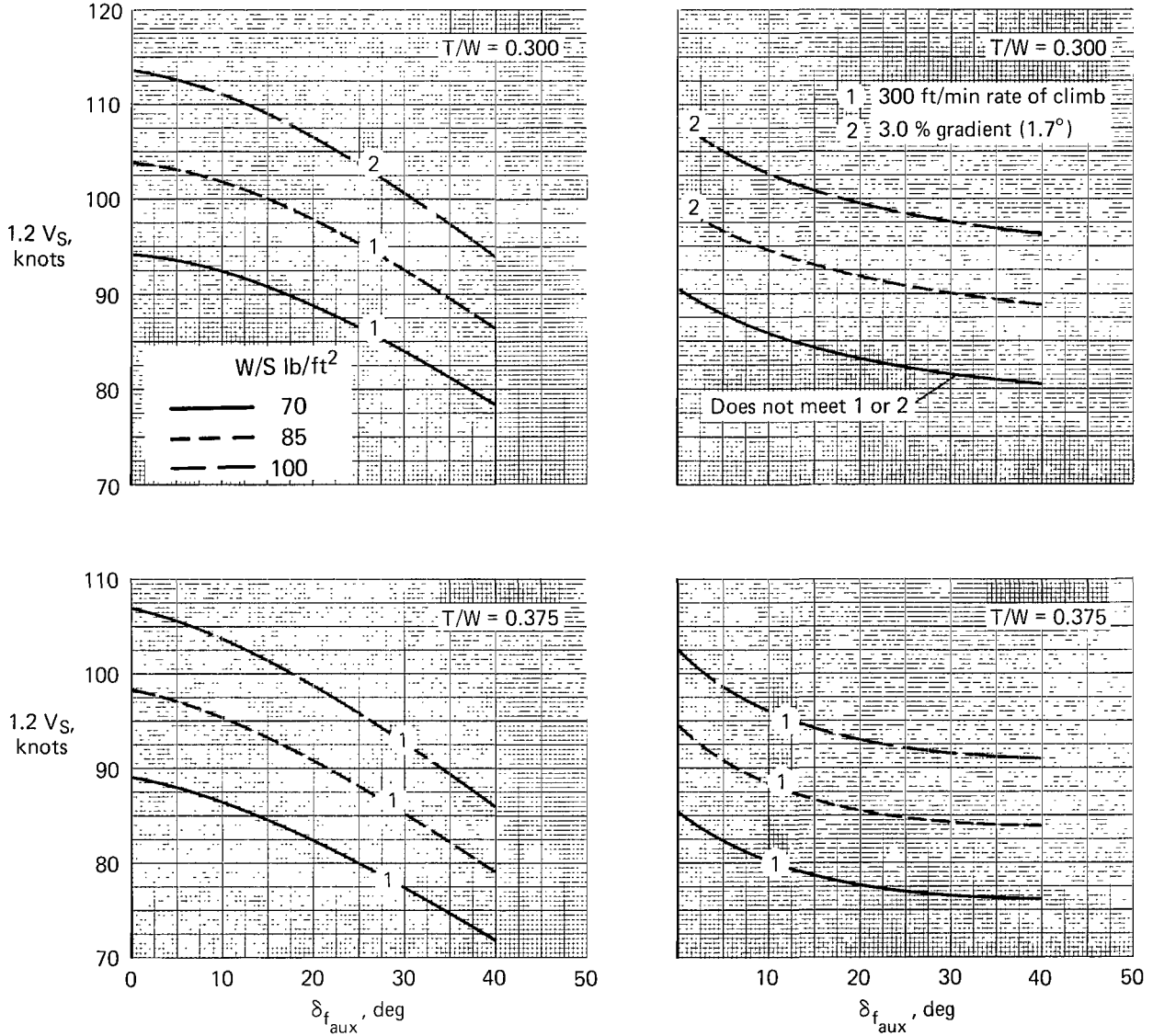

Figure 27.- Variation of forward speed with auxiliary flap deflection during steady climb for 1 g flight.

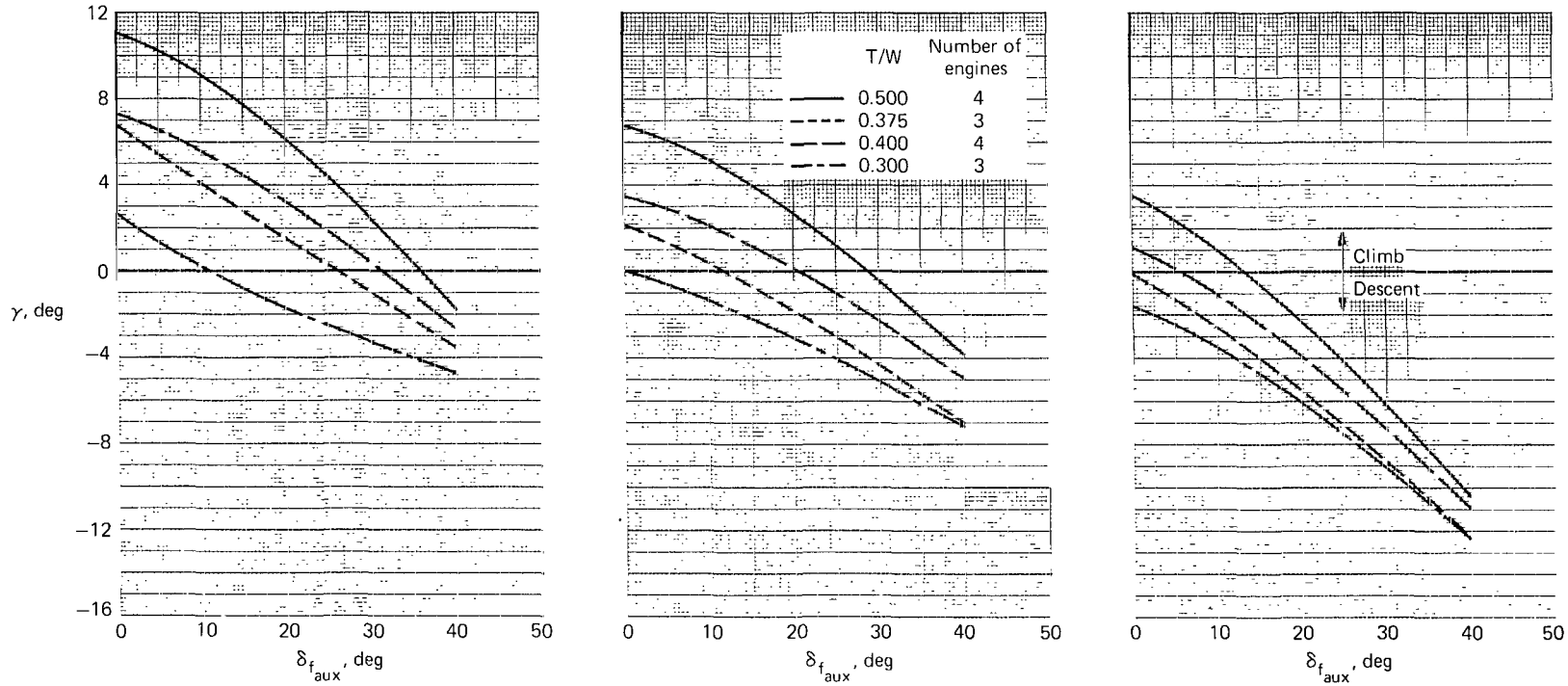

(a) $\delta_{f_m} = 30°$ (b) $\delta_{f_m} = 40°$ (c) $\delta_{f_m} = 50°$

Figure 28.- Variation of flight path angle with auxiliary flap deflection at 1.3 V_S (1 g flight).

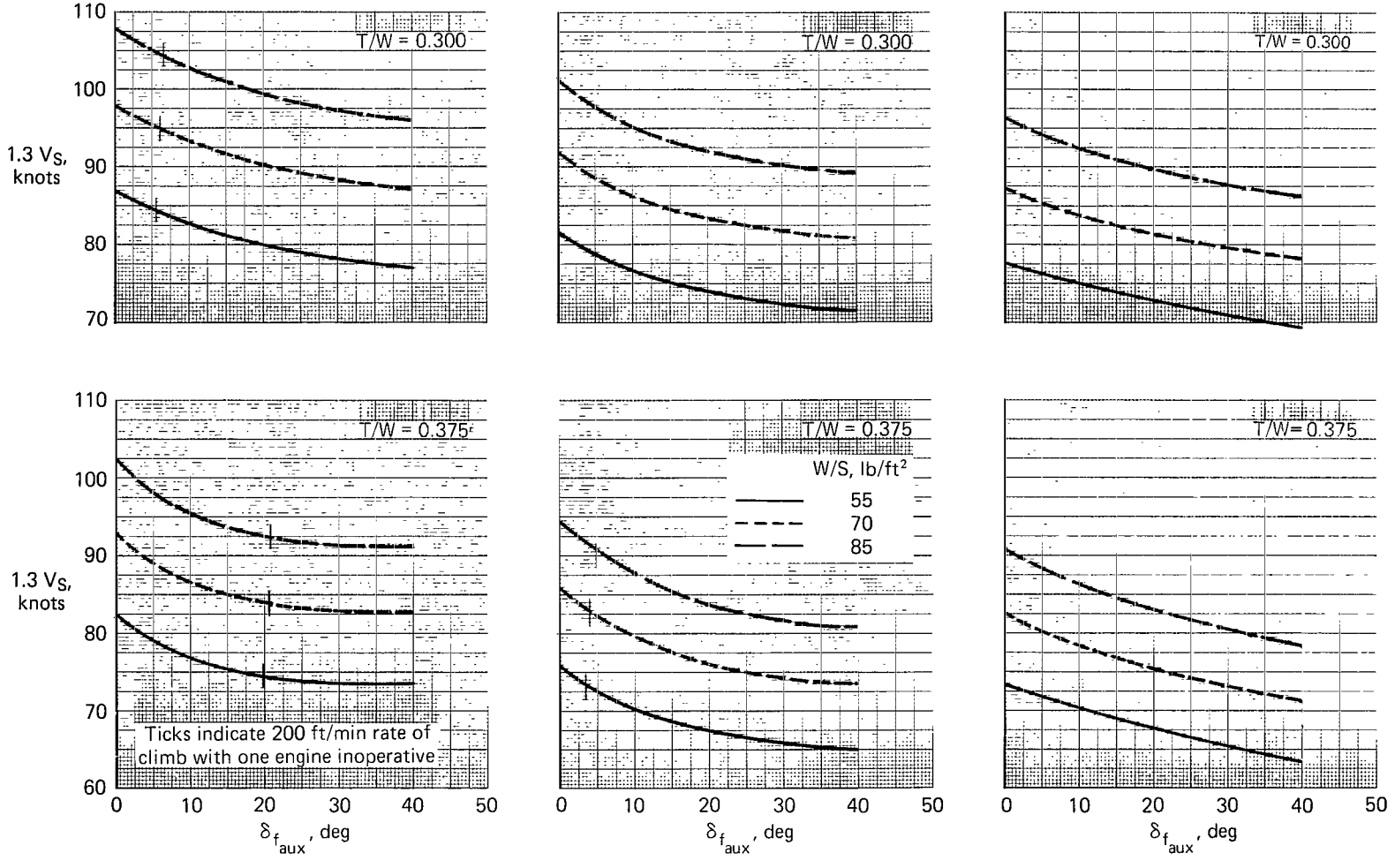

(a) $\delta_{f_m} = 30°$ (b) $\delta_{f_m} = 40°$ (c) $\delta_{f_m} = 50°$

Figure 29.- Variation of approach speed with auxiliary flap deflection for 1 g flight.

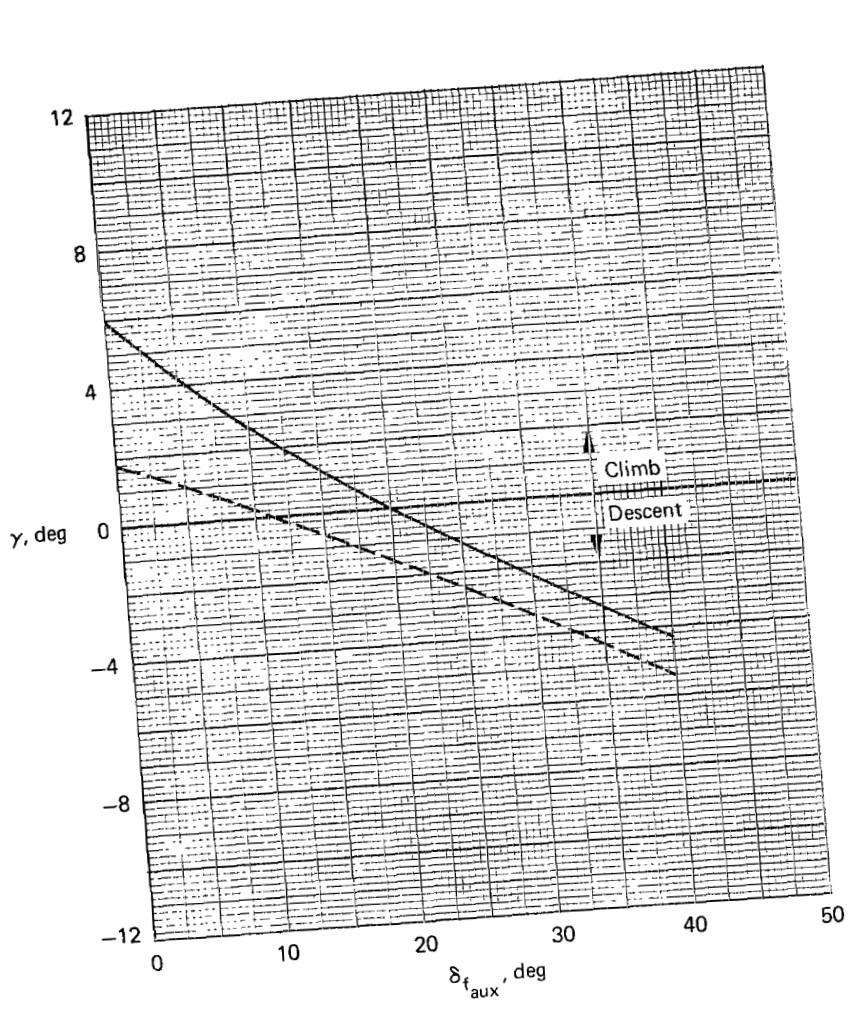

(a) $\delta_{f_m} = 30°$

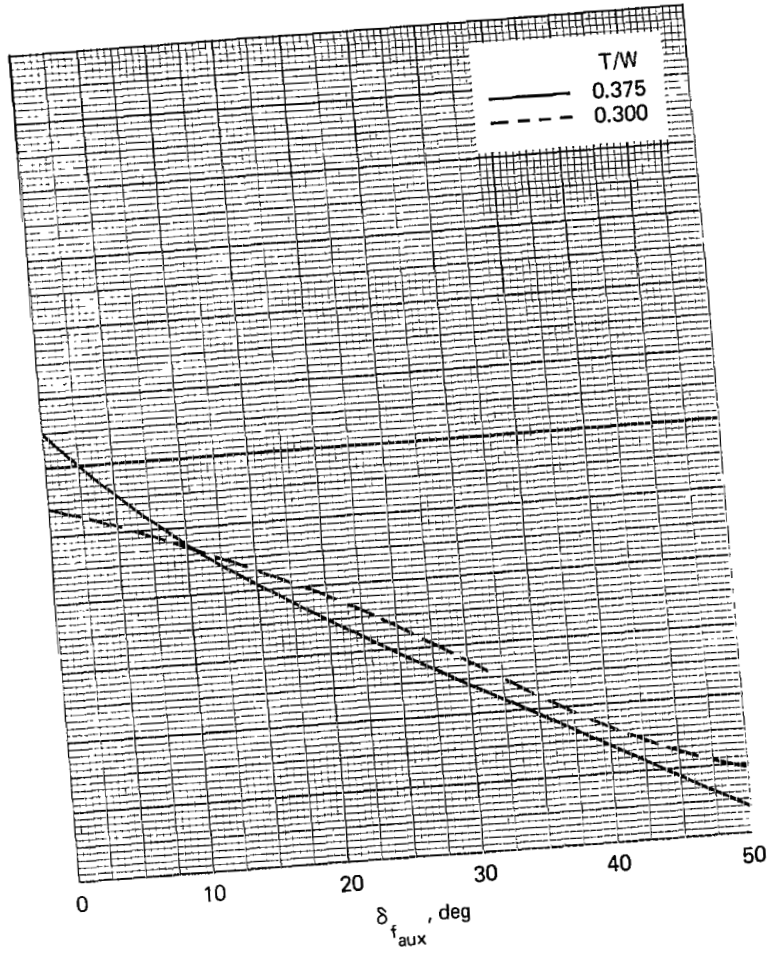

(b) $\delta_{f_m} = 40°$

Figure 30.- Variation of flight path angle with auxiliary flap deflection at 1.2 V_S (1 g flight).

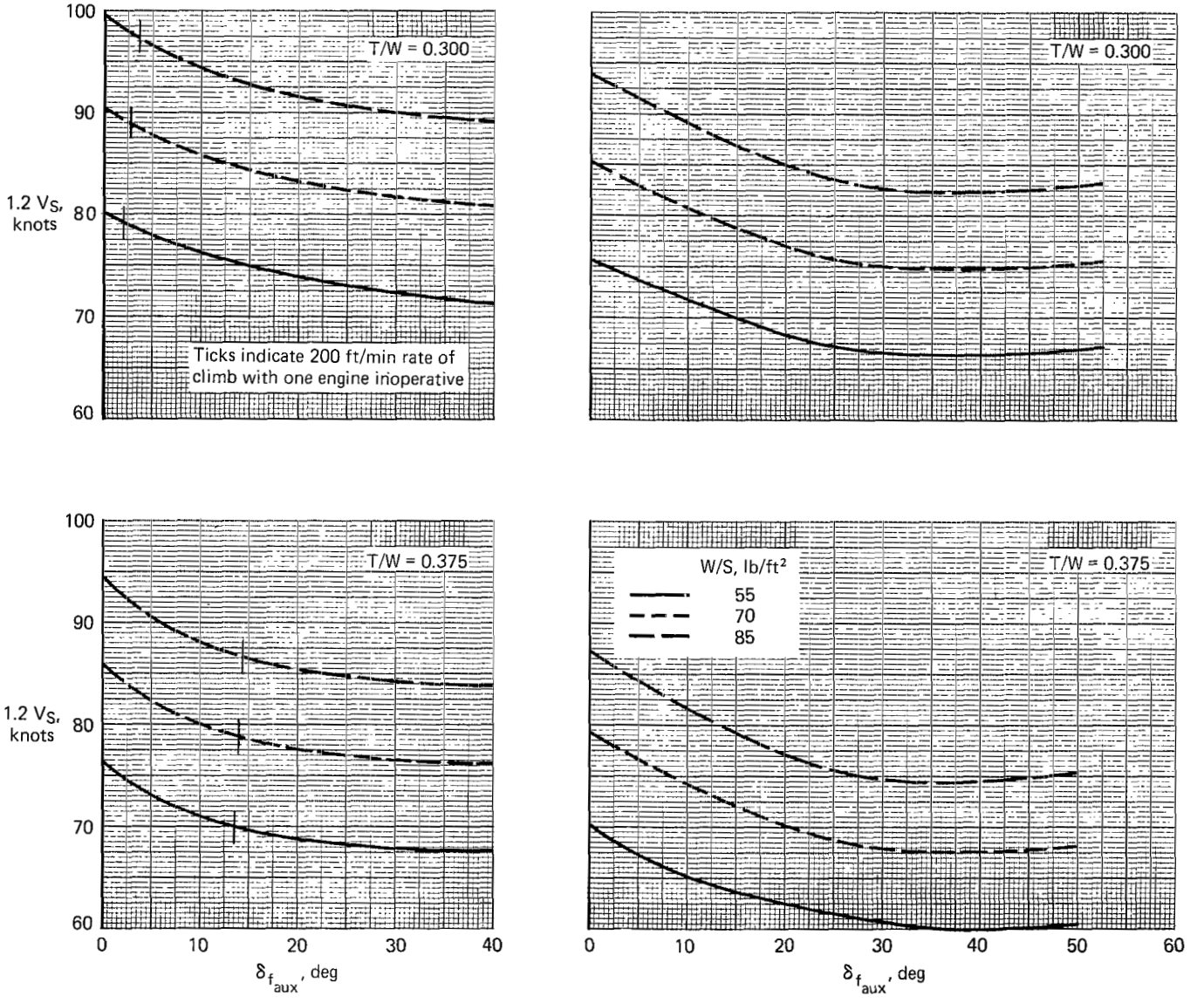

(a) $\delta_{f_m} = 30°$

(b) $\delta_{f_m} = 40°$

Figure 31.- Variation of approach speed with auxiliary flap deflection for 1 g flight.

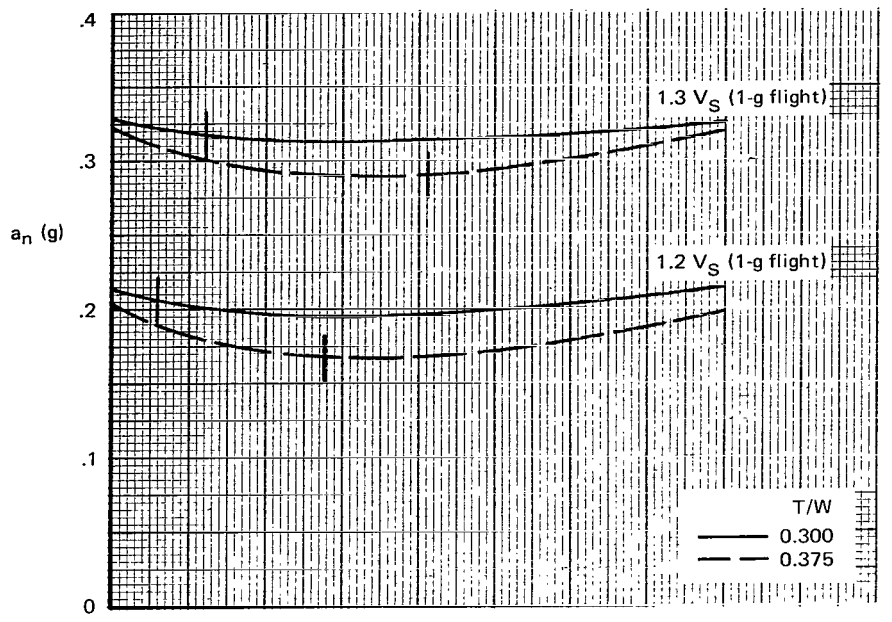

(a) $\delta_{f_m} = 30°$

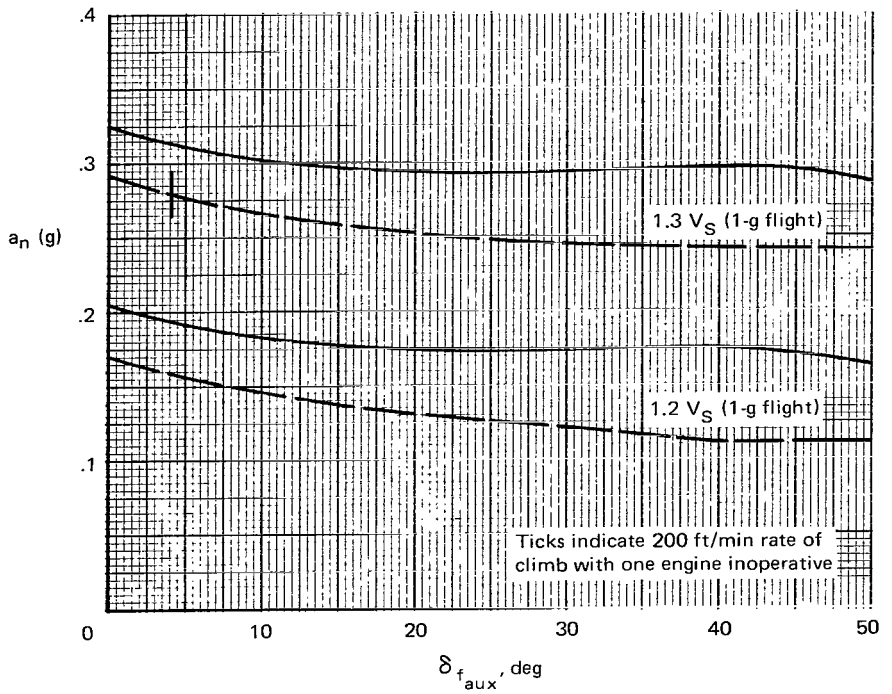

(b) $\delta_{f_m} = 40°$

Figure 32.- Variation of maximum pull-up incremental normal acceleration with auxiliary flap deflection.

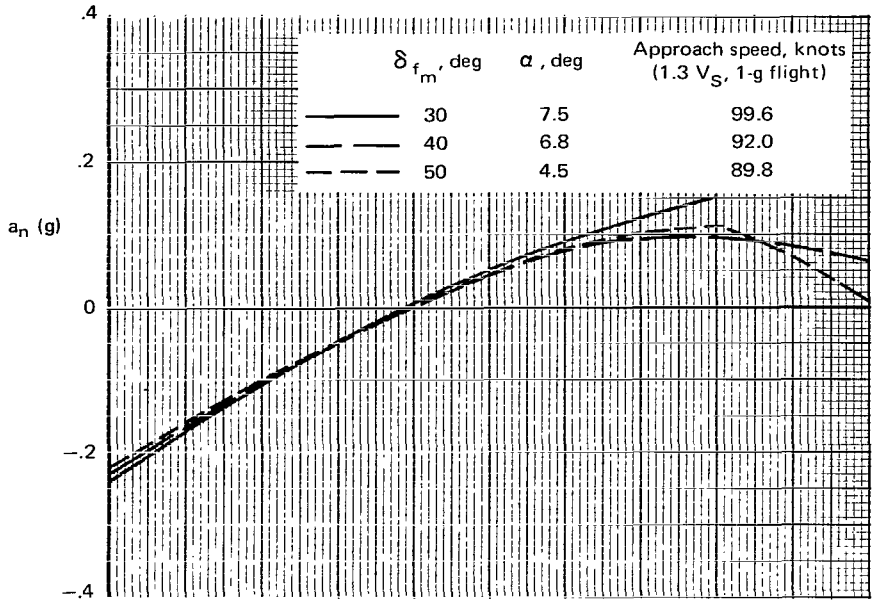

(a) T/W = 0.30

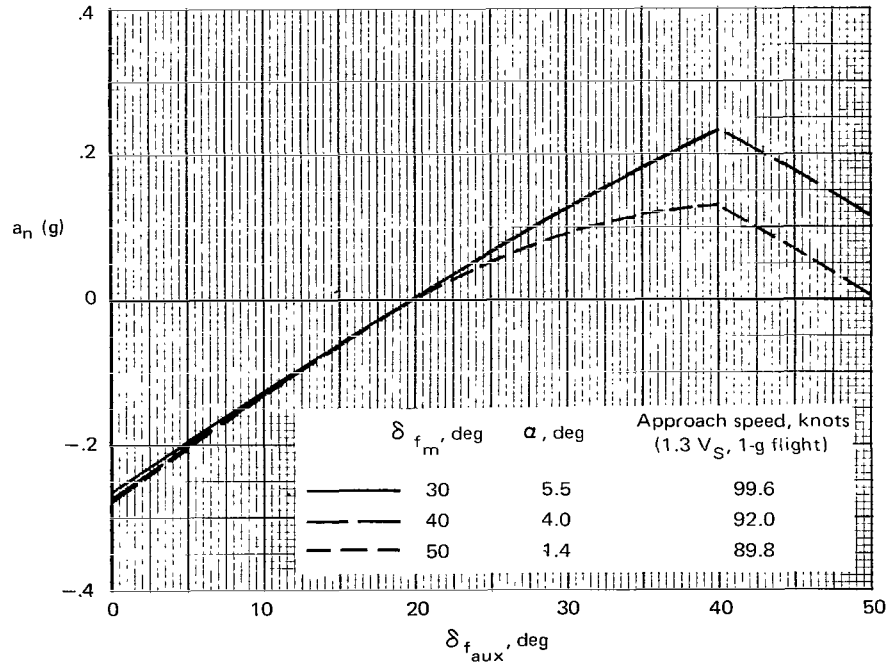

(b) T/W = 0.40

Figure 33.- Variation of incremental normal acceleration due to auxiliary flap deflection at constant angle of attack; W/S = 85 lb/ft^2.

026 001 C1 U 01 710813 S00903DS
DEPT OF THE AIR FORCE
AF SYSTEMS COMMAND
AF WEAPONS LAB (WLOL)
ATTN: E LOU BOWMAN, CHIEF TECH LIBRARY
KIRTLAND AFB NM 87117

"The aeronautical and space activities of the United States shall be conducted so as to contribute . . . to the expansion of human knowledge of phenomena in the atmosphere and space. The Administration shall provide for the widest practicable and appropriate dissemination of information concerning its activities and the results thereof."

—NATIONAL AERONAUTICS AND SPACE ACT OF 1958

NASA SCIENTIFIC AND TECHNICAL PUBLICATIONS

TECHNICAL REPORTS: Scientific and technical information considered important, complete, and a lasting contribution to existing knowledge.

TECHNICAL NOTES: Information less broad in scope but nevertheless of importance as a contribution to existing knowledge.

TECHNICAL MEMORANDUMS: Information receiving limited distribution because of preliminary data, security classification, or other reasons.

CONTRACTOR REPORTS: Scientific and technical information generated under a NASA contract or grant and considered an important contribution to existing knowledge.

TECHNICAL TRANSLATIONS: Information published in a foreign language considered to merit NASA distribution in English.

SPECIAL PUBLICATIONS: Information derived from or of value to NASA activities. Publications include conference proceedings, monographs, data compilations, handbooks, sourcebooks, and special bibliographies.

TECHNOLOGY UTILIZATION PUBLICATIONS: Information on technology used by NASA that may be of particular interest in commercial and other non-aerospace applications. Publications include Tech Briefs, Technology Utilization Reports and Technology Surveys.

Details on the availability of these publications may be obtained from:

SCIENTIFIC AND TECHNICAL INFORMATION OFFICE

NATIONAL AERONAUTICS AND SPACE ADMINISTRATION

Washington, D.C. 20546